Institut Langevin
ONDES ET IMAGES

Reflection Matrix Imaging in Wave Physics

Alexandre Aubry

Institut Langevin, ESPCI Paris, CNRS, PSL University, Paris, France

PSL UNIVERSITÉ PARIS

ESPCI PARIS

cnrs dépasser les frontières

INVESTISSEMENTS D'AVENIR

erc European Research Council Established by the European Commission

IDEFIX Seminar – INRIA, Institut Polytechnique de Paris, EDF R&D – March 22nd, 2022

Institut Langevin
ONDES ET IMAGES

Conventional wave imaging in inhomogeneous media

Optical microscopy

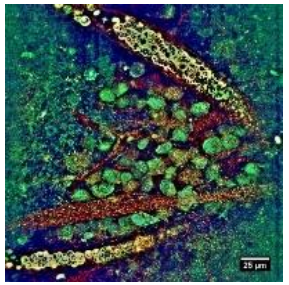

Apelian *et al.*
Opt. Exp. 2016

biological tissues

Badon et al., *Sci. Adv.*, 2016 - 2020

Ultrasound imaging

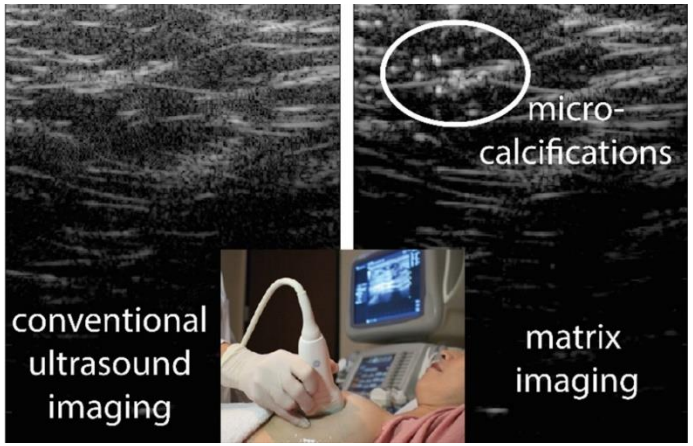

liver/breast imaging

Lambert et al., *PNAS*, *PRX*, 2020

Seismology

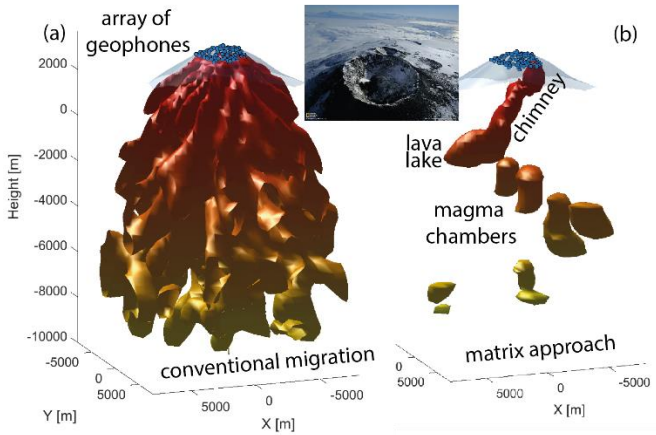

fault zones, volcanoes

Touma *et al.*, *Geophys. J. Int.*, 2021

Blondel et al., *JGR*, 2018

Same limitations due to the medium inhomogeneities (aberrations/multiple scattering)

Our holy grail:

Universal and *non-invasive* approach of wave imaging in complex media

Principle of a microscope in reflection

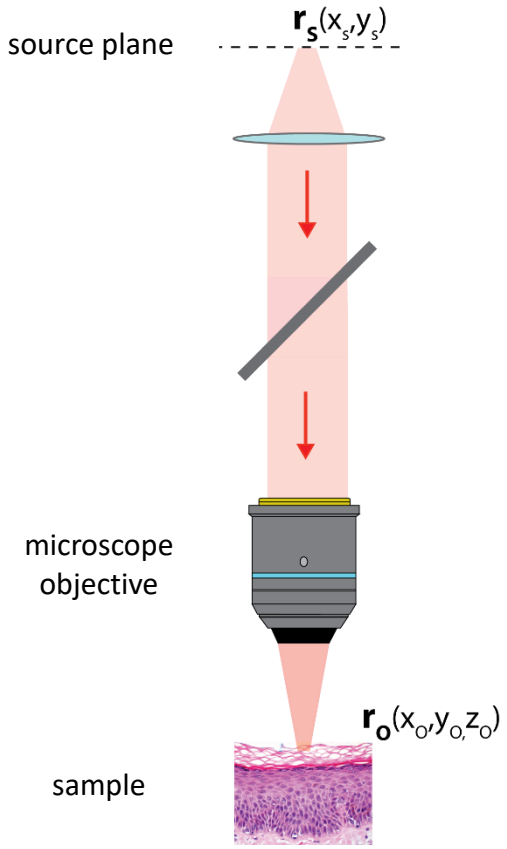

Introduction: Limitations of optical microscopy

Institut Langevin
ONDES ET IMAGES

Principle of a microscope in reflection

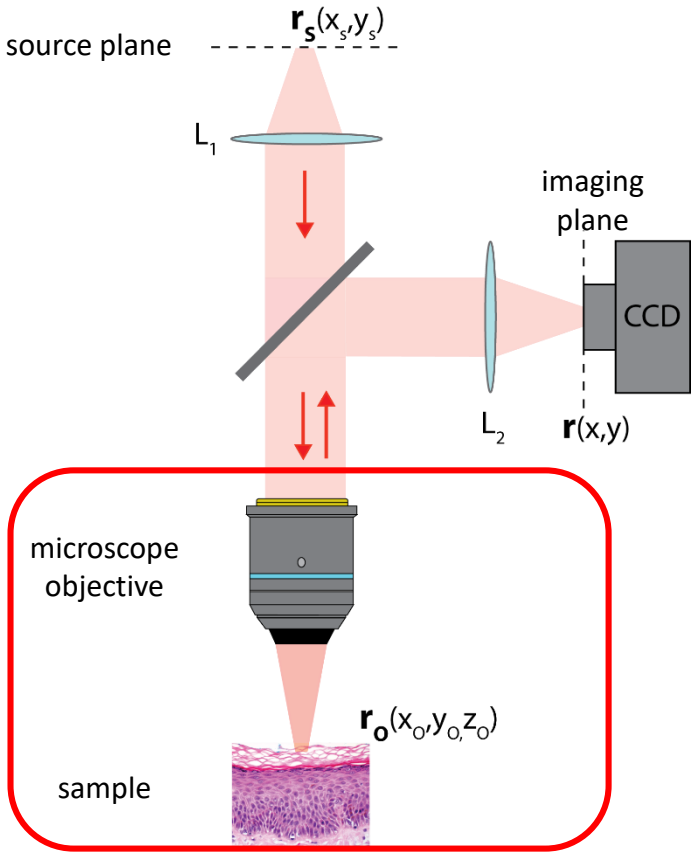

Introduction: Limitations of optical microscopy

Institut Langevin
ONDES ET IMAGES

Principle of a microscope in reflection

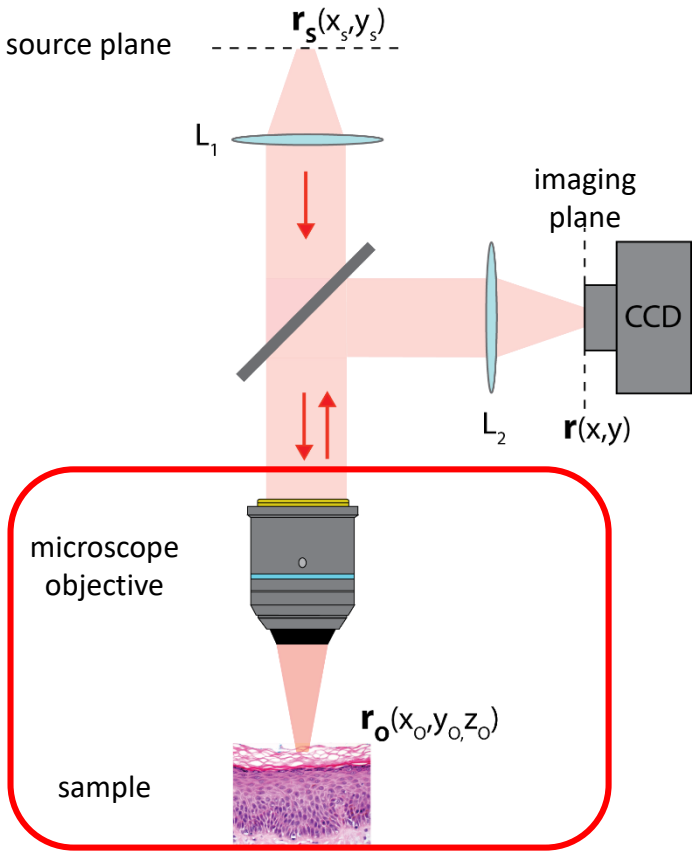

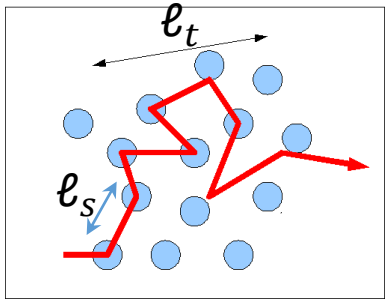

SINGLE SCATTERING

BALLISTIC PATHS

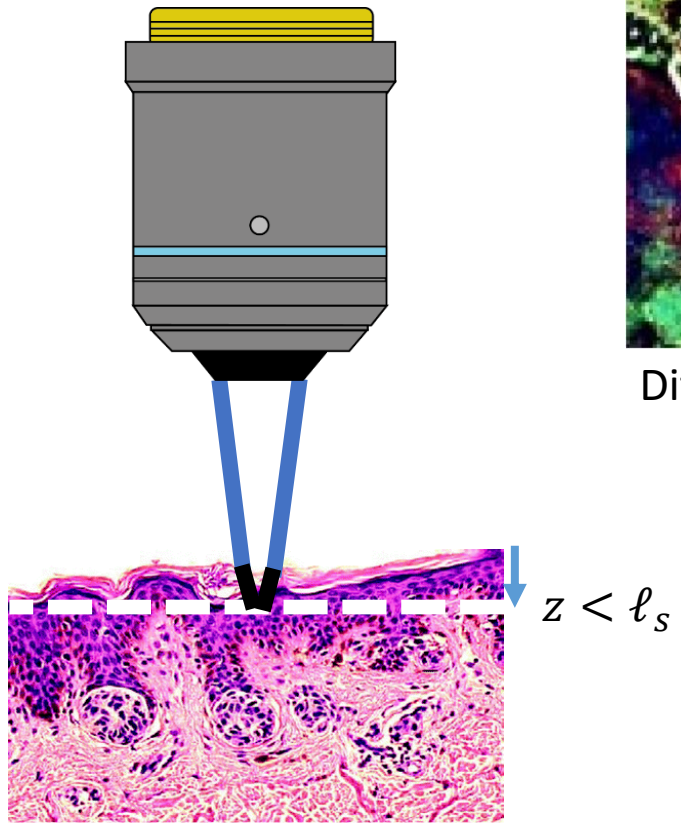

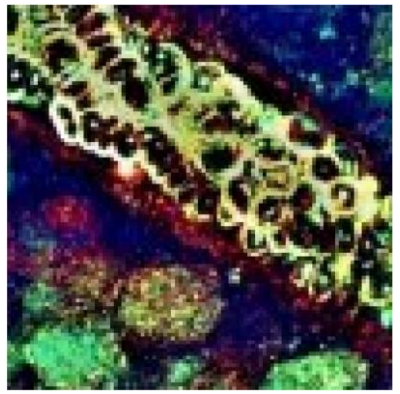

Diffraction-limited resolution

ℓ_s: scattering mean free path

$\ell_s \sim 50 - 200\ \mu m$ in biological tissues

Introduction: Limitations of optical microscopy

Institut Langevin
ONDES ET IMAGES

Principle of a microscope in reflection

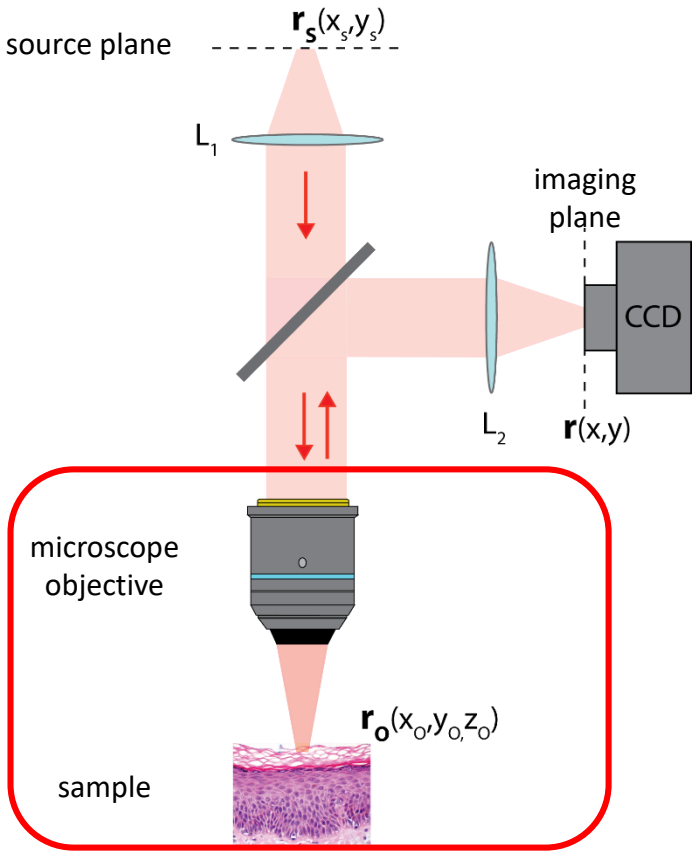

ABERRATIONS / FORWARD MULTIPLE SCATTERING

WAVE-FRONT DISTORTIONS

Strehl ratio

$$S = \frac{\mathrm{I_{real}(focal)}}{\mathrm{I_{ideal}(focal)}} < 1$$

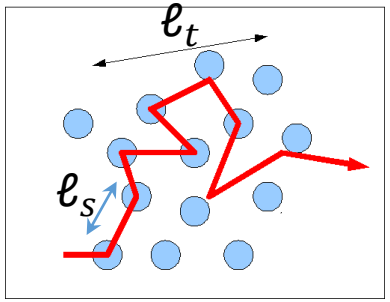

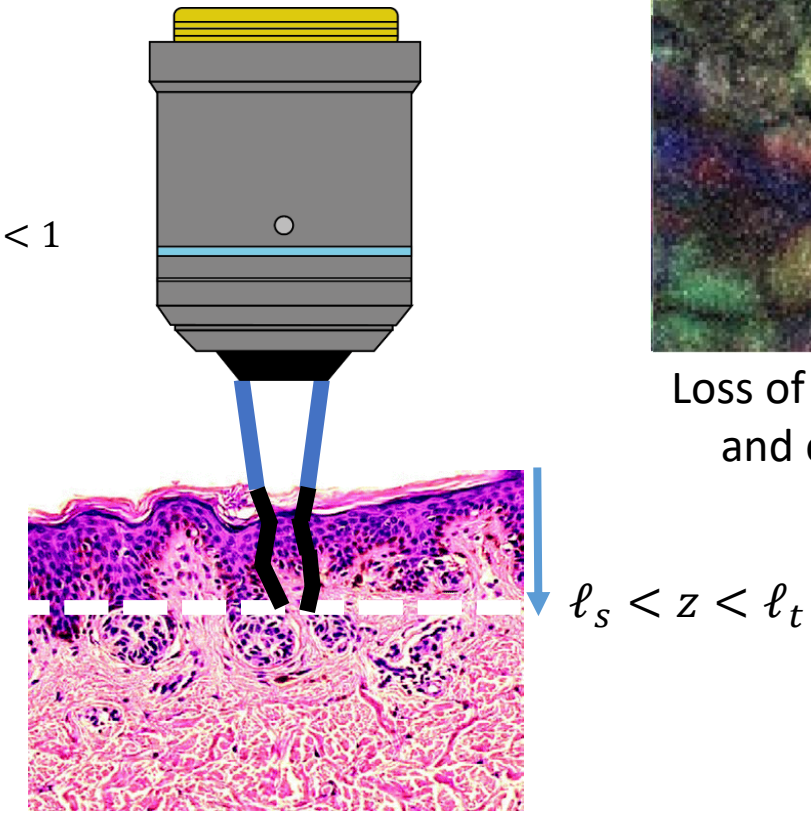

$\ell_s < z < \ell_t$

Loss of resolution and contrast

ℓ_t: transport mean free path

$\ell_t \sim 1$ mm in biological tissues

Introduction: Limitations of optical microscopy

Institut Langevin
ONDES ET IMAGES

Principle of a microscope in reflection

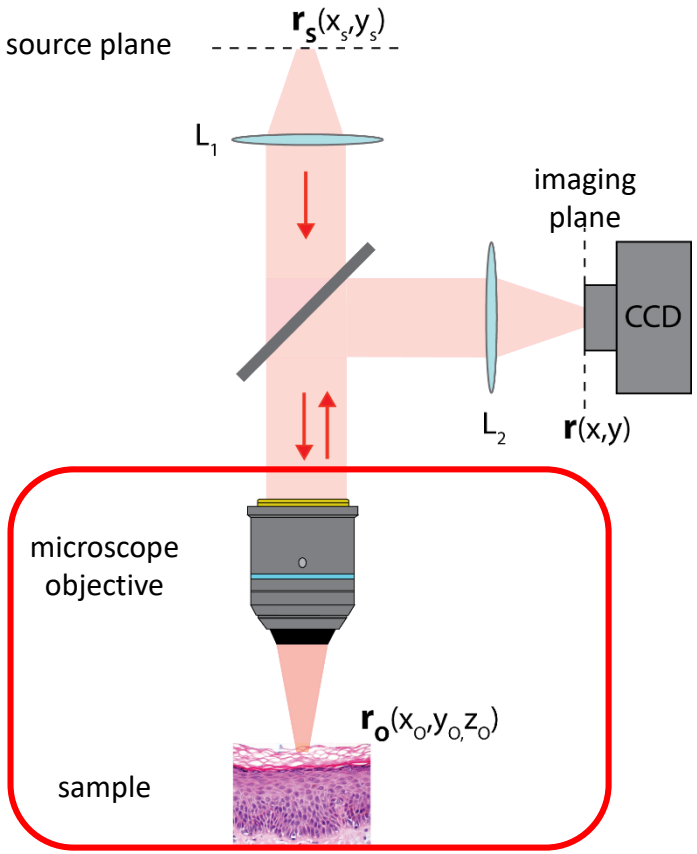

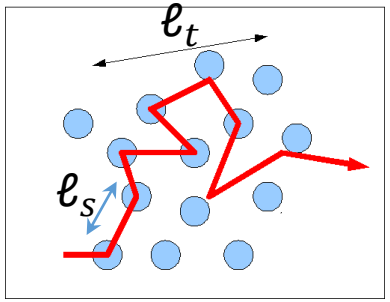

DEEP MULTIPLE SCATTERING

RANDOM PATHS / DIFFUSION

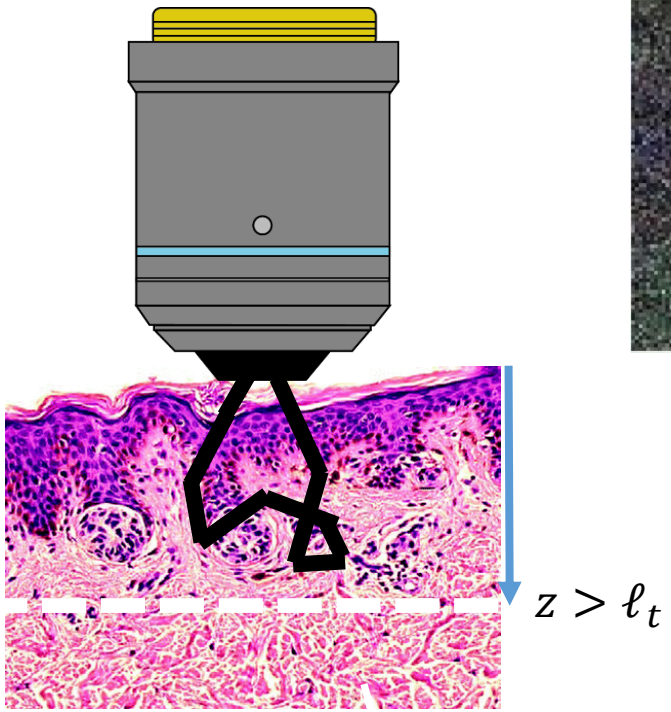

Random speckle image

ENHANCE THE SINGLE SCATTERING CONTRIBUTION

Spatial discrimination

Confocal microscopy

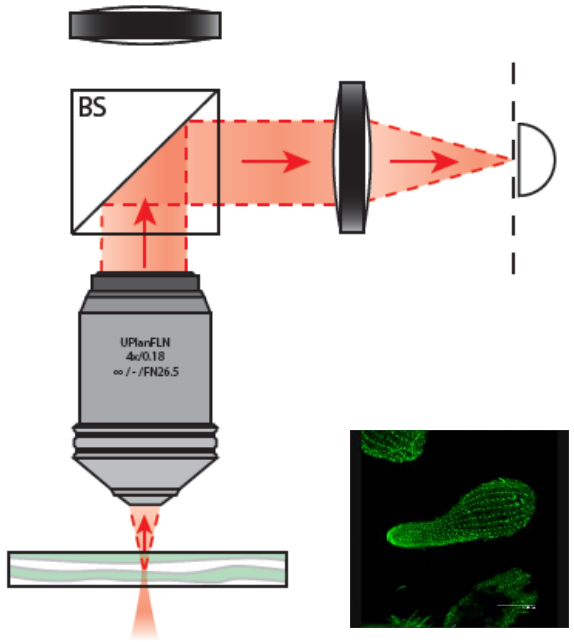

M. Minski, *Microscopy apparatus (1961)*

Temporal discrimination

Optical coherence tomography

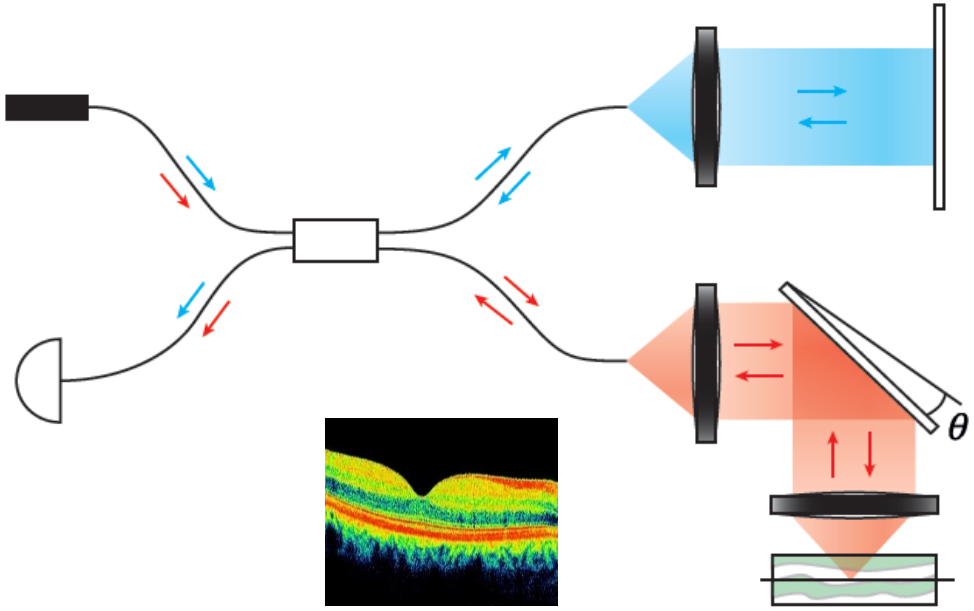

Huang, *et al.*, science 254, 1178–1181 (1991)

Introduction: The multiple scattering limit in microscopy

Institut Langevin
ONDES ET IMAGES

CAN WE GO DEEPER?

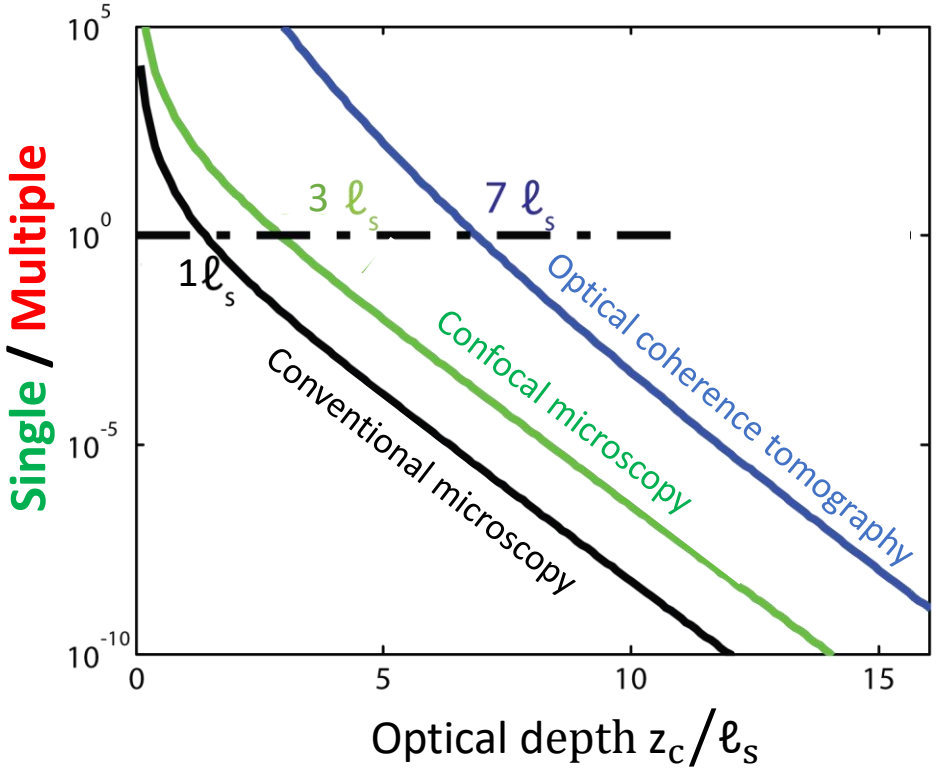

A. Badon *et al.*, Opt. Exp., 2017

TACKLE
WAVE
DISTORTIONS

REMOVE
MULTIPLE
SCATTERING
BACKGROUND

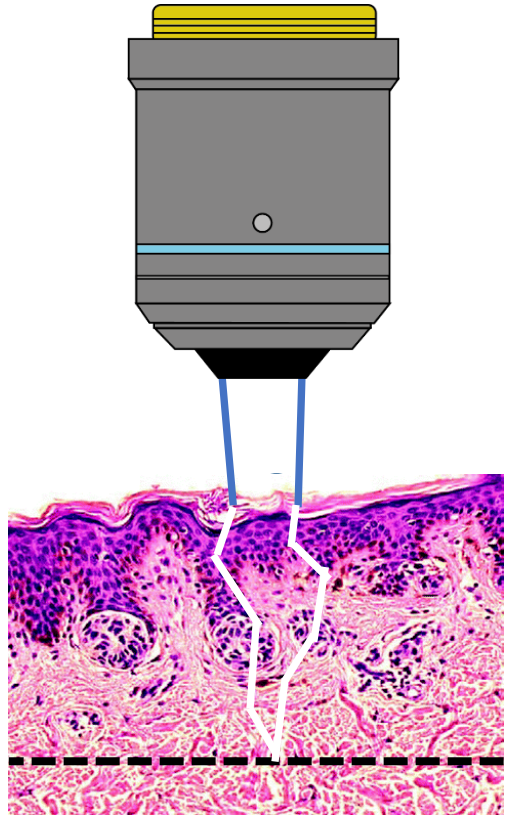

$L > \ell_t$

ℓ_t: transport mean free path

$\ell_t \sim 1$ mm in biological tissues

Introduction: Adaptive optics applied to optical microscopy

Institut Langevin
ONDES ET IMAGES

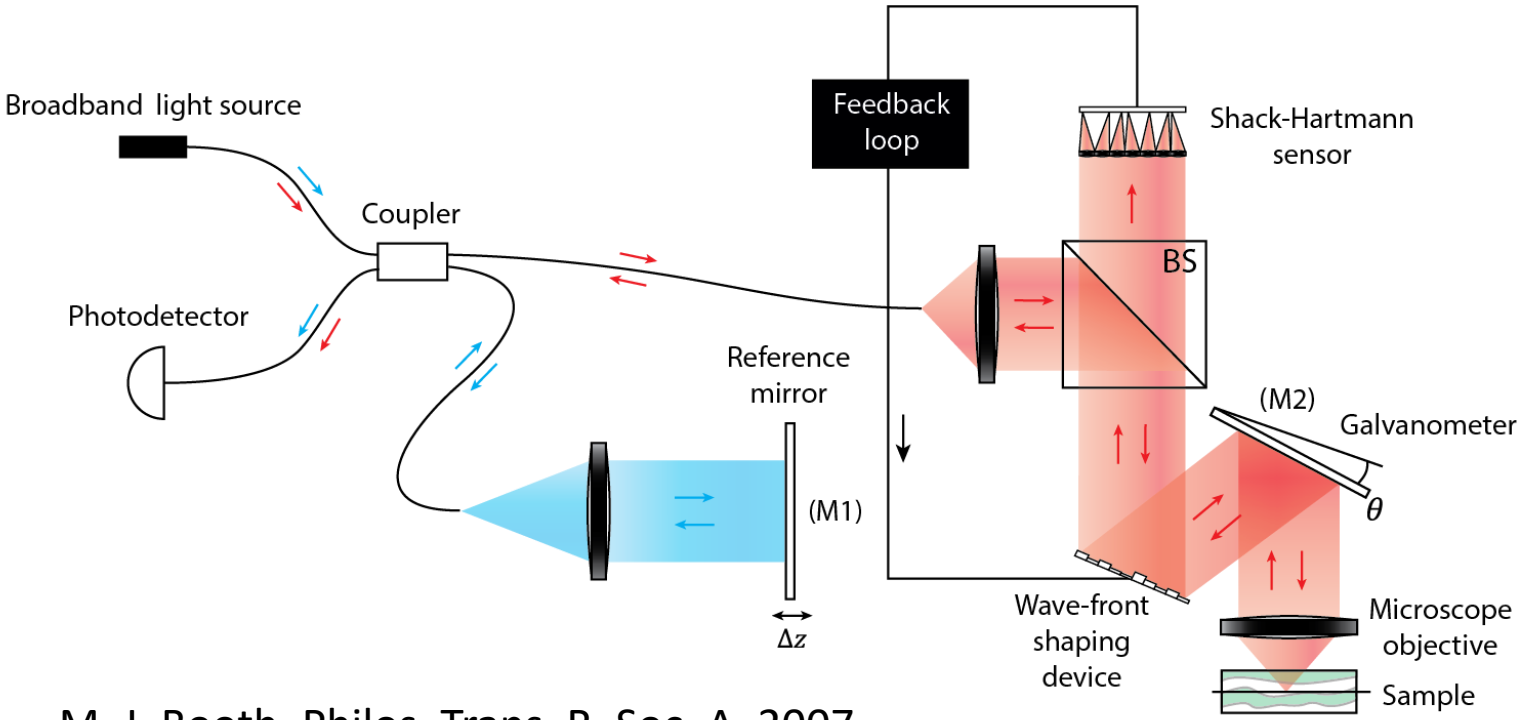

M. J. Booth, Philos. Trans. R. Soc. A, 2007

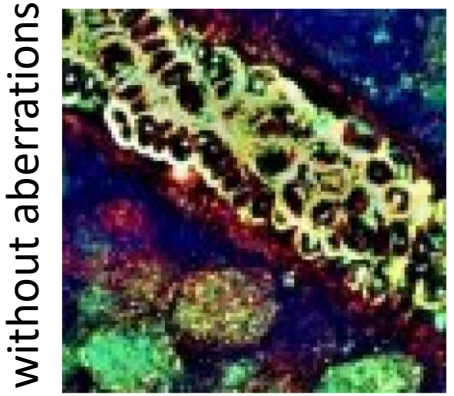

no correction

AO correction

Isoplanatic area (few µm at a depth of 1 l_t)

Adaptive focusing law only valid over a single isoplanatic patch

Introduction: Spatially-distributed aberrations

Institut Langevin
ONDES ET IMAGES

Confocal imaging

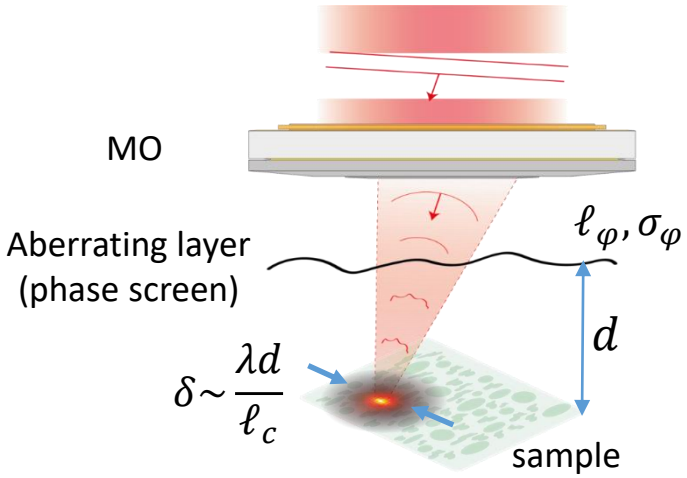

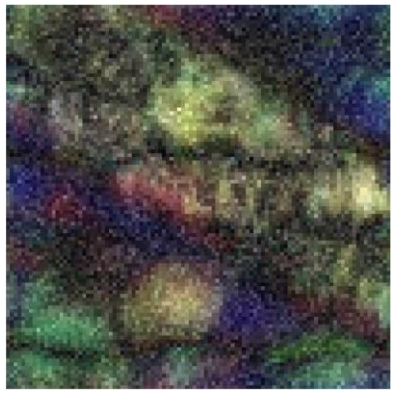

Adaptive optics + Confocal imaging

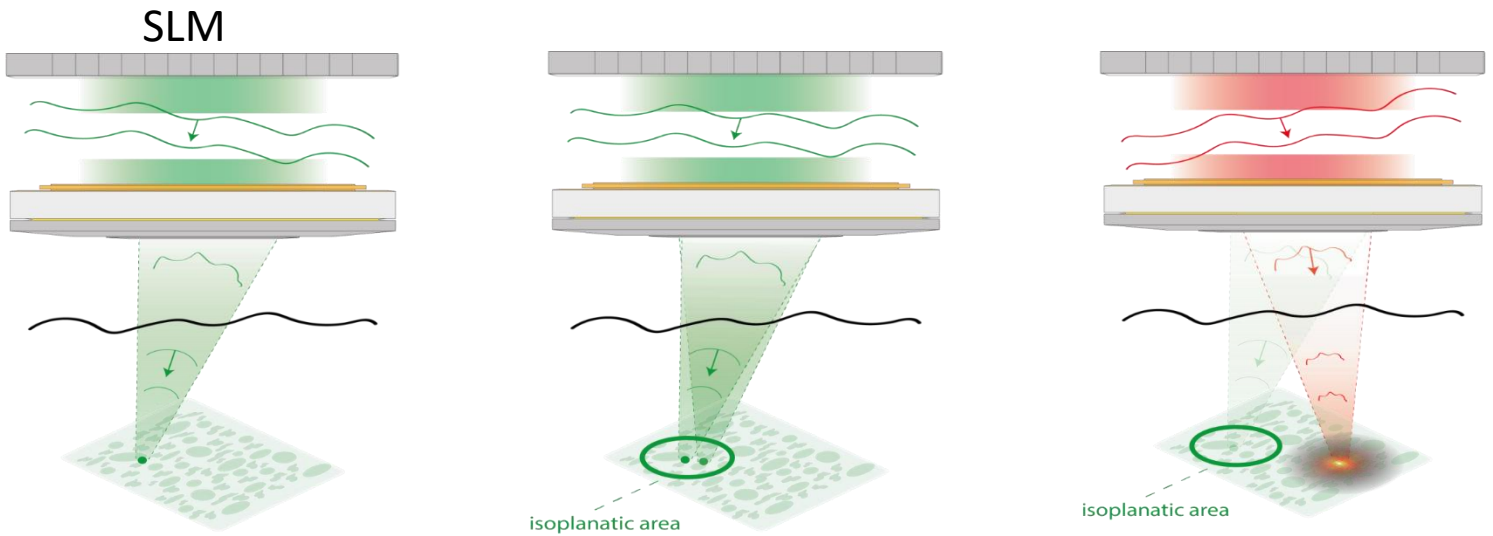

$$\ell_c \sim \frac{2\ell_\varphi}{\sqrt{1+2\sigma_\varphi^2}}$$

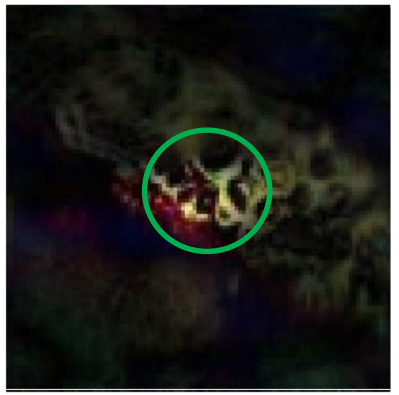

Isoplanatic area
~
Coherence length ℓ_c of the aberrating layer

Adaptive focusing law only valid over a single isoplanatic patch

J. Mertz *et al.*, *Appl. Opt.*, 2015

Introduction: Adaptive optics applied to optical microscopy

Institut Langevin
ONDES ET IMAGES

Broadband light source

Photodetector

M. J. Booth, Phil

rrations

J. Mertz *et al.*, Appl. Opt. , 2015

AO correction

Isoplanatic area (few µm at a depth of 1 l_t)

⊖ Bulky/Complex optical devices
Time/Memory consuming
Limited field-of-view

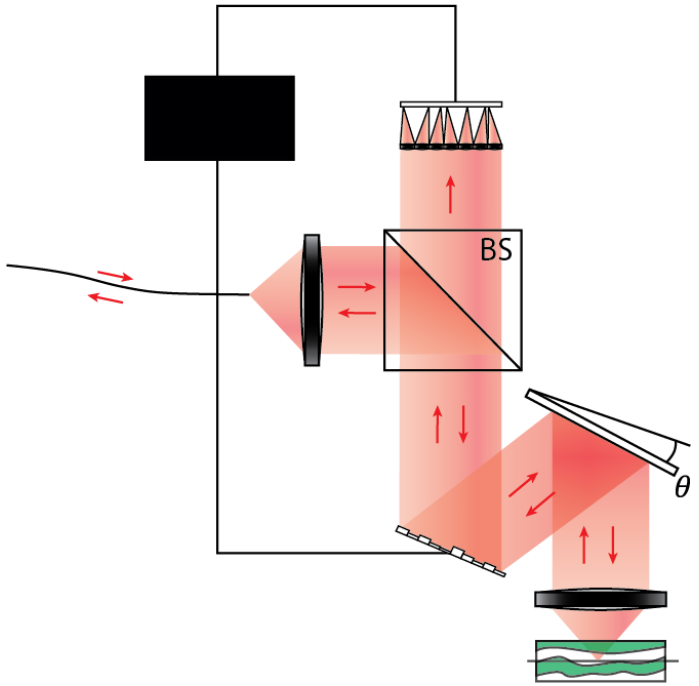

An alternative to adaptive optics?

Introduction: Transmission matrix for optimal focusing

Institut Langevin
ONDES ET IMAGES

Focusing through strongly scattering media

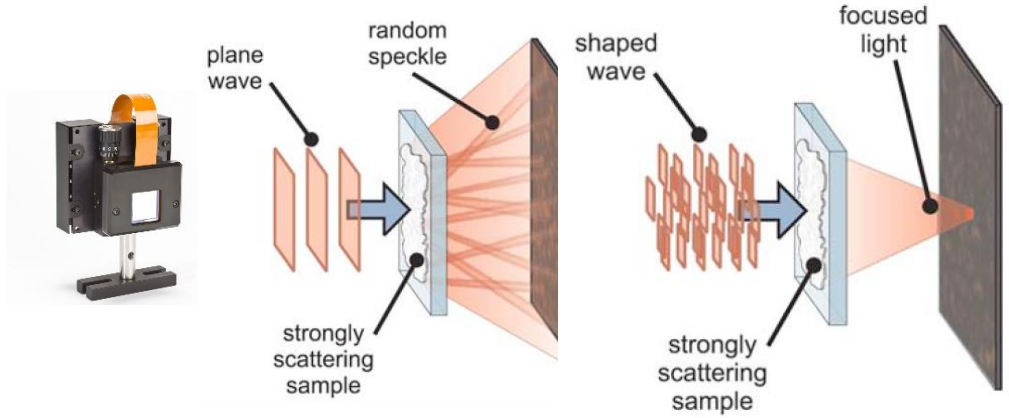

Vellekoop and Mosk, *Opt. Lett.* (2007)

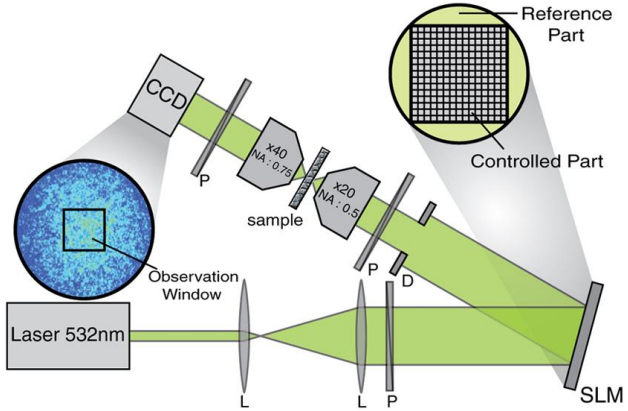

Popoff *et al., Phys. Rev. Lett.* (2010)

Transmission matrix

between the pixels of a SLM and of a CCD camera

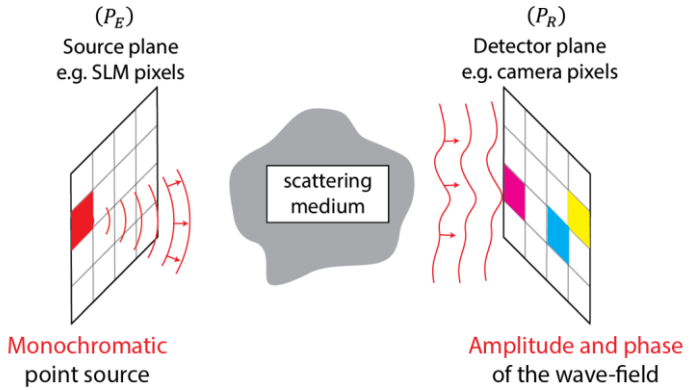

Transmission matrix

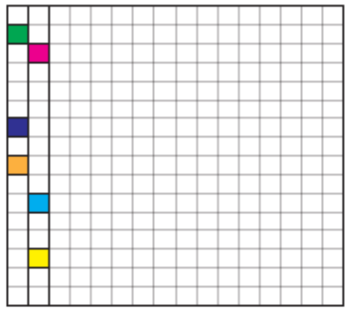

Response matrix

$$\mathbf{T} = \left[T(SLM_i, CCD_j) \right]$$

CCD pixels

$$\begin{pmatrix} t_{1,1} & t_{1,2} & \cdots & t_{1,N} \\ t_{2,1} & & & \\ \vdots & & \ddots & \vdots \\ t_{N,1} & & \cdots & t_{N,N} \end{pmatrix}$$

T contains all the information available on the medium

Introduction: Transmission matrix for optimal focusing

Institut Langevin
ONDES ET IMAGES

Focusing through strongly scattering media

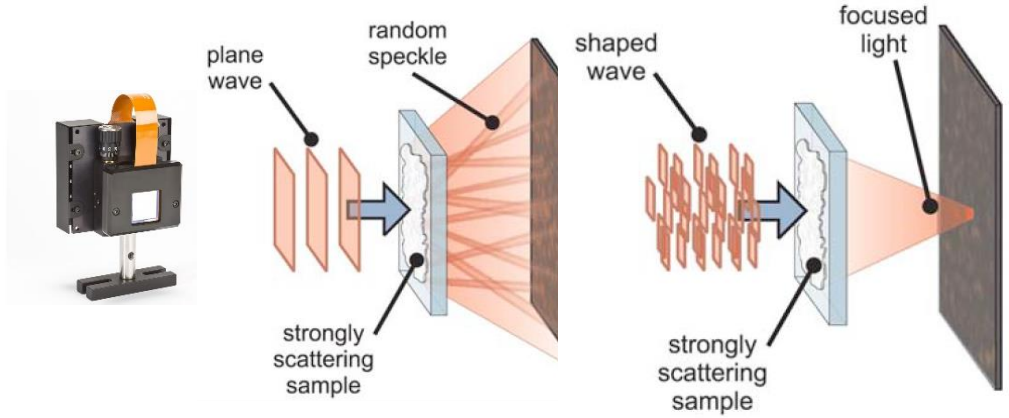

Vellekoop and Mosk, *Opt. Lett.* (2007)

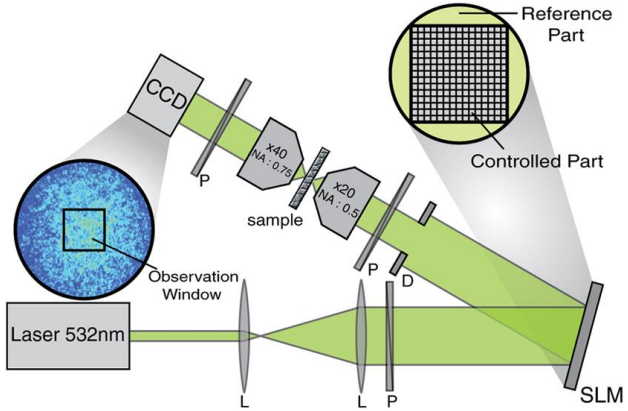

Popoff *et al., Phys. Rev. Lett.* (2010)

Phase conjugation/inversion

T-matrix

Scattering medium = black box

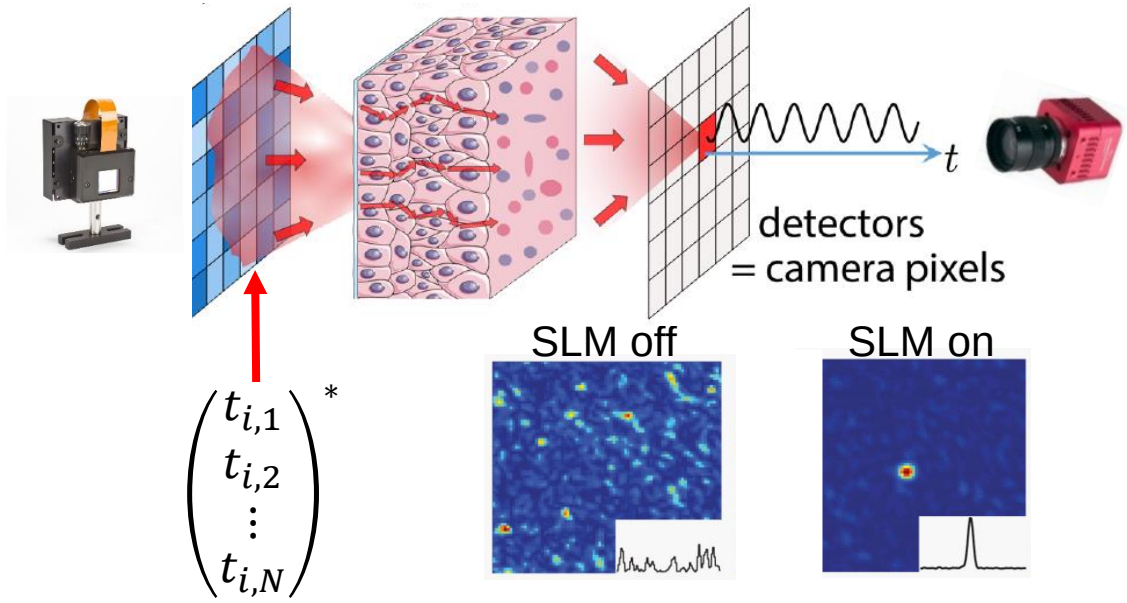

Any turbid medium
can behave as a lens

Introduction: Transmission matrix for imaging?

Institut Langevin
ONDES ET IMAGES

Focusing through strongly scattering media

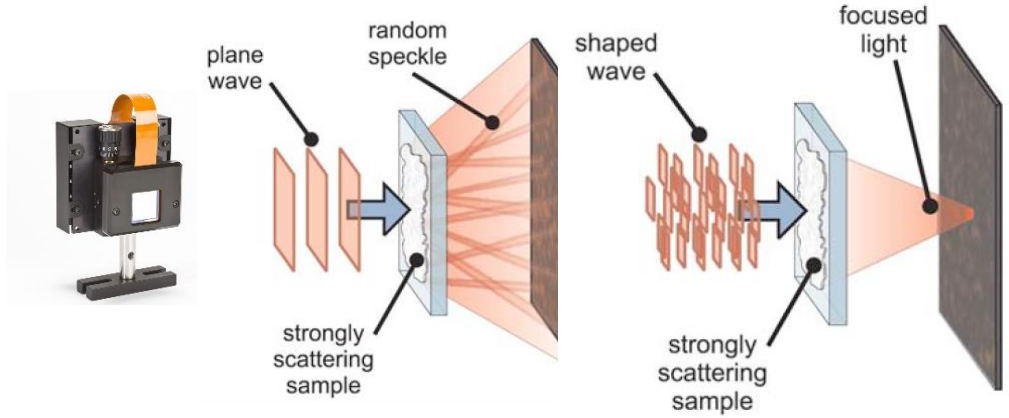

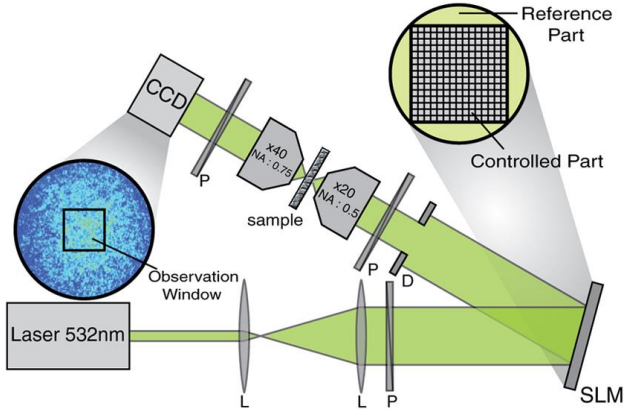

Popoff *et al., Phys. Rev. Lett.* (2010)

HOLY GRAIL FOR IMAGING:

TRANSMISSION MATRIX INSIDE THE MEDIUM

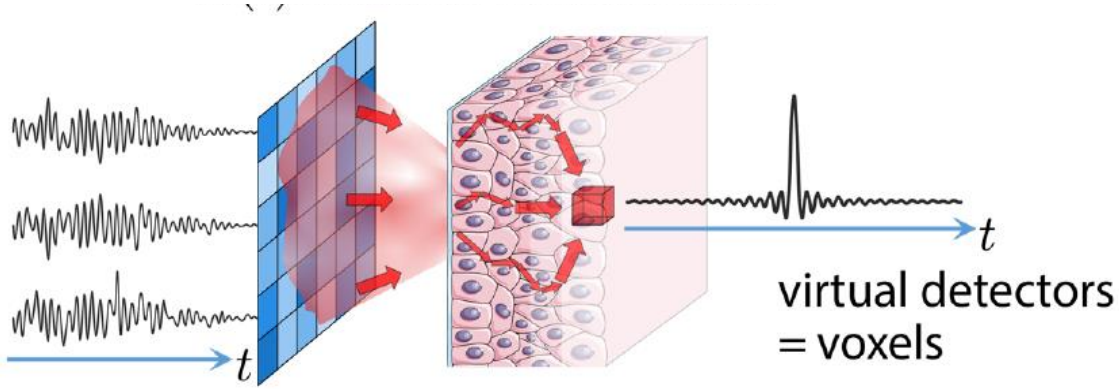

OPEN THE BLACK BOX
BUT
HIGHLY INVASIVE…

Introduction: Reflection matrix for imaging?

Institut Langevin
ONDES ET IMAGES

Reflection matrix:
From ultrasound imaging
to optical microsocpy

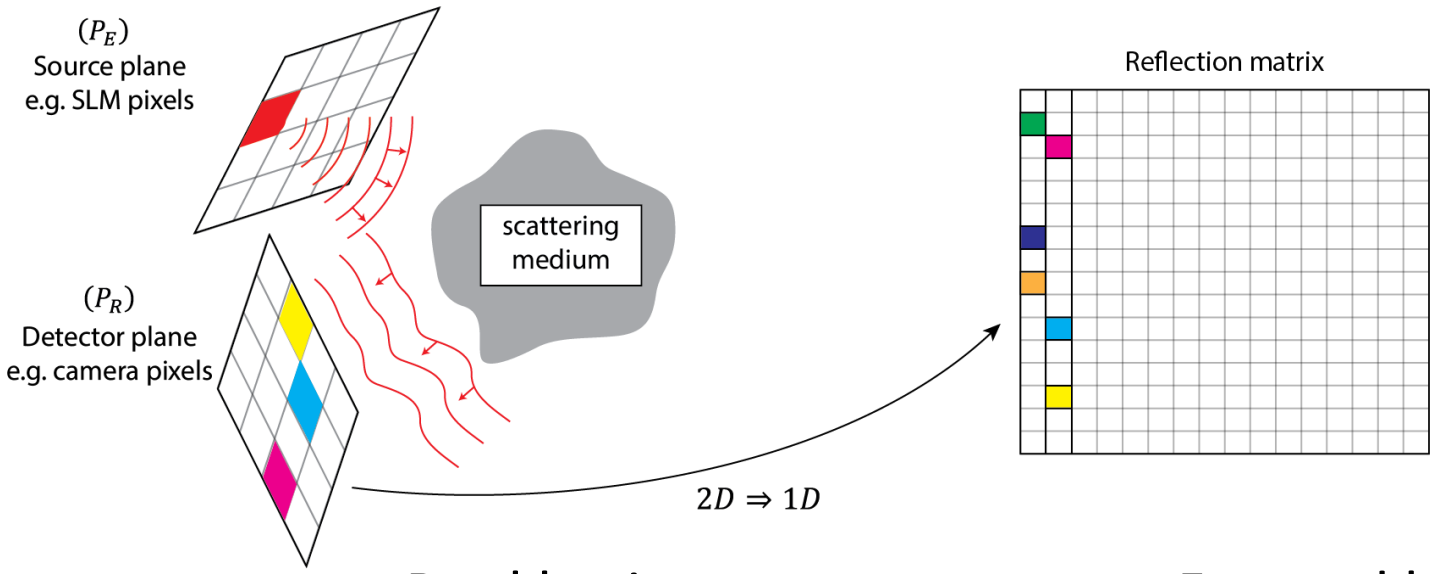

« Far-field » basis (k_{in},k_{out})

S. Kang *et al., Nat. Photon.,* 2015, 2017
M. Kim *et al., Nature Com.*, 2019

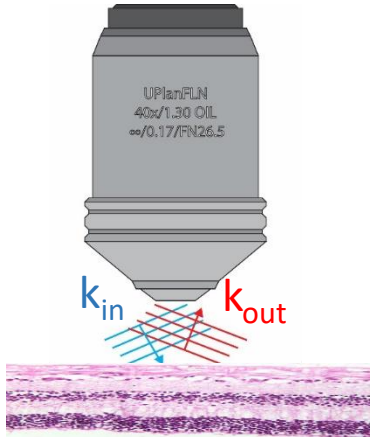

Dual basis (r_{in}, k_{out})

W. Lambert et al., *PNAS* (2020)
A. Badon et al., *Sci. Adv.* (2020)

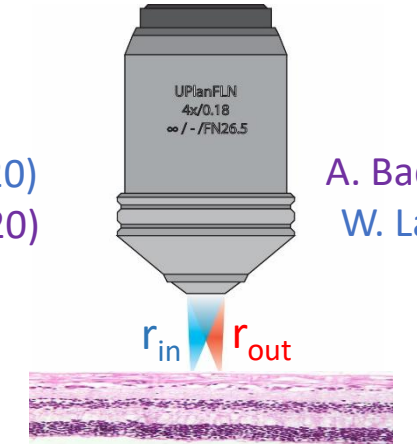

Focused basis (r_{in}, r_{out})

A. Badon *et al., Sci. Adv.* (2016)
W. Lambert *et al., PRX* (2020)

OBJECTIVE: Retrieve the TRANSMISSION matrix INSIDE the medium
from a REFLECTION matrix recorded OUTSIDE?

Focused Reflection Matrix

A coherent proof-of-concept

Coherent optical system: Time-gated reflection matrix

Amaury Badon

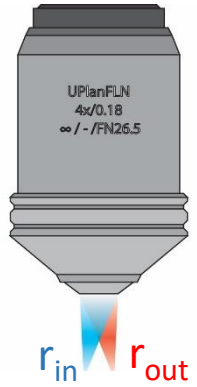

SLM diffraction grating

Coherence time gating / Phase shifting interferometry

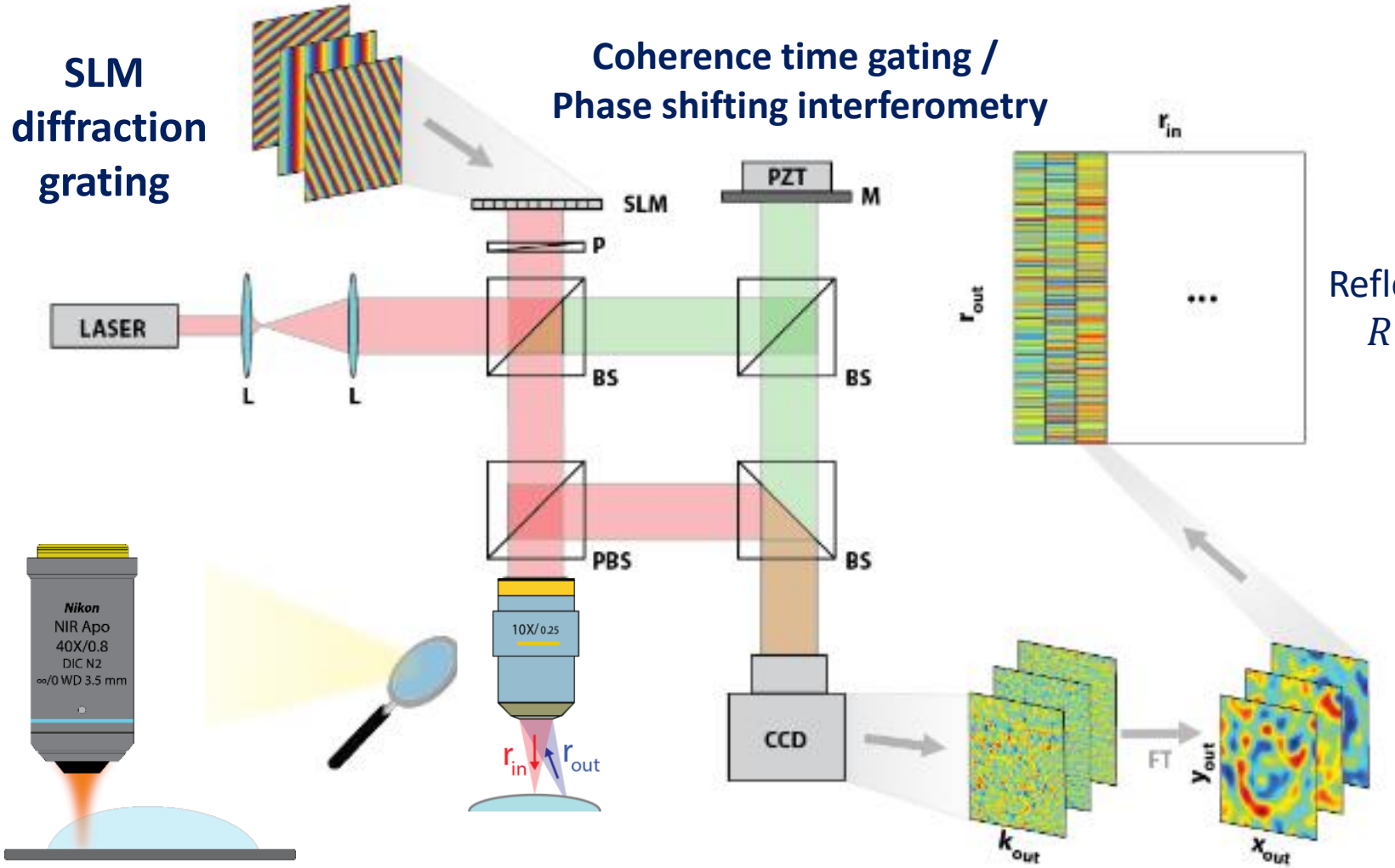

Reflection matrix

$R(\mathbf{r}_{in}, \mathbf{r}_{out})$

A. Badon *et al.*, *Sci. Adv.* **2**, e1600370 (2016).

Focused reflection matrix

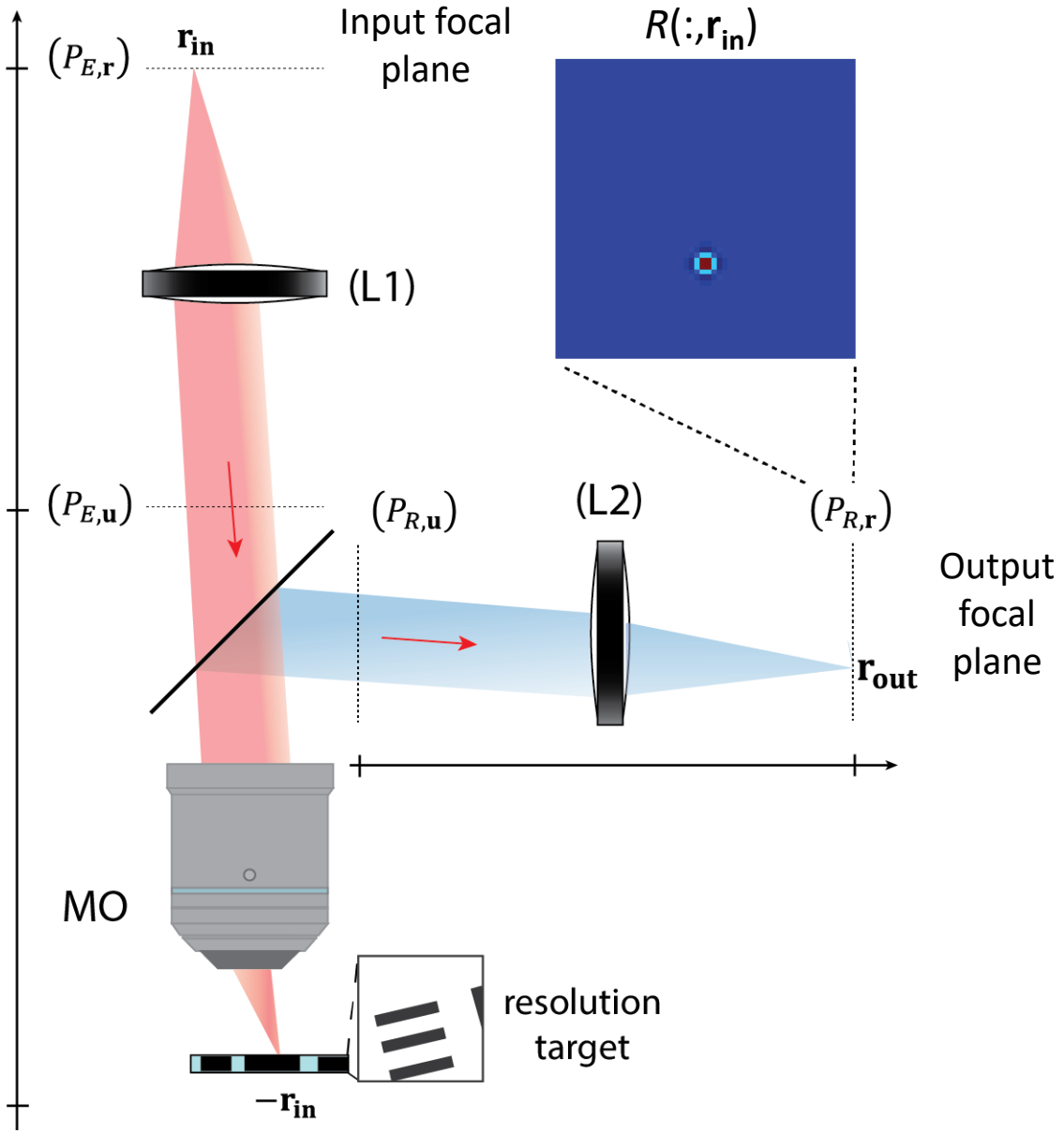

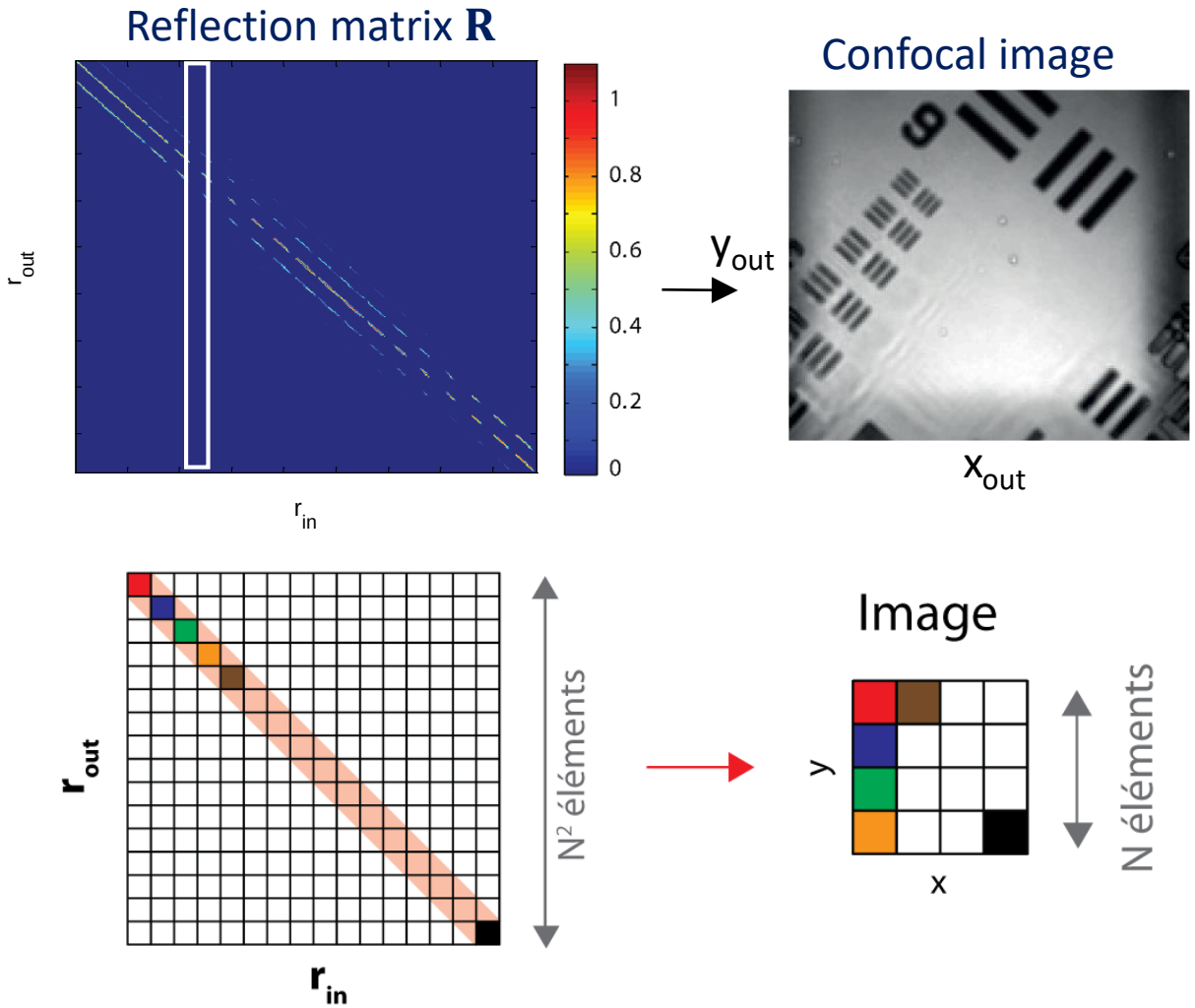

Impulse responses between $\mathbf{r_{in}}$ and $\mathbf{r_{out}}$ (cross-talk)
4D-matrix, but concatenated in 2D for sake of simplicity

A. Badon *et al., Sci. Adv.* **2**, e1600370 (2016).

Focused reflection matrix

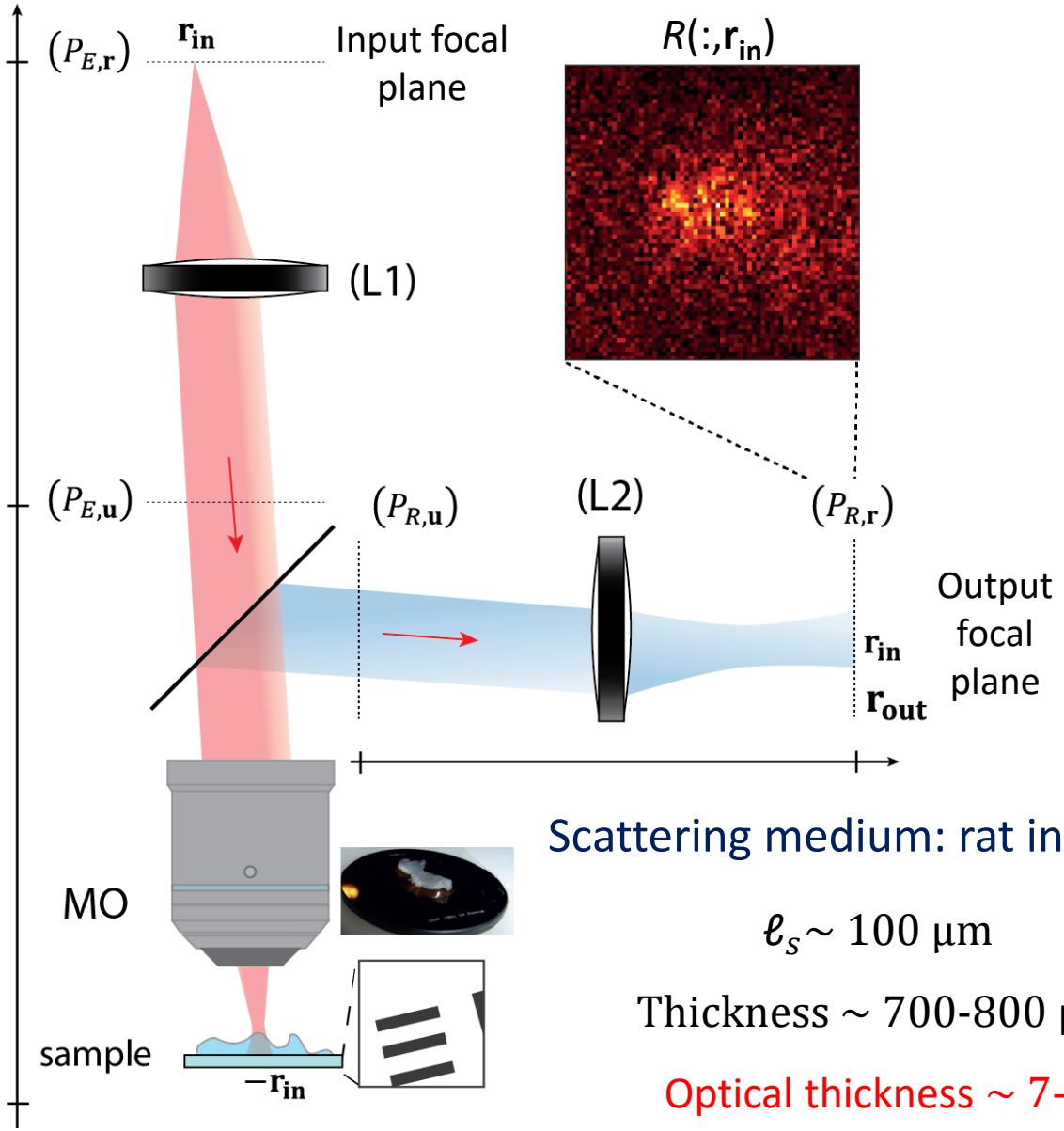

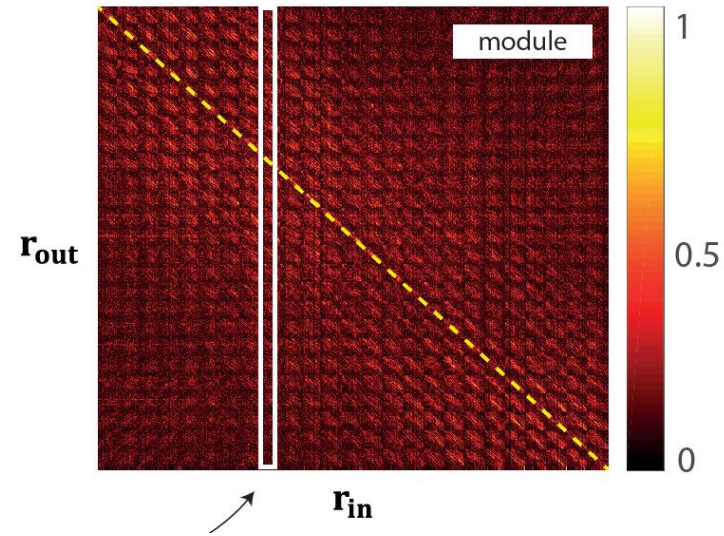

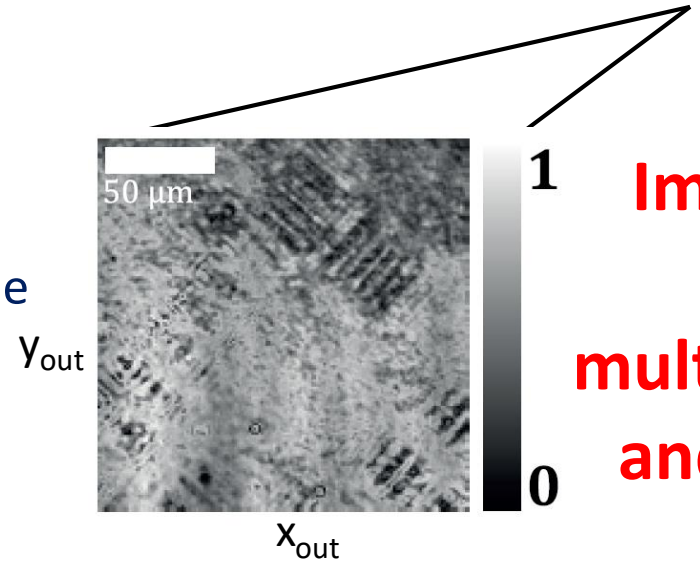

Scattering medium: rat intestine

$\ell_s \sim 100$ µm

Thickness ~ 700-800 µm

Optical thickness ~ 7-8

Imaging failure because of multiple scattering and aberrations

A. Badon *et al., Sci. Adv.* **2**, e1600370 (2016).

Distorsion Matrix

A coherent proof-of-concept

Dual reflection matrix

Amaury Badon

Victor Barolle

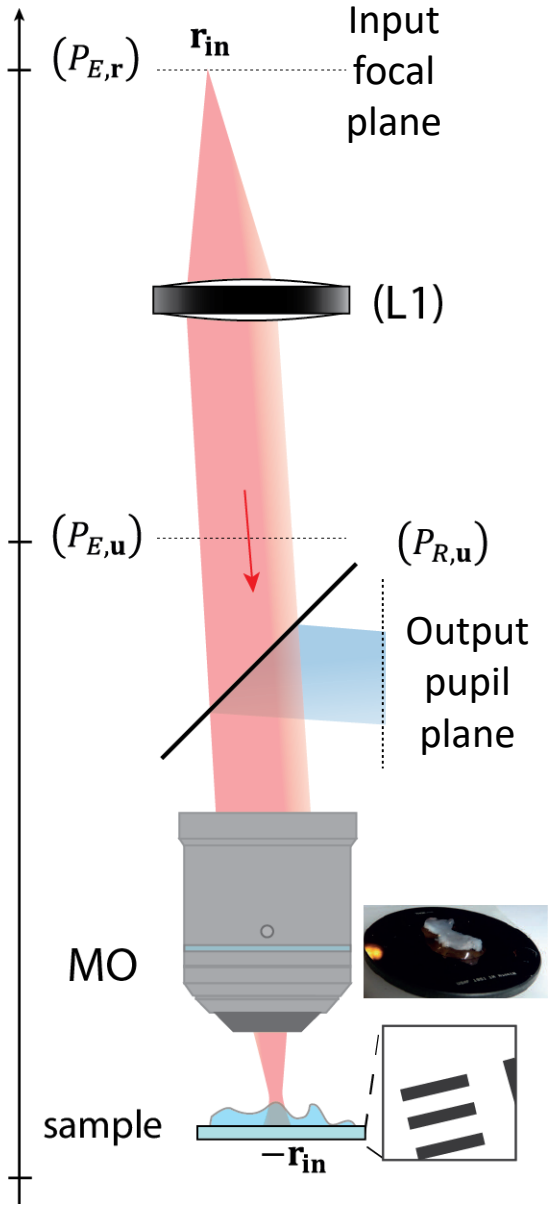

Dual bases: Input focusing ↔ Output pupil

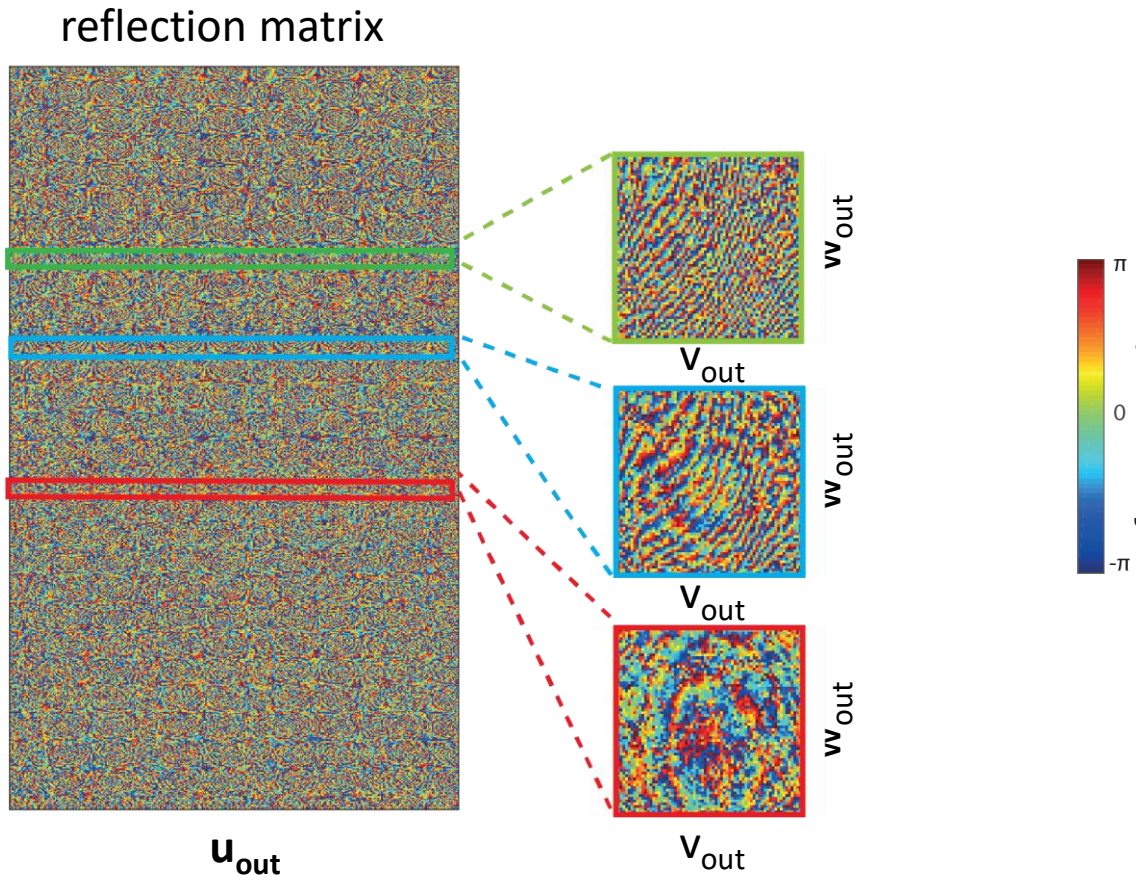

No correlations between the lines/columns of R

A. Badon *et al., Sci. Adv.* **6,** eaay7170 (2020)

Distortion matrix concept

Institut Langevin
ONDES ET IMAGES

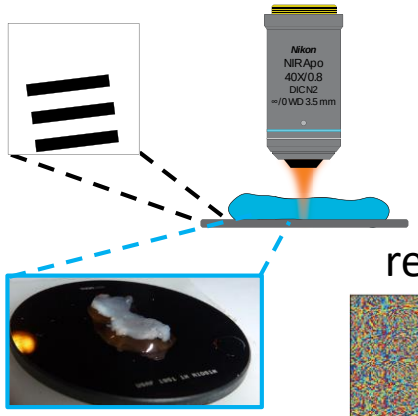

Trick: Extract the distorted component of the reflected wave-front

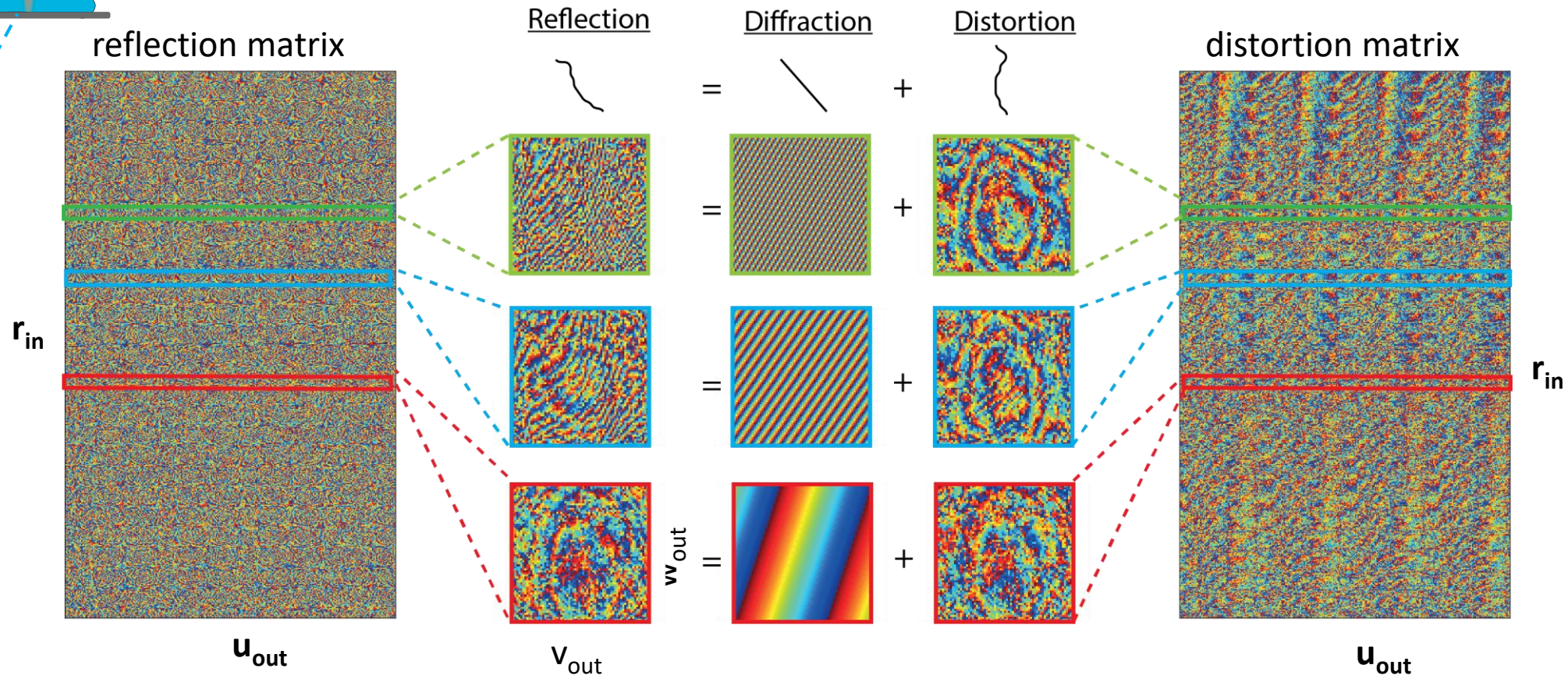

The distortion matrix reveals the hidden correlations of the reflected wave-field

A. Badon *et al., Sci. Adv.* **6,** eaay7170 (2020)

Covariance matrix / Time-reversal operator

Institut Langevin
ONDES ET IMAGES

Correlations beween input focusing illuminations shall yield the aberration transmittance

pupil aberration transmittance
$\hat{H}_{out}(\mathbf{u_{out}})$

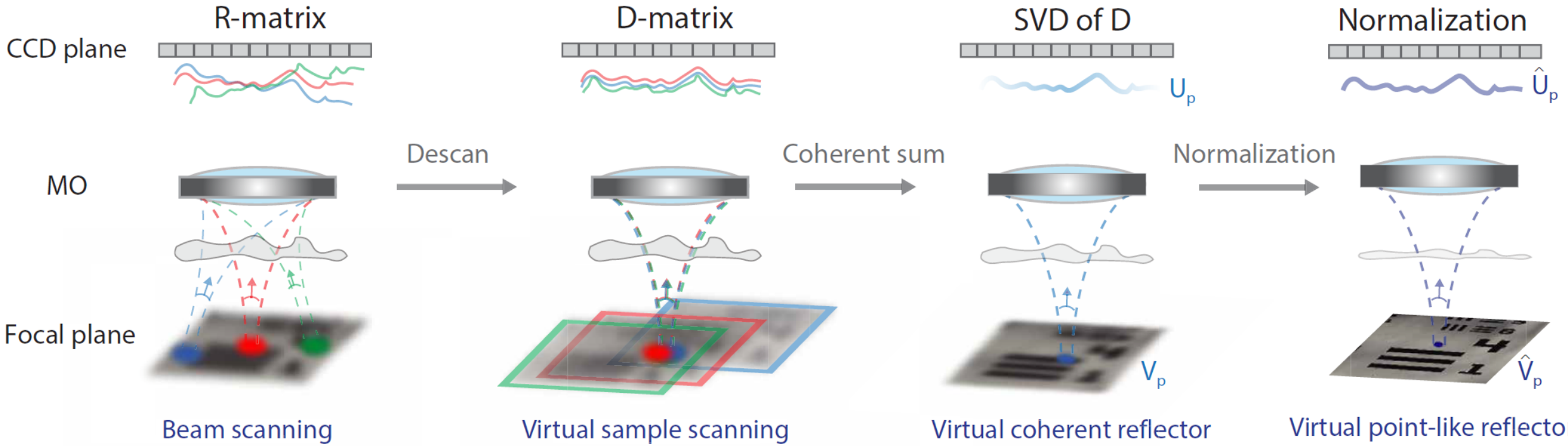

$\rho(\mathbf{r_{in}})H_{in}(\mathbf{r_{in}})$

reflectivity × input PSF

But need to average over a suffiently large number of input focusing points : $N_{in} \gg (\delta_{in}/\delta_0)^2$

A. Badon *et al., Sci. Adv.* **6,** eaay7170 (2020)

Singular value decomposition of the D-matrix

Institut Langevin
ONDES ET IMAGES

In practice, a singular value decomposition of **D** is performed to **remove diffuse multiple scattering** and **noise**

$$\mathbf{D} = \sum_{p=1}^{N} \sigma_p \mathbf{U_p} \mathbf{V_p}^{\dagger}$$

Singular values

Output singular vectors

Input singular vectors

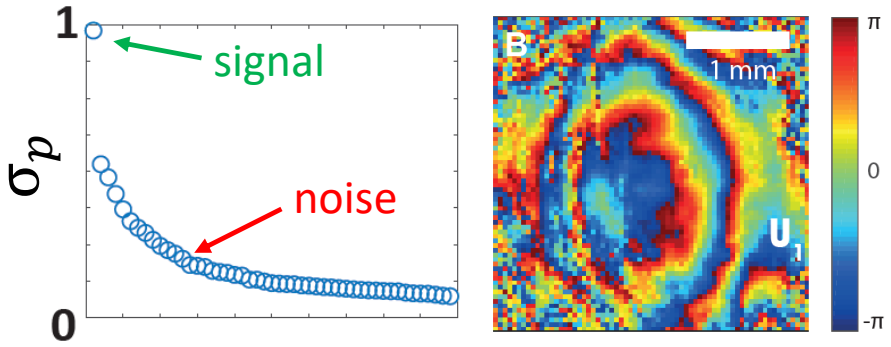

$\mathbf{U_1}$ (phase)

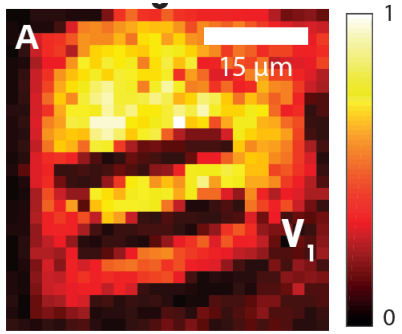

$\mathbf{V_1}$ (modulus)

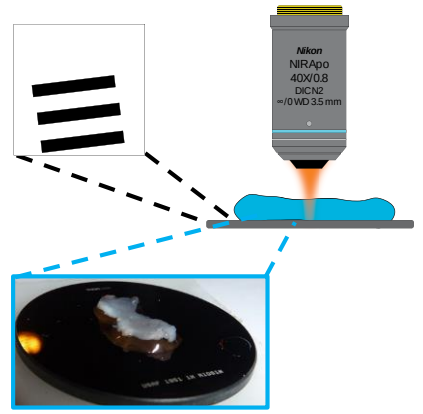

Isoplanatic case

Signal subspace of rank 1

U_1: Pupil transmittance

V_1: Reflectivity × input PSF

A. Badon *et al.*, *Sci. Adv.* **6,** eaay7170 (2020)

Conventional vs Matrix imaging

Institut Langevin
ONDES ET IMAGES

Conventional imaging

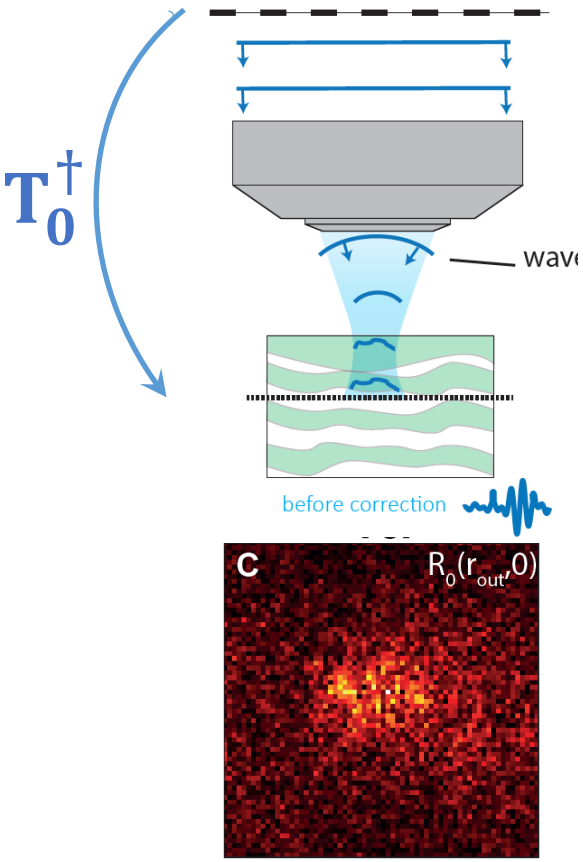

PSF width:
$\delta \sim 15$ µm

Free space T-matrix: $\mathbf{T_0}$ (FT operator)

T-matrix estimator: $\hat{\mathbf{T}} = \mathbf{T_0} \circ \mathbf{U_1}$

Focused R-matrix: $\mathbf{R_F} = \hat{\mathbf{T}}^\dagger \times \mathbf{R}$

Full-field image

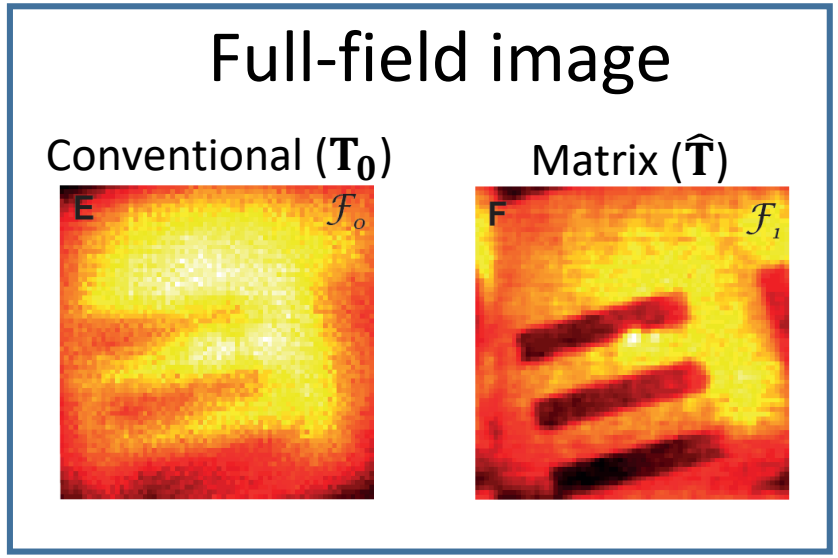

Strehl ratio increased by a factor 150
Resolution improved by a factor 15

Matrix imaging

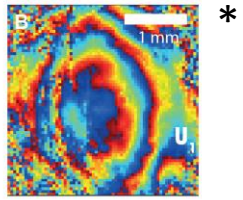

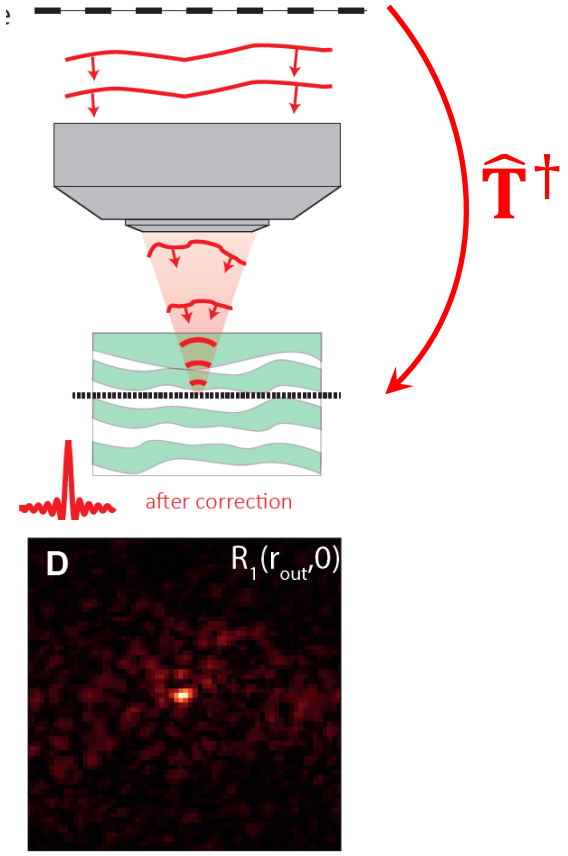

$\delta \sim 0.9$ µm
($\delta_{th} \sim 0.7$ µm)

Imaging through an opaque cornea: Beyond isoplanicity

Institut Langevin
ONDES ET IMAGES

700-µm-thick edematous primate cornea ($\ell_s \sim 70$ µm)
Optical thickness $\sim 10\ell_s$

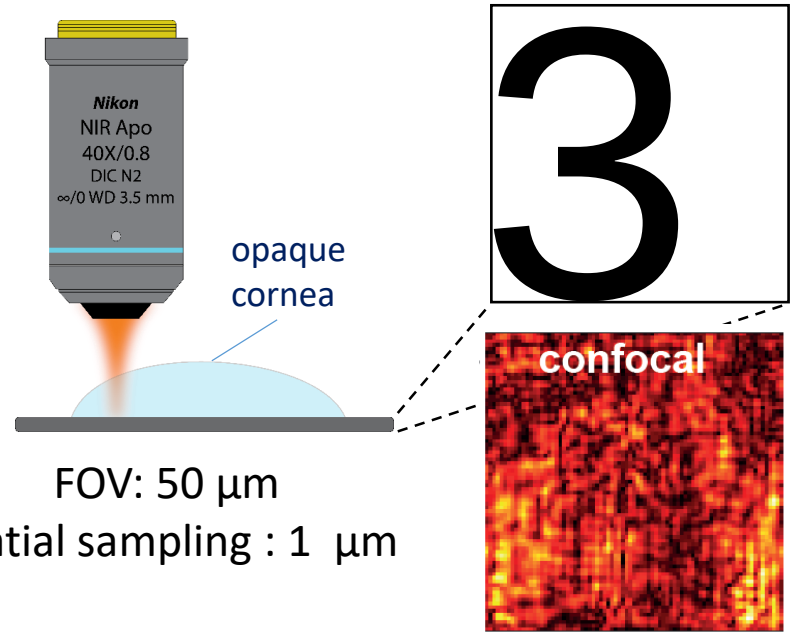

FOV: 50 µm
Spatial sampling : 1 µm

Singular value decomposition of **D**

$$\mathbf{D} = \sum_p \sigma_p \mathbf{U_p} \mathbf{V_p}^\dagger$$

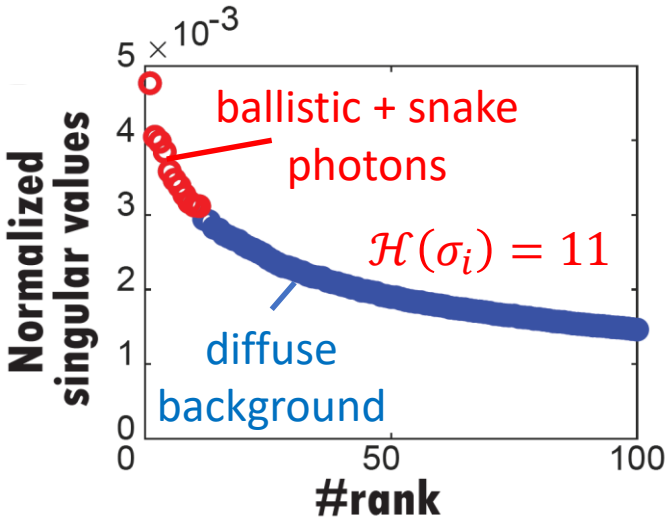

Effective rank of the imaging process = Entropy of singular values

$$\mathcal{H}(\sigma_i) = -\sum_{i=1}^{N} \sigma_i^2 \log_2(\sigma_i^2)$$

Entropy of D scales as the number of isoplanatic patches

A. Badon *et al.*, *Sci. Adv.* **6,** eaay7170 (2020)

Imaging through an opaque cornea

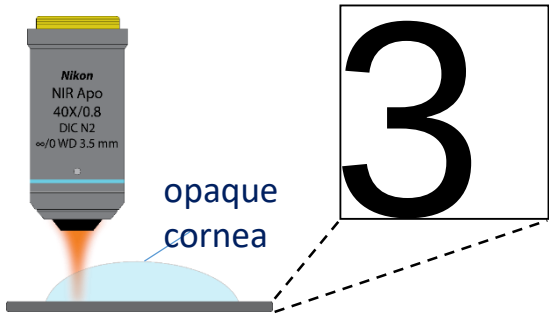

The SVD of **D** decomposes the field-of-view onto a set of orthogonal isoplanatic modes ($\mathbf{V_p}$), each one being associated with a different transmittance ($\mathbf{U_p}$) in the pupil plane

A. Badon *et al., Sci. Adv.* **6,** eaay7170 (2020)

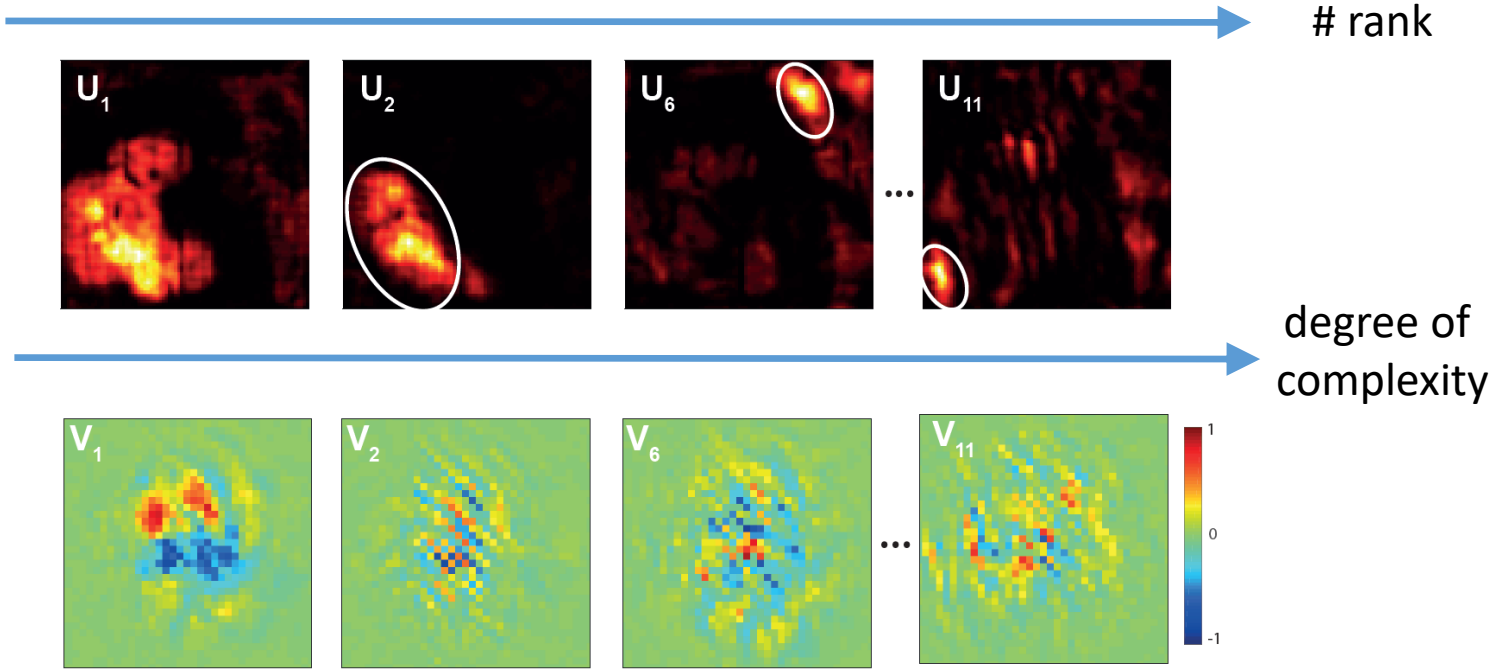

Adequate basis to characterize and quantify high-order aberrations

Confocal vs Matrix imaging

Institut Langevin
ONDES ET IMAGES

Coherent combination of pupil singular vectors: $\widehat{\mathbf{T}} = \mathbf{T_0} \circ \sum_{p=1}^{\mathcal{H}(\sigma_i)} \mathbf{U_p^\dagger}$

Conventional imaging

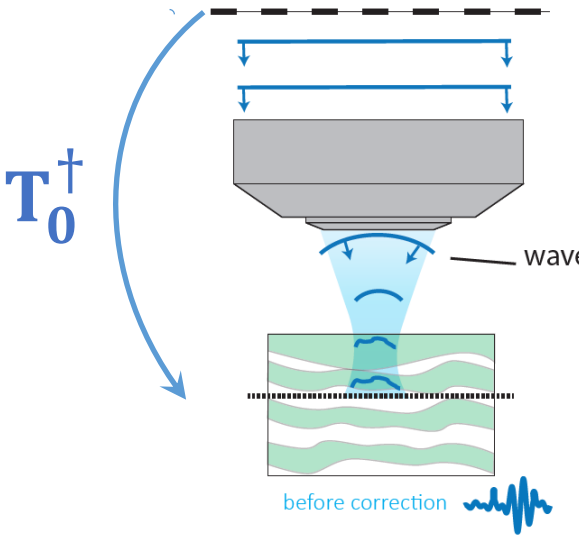

Adapted confocal images

Confocal ($\mathbf{T_0}$)

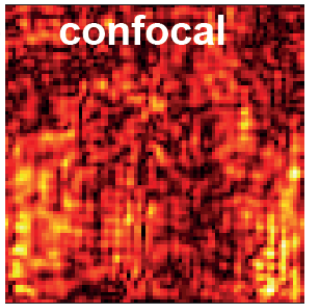

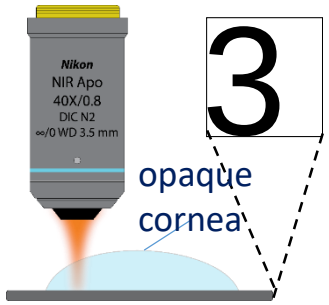

Matrix ($\widehat{\mathbf{T}}$)

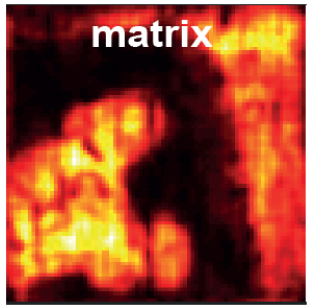

Strehl ratio increased by a factor 230

Matrix imaging

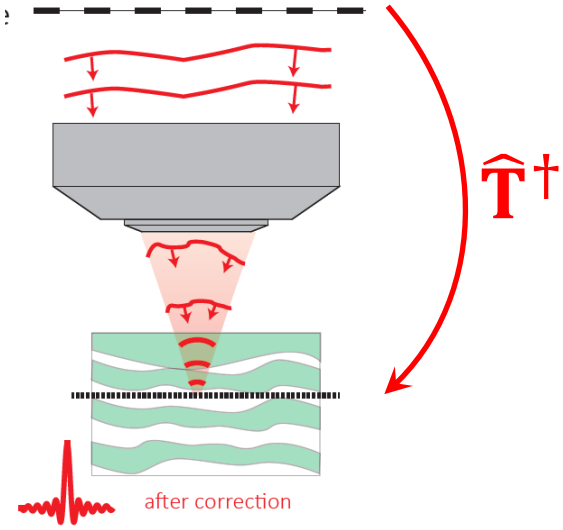

Full-field aberration correction (beyond the isoplanatic hypothesis)

A. Badon *et al., Sci. Adv.* **6,** eaay7170 (2020)

Conclusion

Institut Langevin
ONDES ET IMAGES

Deep matrix imaging:

Correlation-based discrimination between
- single scattering paths
- forward multiple scattering paths
- random walks

Computational approach (post-processing)
Overcome the intrinsic limit of adaptive optics (isoplanicity)
Penetration depth > 10 l_s

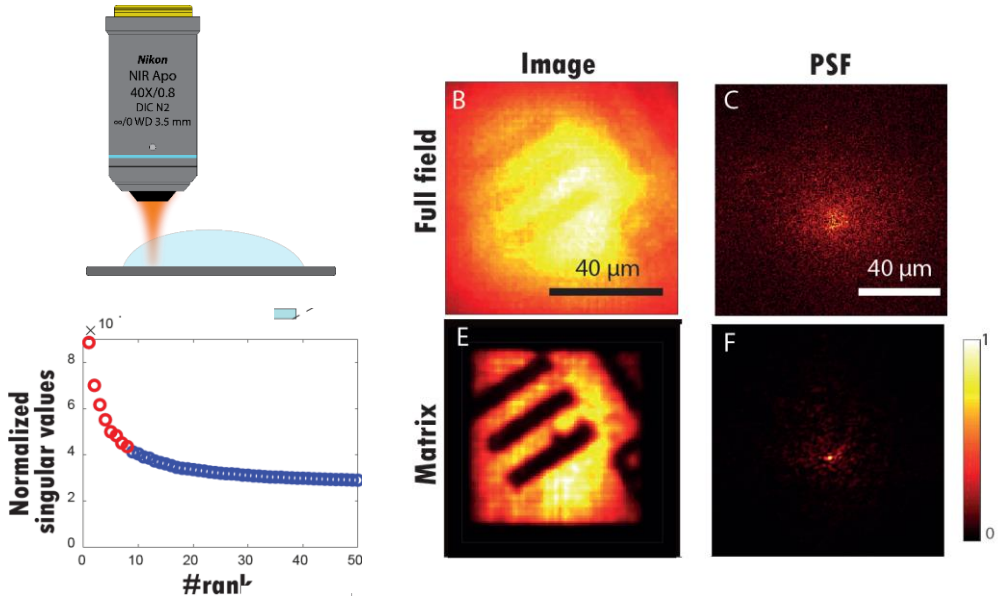

Coherent optical system:

Academic proof-of-concept
Invasive - Scanning technique
Limited FOV (~10^3 pixels) / Long acquisition time
Moderate axial sectioning (~10 µm)
Only 2D imaging of specular reflectors so far…

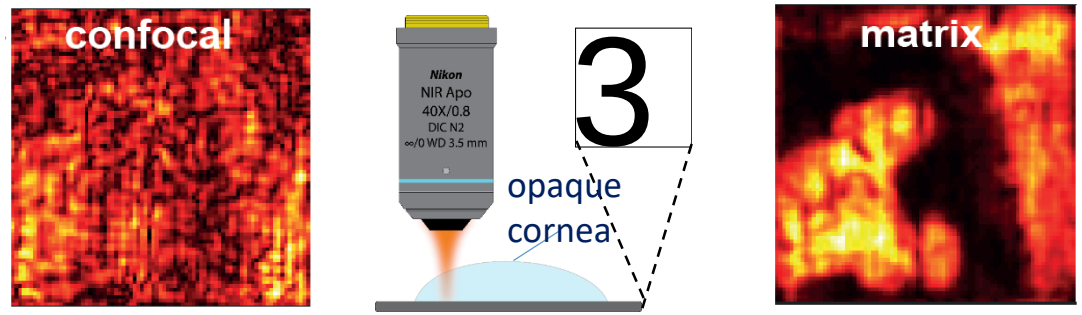

A. Badon *et al., Sci. Adv.* **6,** eaay7170 (2020)

Passive matrix imaging

An optical proof-of-concept

Passive matrix imaging: Full-field OCT

Institut Langevin
ONDES ET IMAGES

Incoherent optical system derived from full-field optical coherence tomography

Non-invasive
Full-field configuration
Huge FOV (10^9 voxels) / Moderate acquisition time
Excellent lateral and axial resolution


Victor Barolle


Paul Balondrade


Ulysse Najar

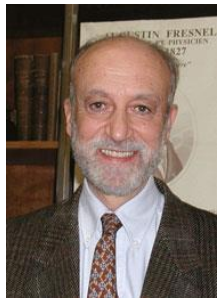
A. C. Boccara

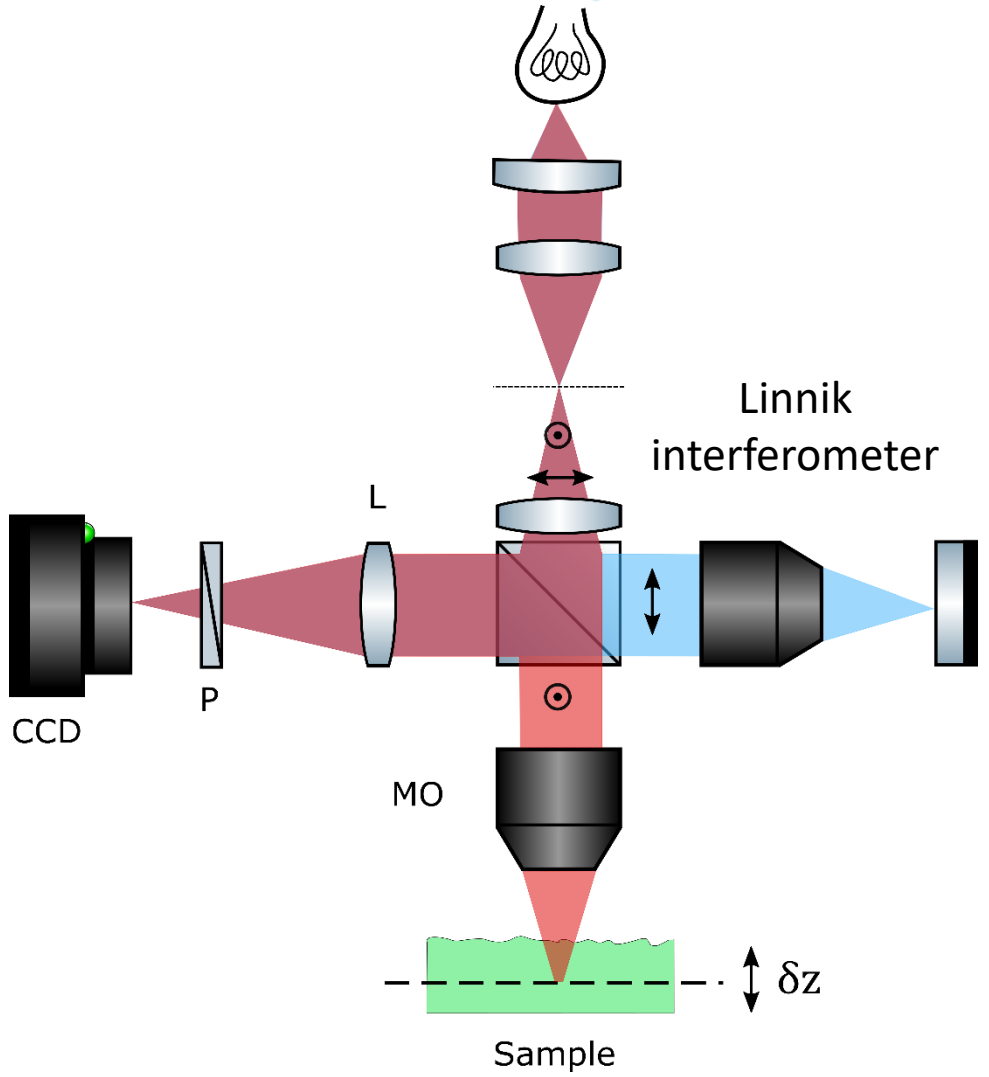

E. Beaurepaire, A. C. Boccara, M. Lebec,
L. Blanchot, and H. Saint-Jalmes, Opt. Lett., 1998

Full-field optical coherence tomography

Institut Langevin
ONDES ET IMAGES

Barolle et al., Opt. Express, 2021

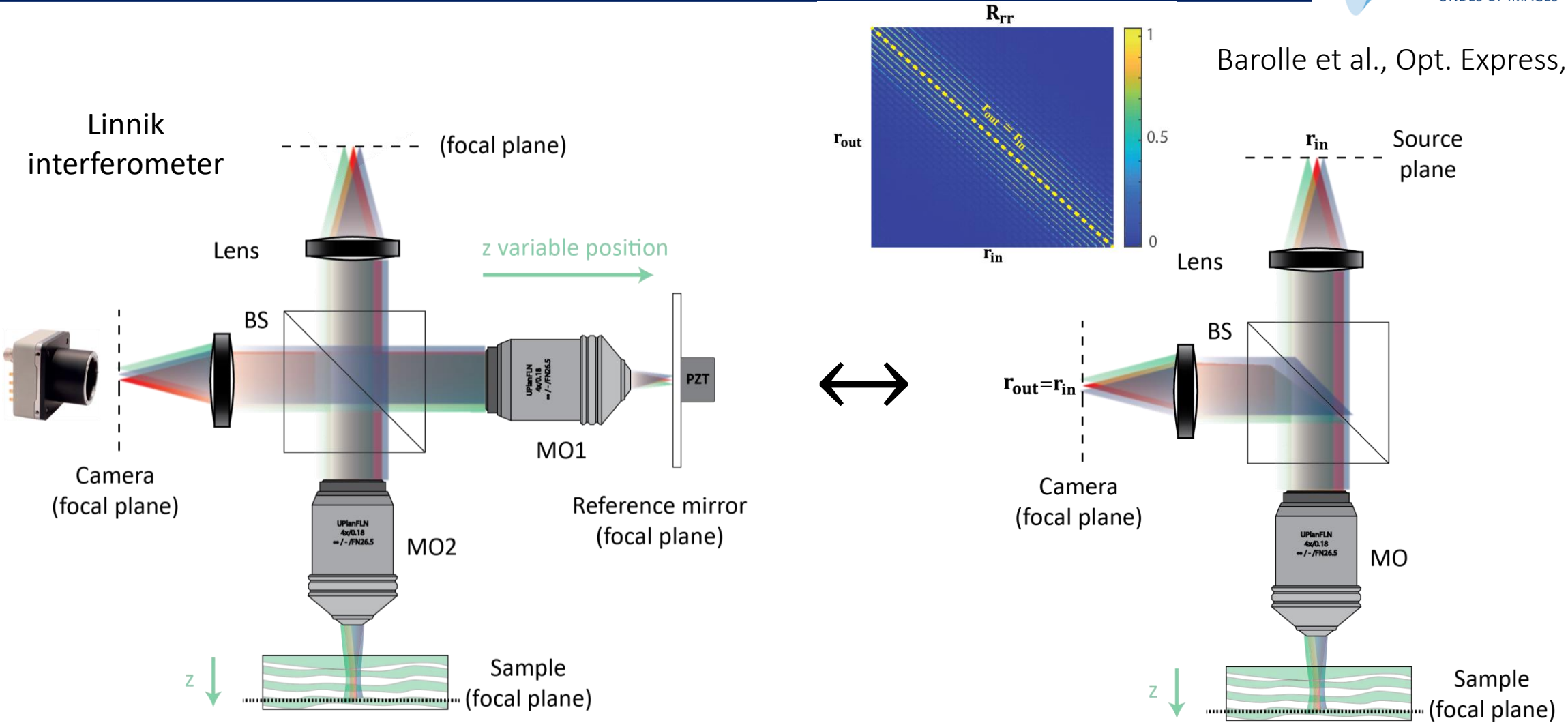

Parralel measurement of an « en-face » confocal image,
i.e whole diagonal of the reflection matrix ($r_{in}=r_{out}$)

Matrix approach of Full-field OCT

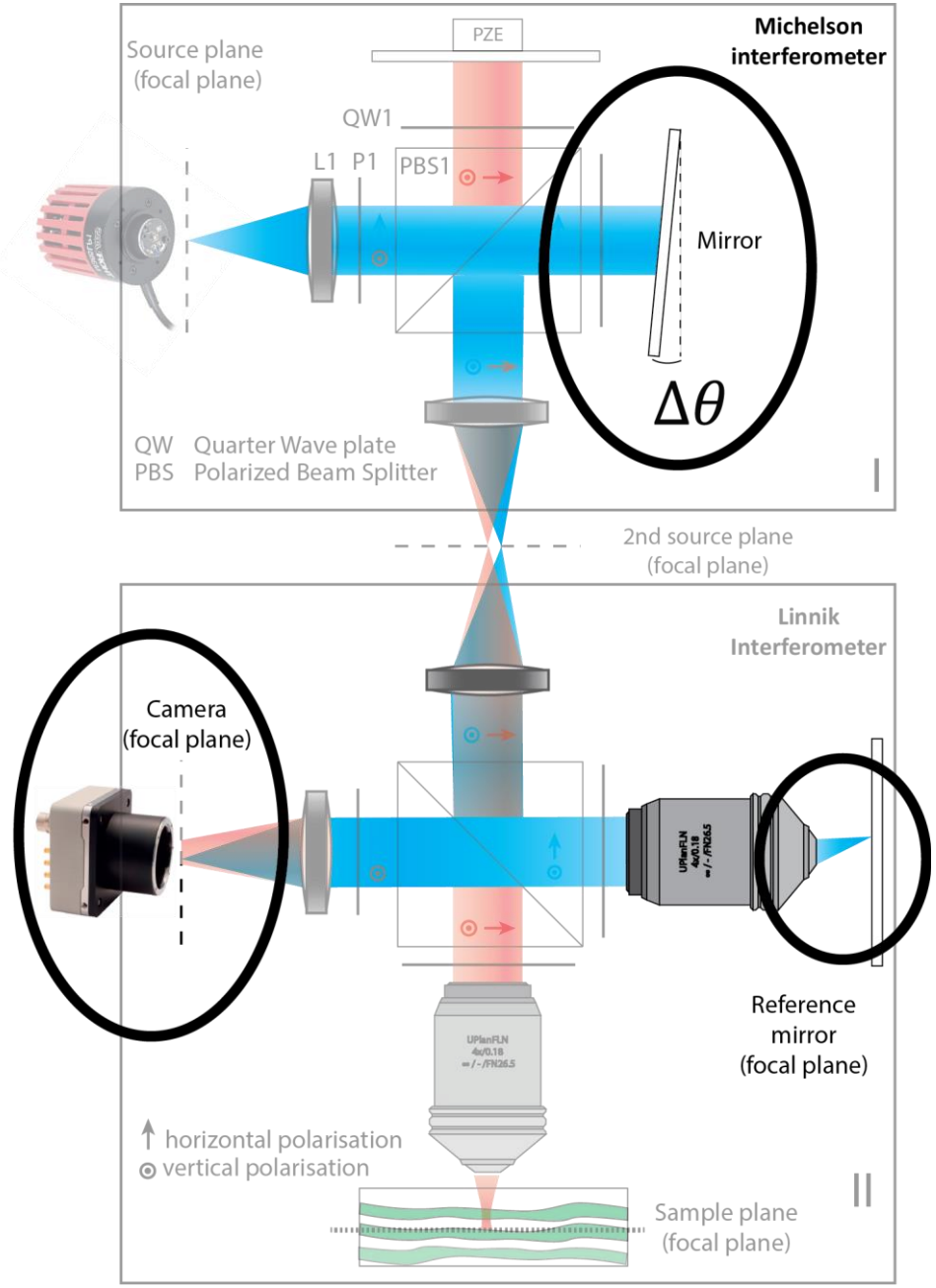

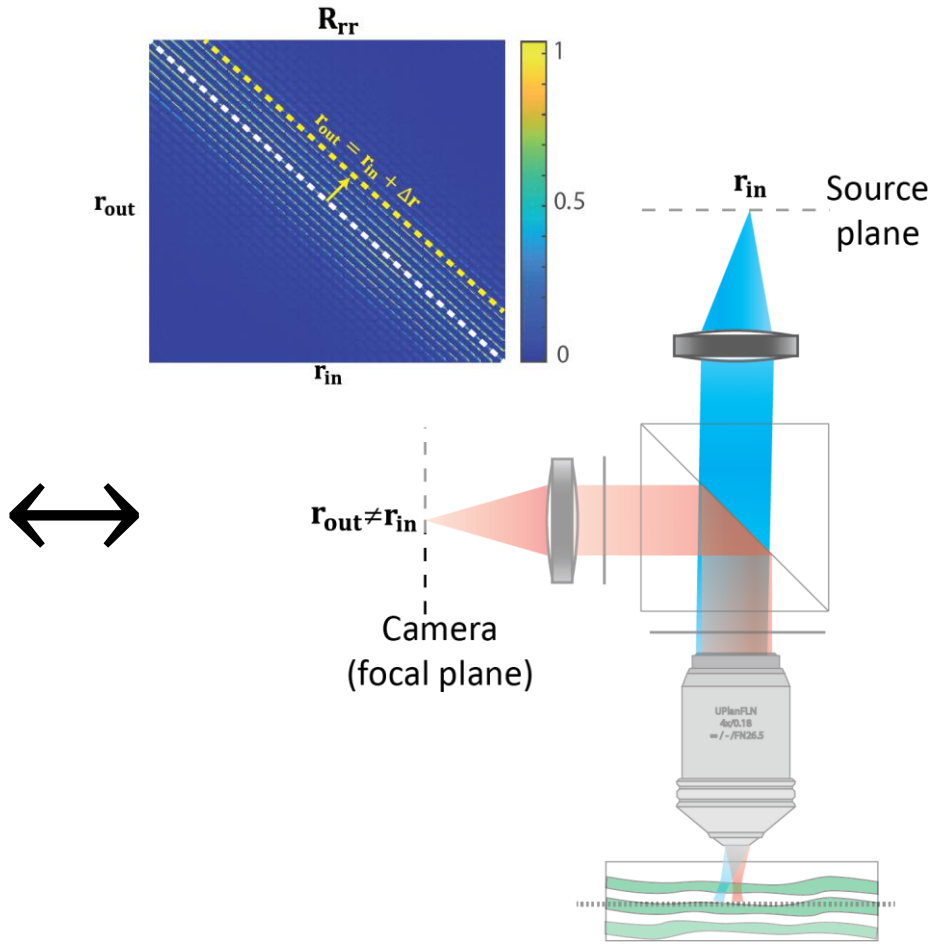

Parallel measurement of the R-matrix sub-diagonals

(r_{in}-r_{out}= Δr)

Passive matrix imaging

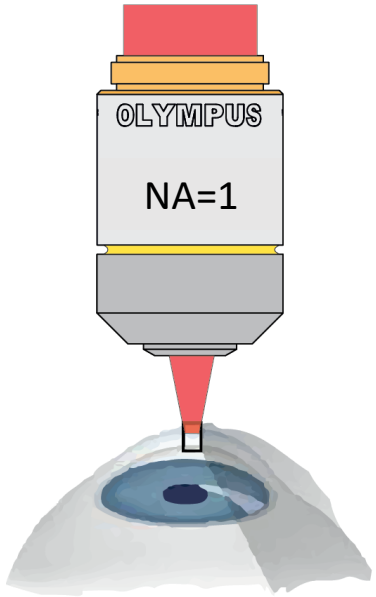

300-µm-thick edematous human cornea

Field-of-view: 200×200 µm^2

High dimension reflection matrix

$10^3 \times 10^3$ **pixels**

descanned reflection matrix

$R(\mathbf{r'}_{\mathbf{out}}|\mathbf{r}_{\mathbf{in}})$

$\mathbf{r}_{\mathbf{in}}$

$\mathbf{r'}_{\mathbf{out}} = \mathbf{r}_{\mathbf{out}} - \mathbf{r}_{\mathbf{in}}$

$R(\mathbf{r'}_{\mathbf{out}} = 0|\mathbf{r}_{\mathbf{in}})$

en-face OCT (confocal) image

$\mathbf{y}_{\mathbf{out}}$

50 µm

$\mathbf{x}_{\mathbf{out}}$

$\sum_{\mathbf{r}_{\mathbf{in}}} |R(\mathbf{r'}_{\mathbf{out}}|\mathbf{r}_{\mathbf{in}})|^2$

averaged PSF in reflection

1 µm

$\mathbf{y}_{\mathbf{out}} - \mathbf{y}_{\mathbf{in}}$

$\mathbf{x}_{\mathbf{out}} - \mathbf{x}_{\mathbf{in}}$

Intensity (dB)

0 -5 -10 -15 -20 -25 -30

1 0.9 0.8 0.7 0.6 0.5 0.4 0.3 0.2 0.1 0

Transmission matrix

Local distortion matrix analysis

Original confocal image

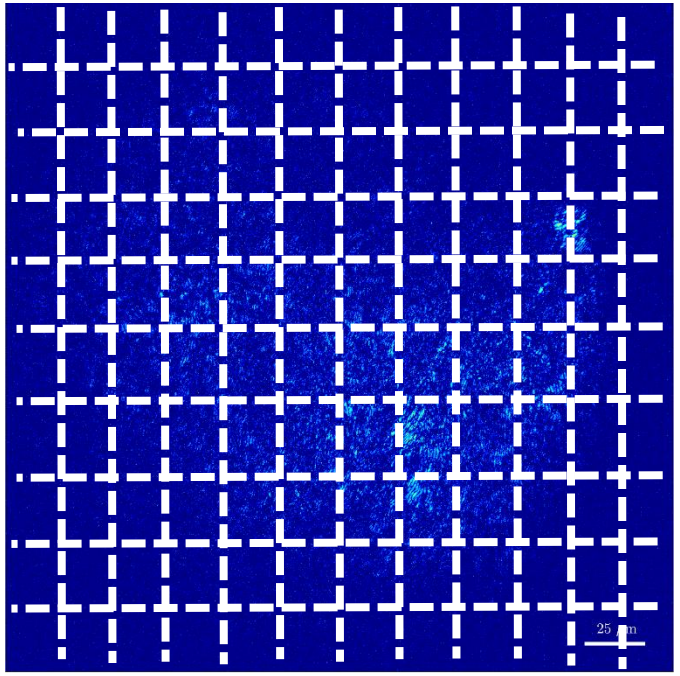

Isoplanatic patches
($\sim 10 \times 10\ \mu m^2$)

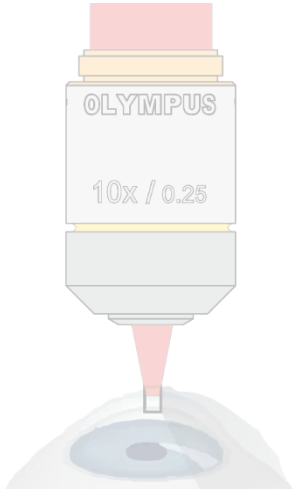

200 µm - depth

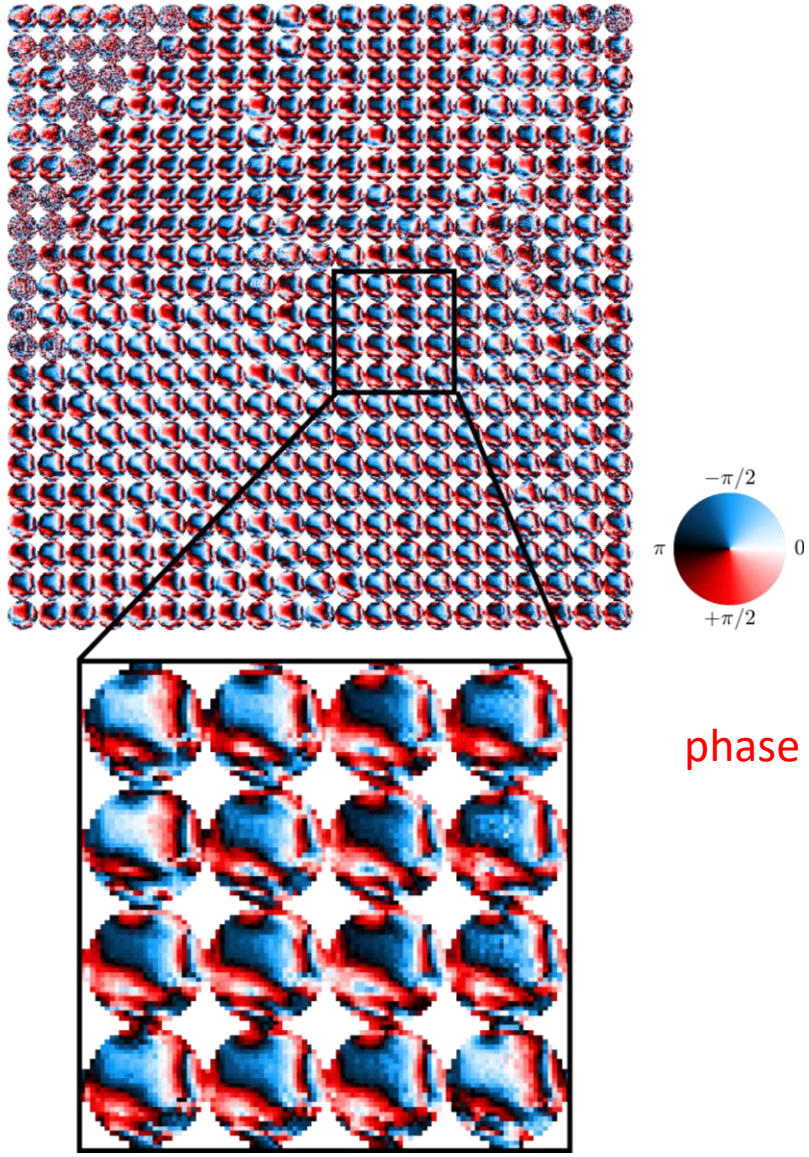

phase

The isoplanatic assumption is everything but true in this configuration

Passive matrix imaging

Transmission matrix correction

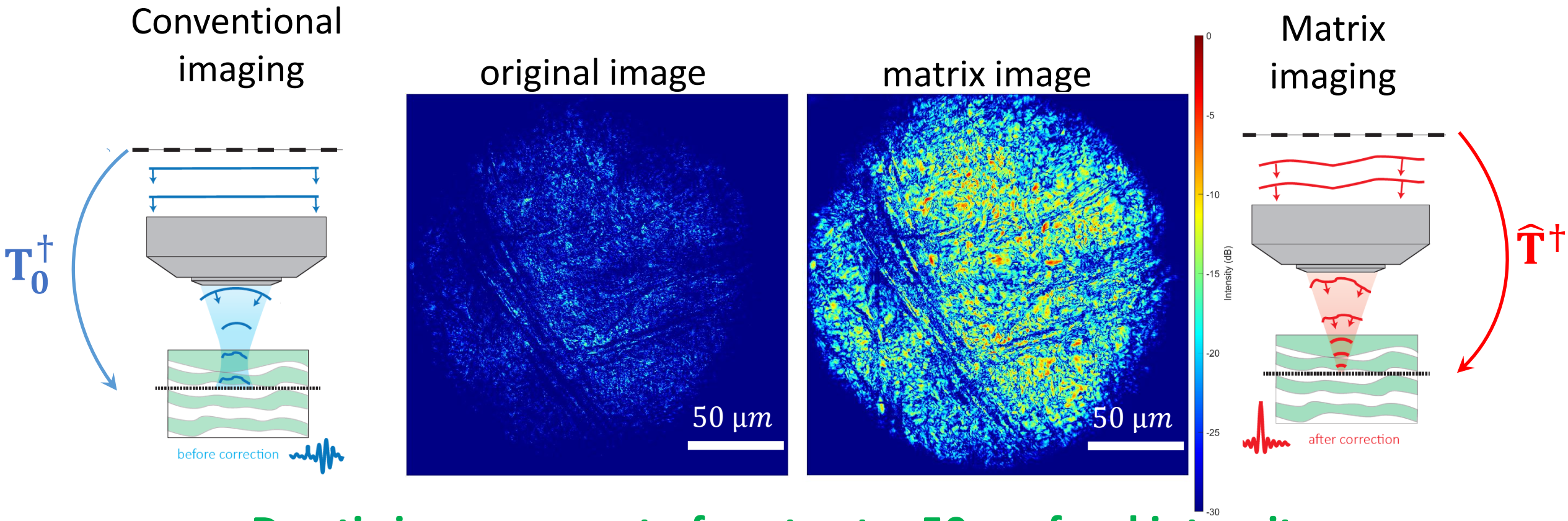

Drastic improvement of contrast: ×50 confocal intensity

Stromal striae (indicator of keratoconus) are revealed by matrix imaging

Transmission matrix correction

Conventional imaging

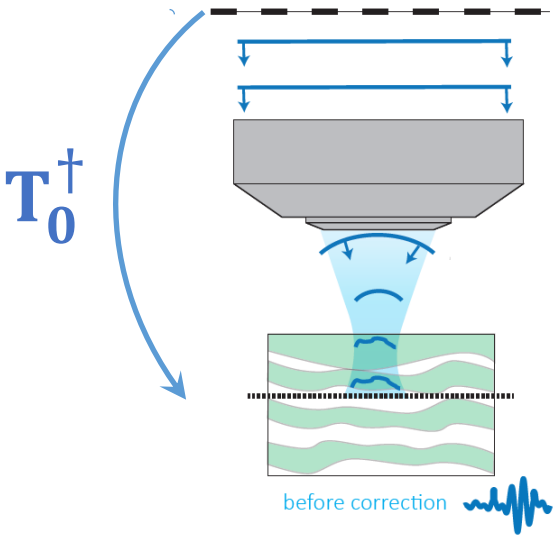

initial PSF

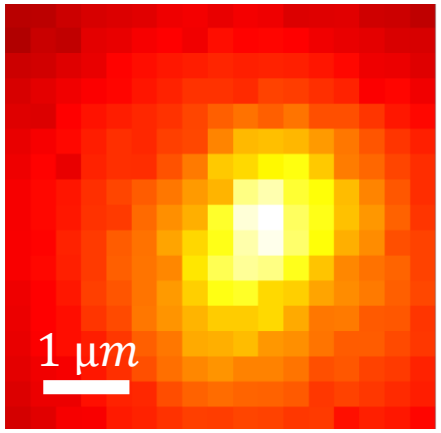

corrected PSF

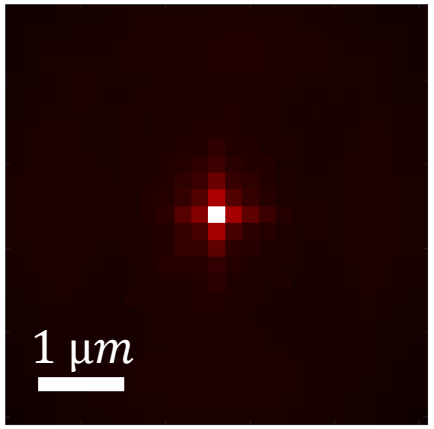

Matrix imaging

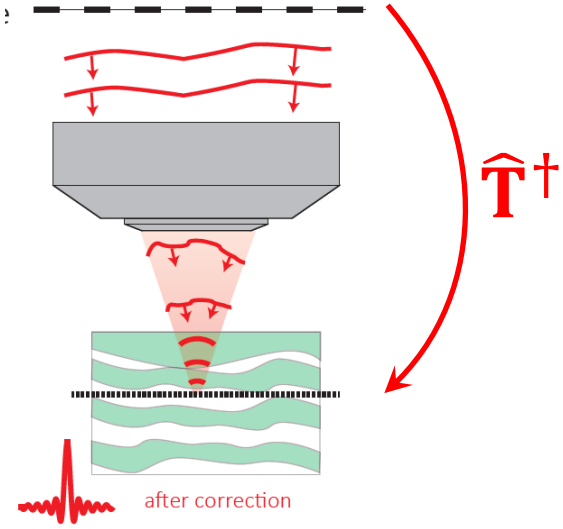

Drastic improvement of resolution (×10): 2.5 µm → 0.25 µm

Passive matrix imaging

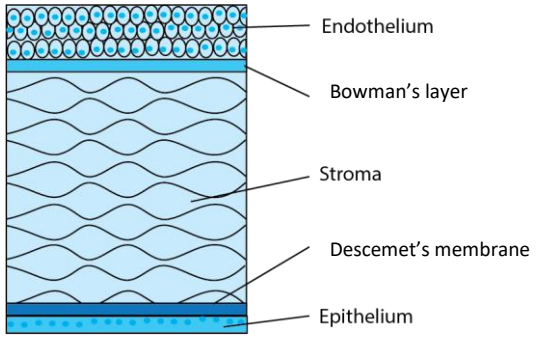

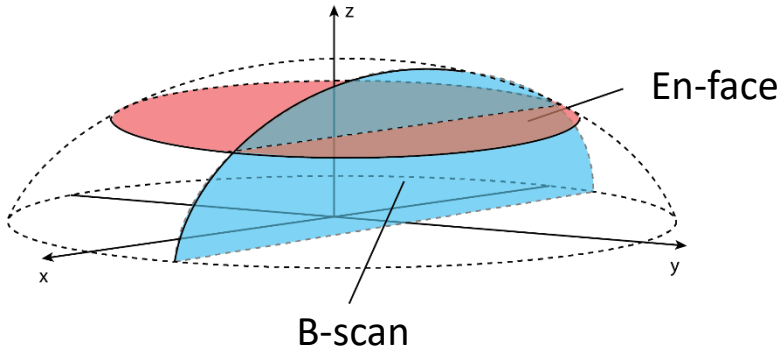

Standard FFOCT

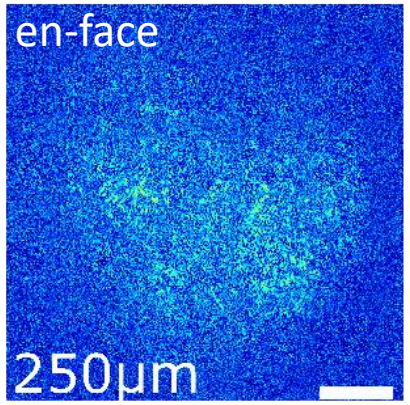

Matrix FFOCT

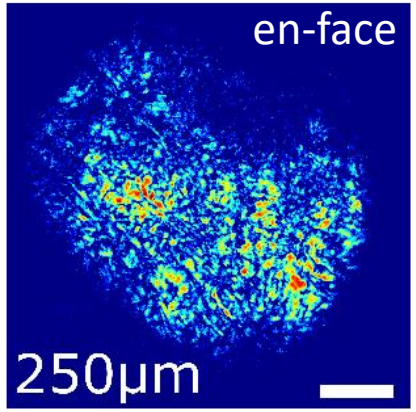

SNR × 30 in depth

Penetration depth ×4

Standard FFOCT

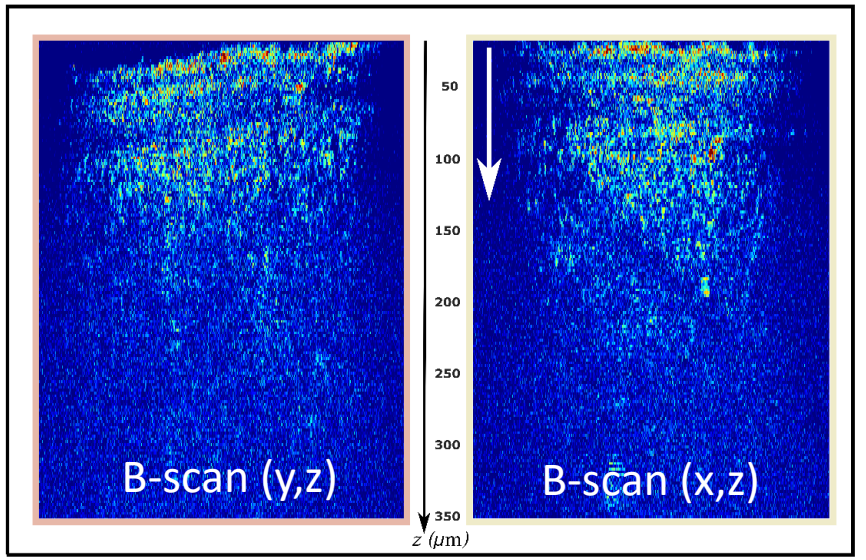

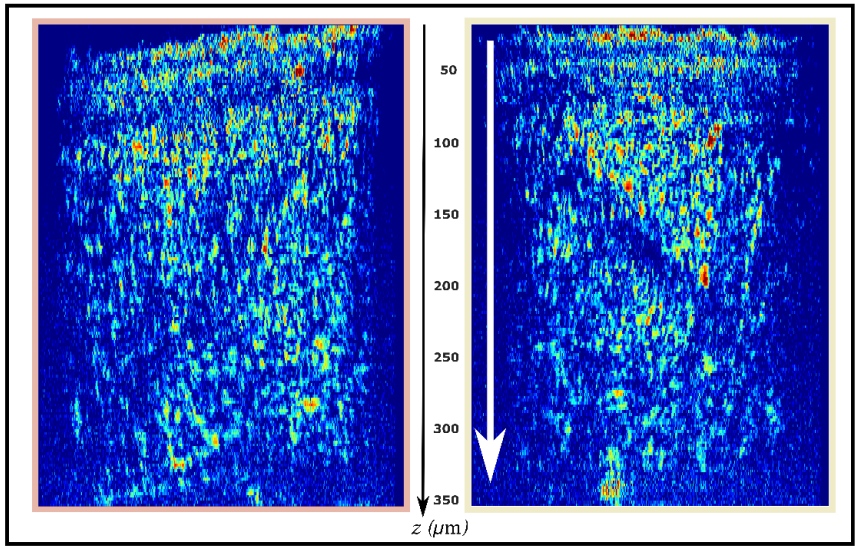

Matrix Approach

Conclusion

Institut Langevin
ONDES ET IMAGES

Passive matrix imaging:

Non-invasive, label-free
Huge FOV (10^9 voxels)
Confocal resolution (0.2 µm)
Penetration depth ~ 10 l_s
Specular / Speckle regimes
Overcome the intrinsic limit of adaptive optics (isoplanicity)

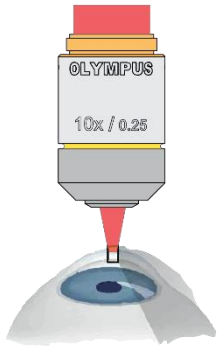

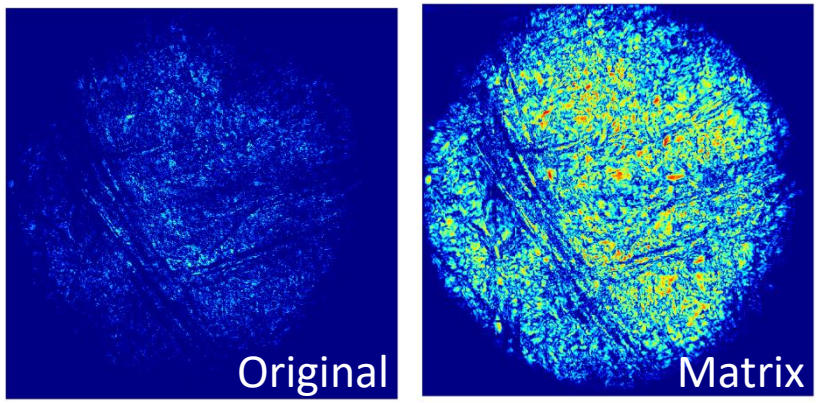

Limits:

No correction of axial/dispersive aberrations
Limited to single scattering and forward multiple scattering (< 1 l_t)
Long acquisition time, low SNR

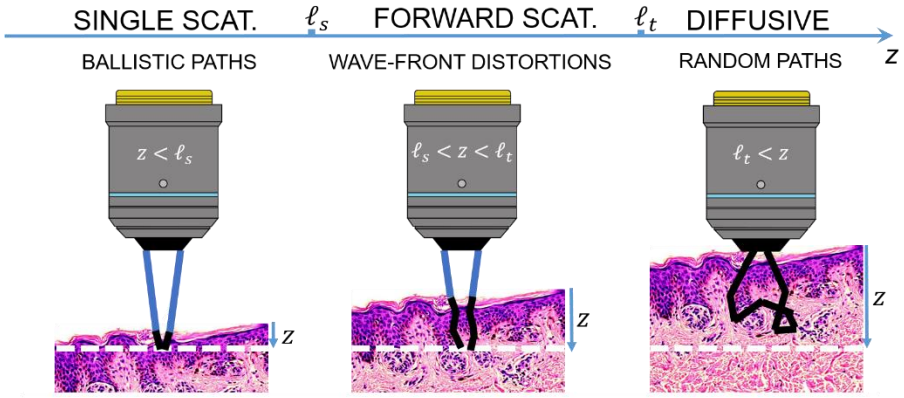

Perspectives:

Spectral domain OCT
Temporal/Frequency degrees of freedom (inspired by **ultrasound**)
Extension to other fields of wave physics (**seismology**, radar *etc.*)

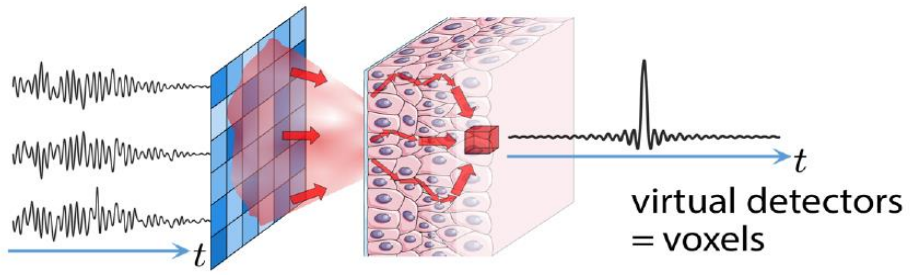

Passive matrix imaging

Application to seismology

Introduction: Reflection seismology

Institut Langevin
ONDES ET IMAGES

Seismic imaging at the *global* scale (« Transmission » configuration)

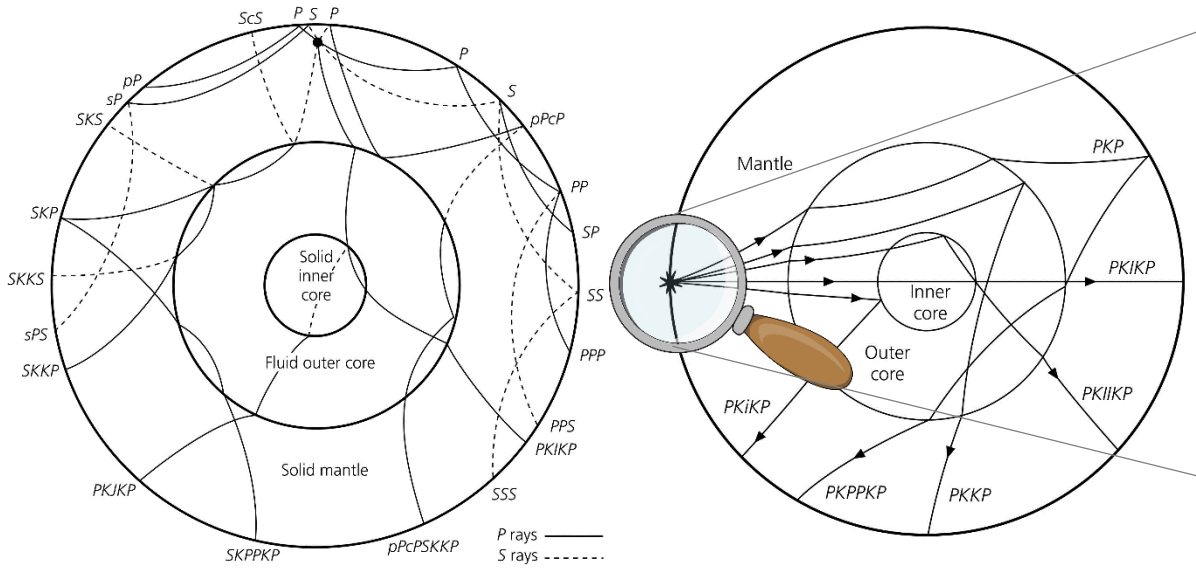

Stein, Wysession, *An Introduction to Seismology, Earthquakes and Earth Structure*, Blackwell Publishing 2003

Seismic imaging at the *local* scale (« Reflection » configuration)

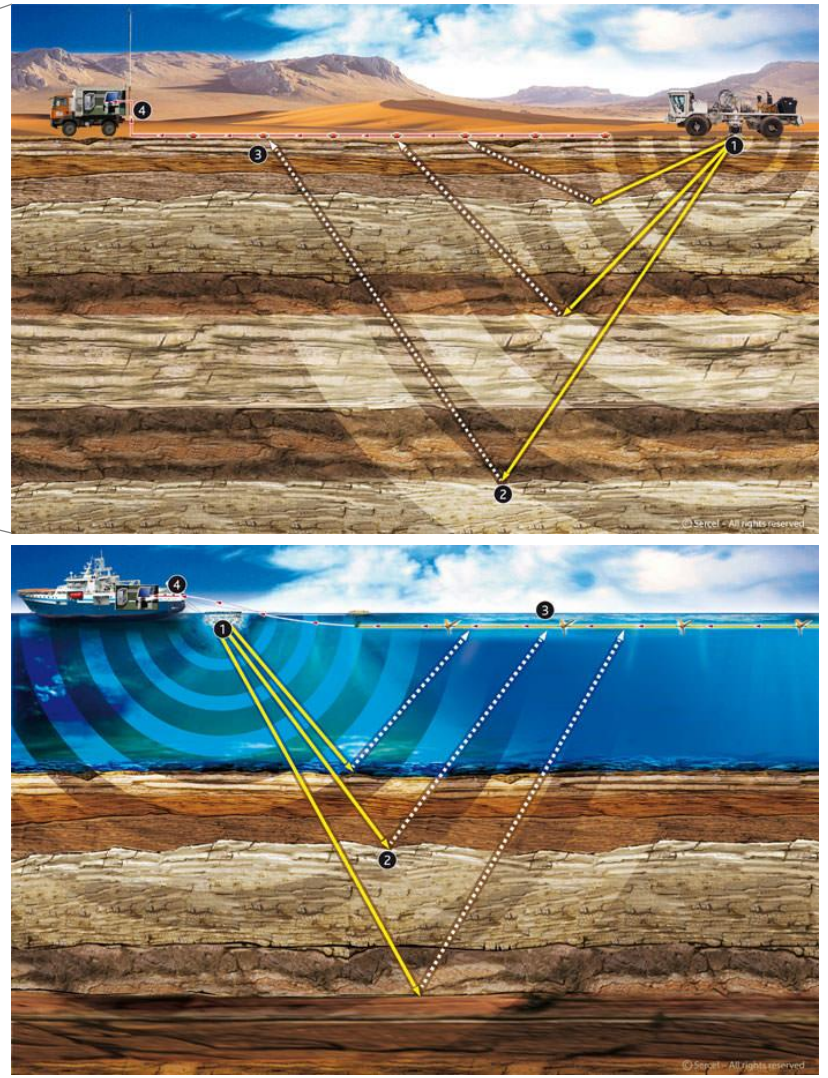

The underground can be probed at the kilometer scale using man-made impulses

The underground heterogeneities **reflect** and **scatter** the seismic bulk waves as they propagate through

Introduction: Fundamental limits of reflection seismology

Institut Langevin
ONDES ET IMAGES

Homogeneous Earth's crust

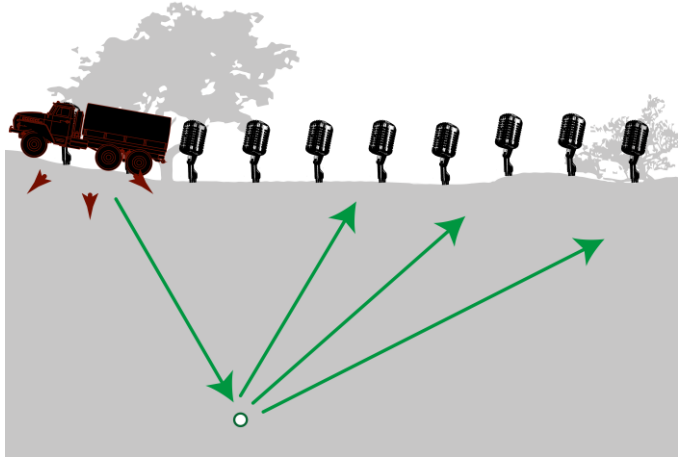

An incident wave is generated at the medium surface

The reflected wave-field is recorded by an **array of geophones**

***Single scattering regime**:*
Travel times directly yield the scatterer position

Heterogeneous Earth's crust

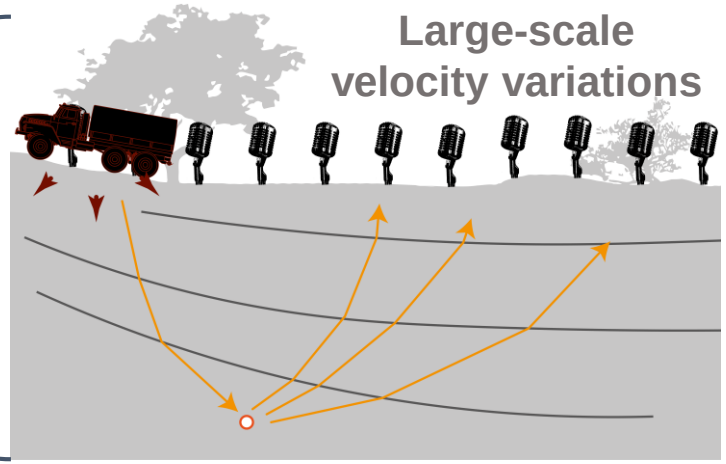

***Aberrations**:* loss in contrast and resolution

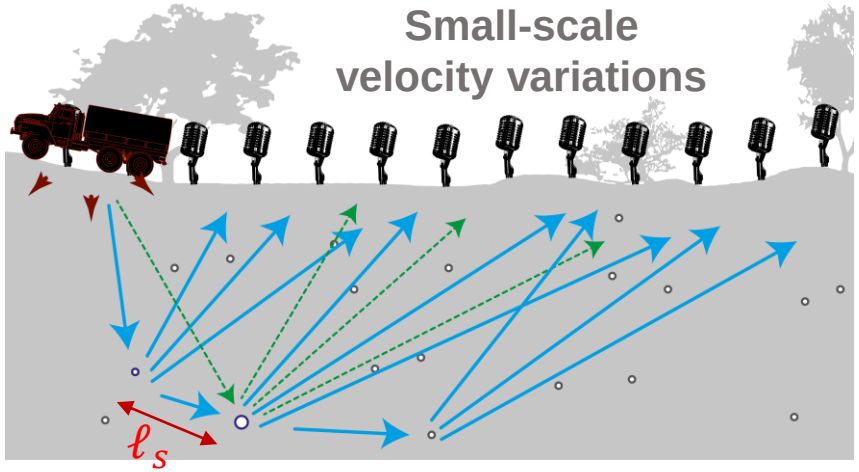

***Multiple scattering**:* Penetration depth limited to ℓ_s

How to go beyond 1 km depth (no coherent source)?

How to overcome multiple scattering and aberration issues ?

Introduction: Green's function retrieval / Passive imaging

Institut Langevin
ONDES ET IMAGES

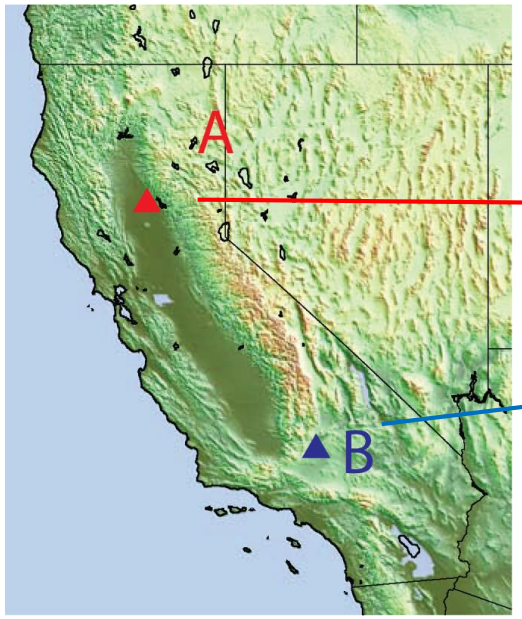

(1) Displacement recorded at two points **A** et **B**

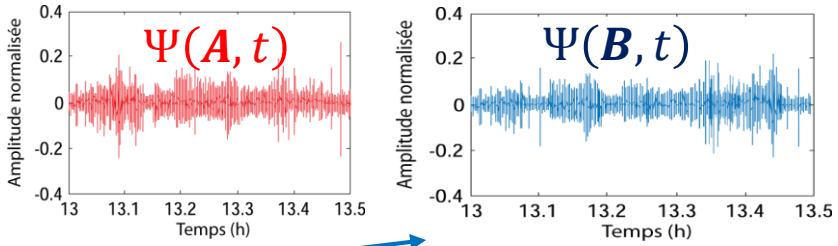

Charcateristic time $\tau_c \sim$ 1s

(2) Green's function retrieval from noise cross-correlation

$$C(\boldsymbol{A},\boldsymbol{B},t) = \int_0^T d\tau \,.\, \Psi(\boldsymbol{A},t+\tau) \,.\, \Psi(\boldsymbol{B},\tau)$$

time reversal analogy /
fluctuation – dissipation theorem

$$T \gg \tau_c : \quad \partial_t C(\boldsymbol{A},\boldsymbol{B},t) = G(\boldsymbol{A},\boldsymbol{B},t) - G(\boldsymbol{A},\boldsymbol{B},-t)$$

Causal Anti-causal

A. Derode *et al., Appl. Phys. Lett.* **83**, 3054 *(2003)*
M. Campillo and A. Paul, *Science* **299,** 5606 (2003)
N. M. Shapiro *et al.,* Science **307**, 5715 (2005)
P. Roux *et al.,* Geophys. J. Int. 206, 980-992 (2016)

$T \sim$ 1 month

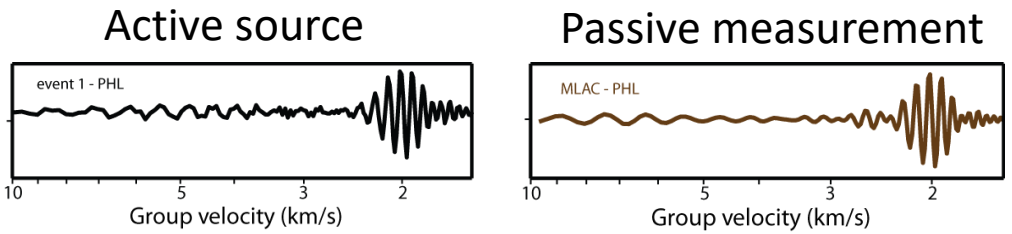

Passive imaging of the Earth's crust (mainly limited to Rayleigh surface wave tomography)

Passive matrix seismic imaging

San Jacinto Fault Zone, one of the most seismically active areas in California

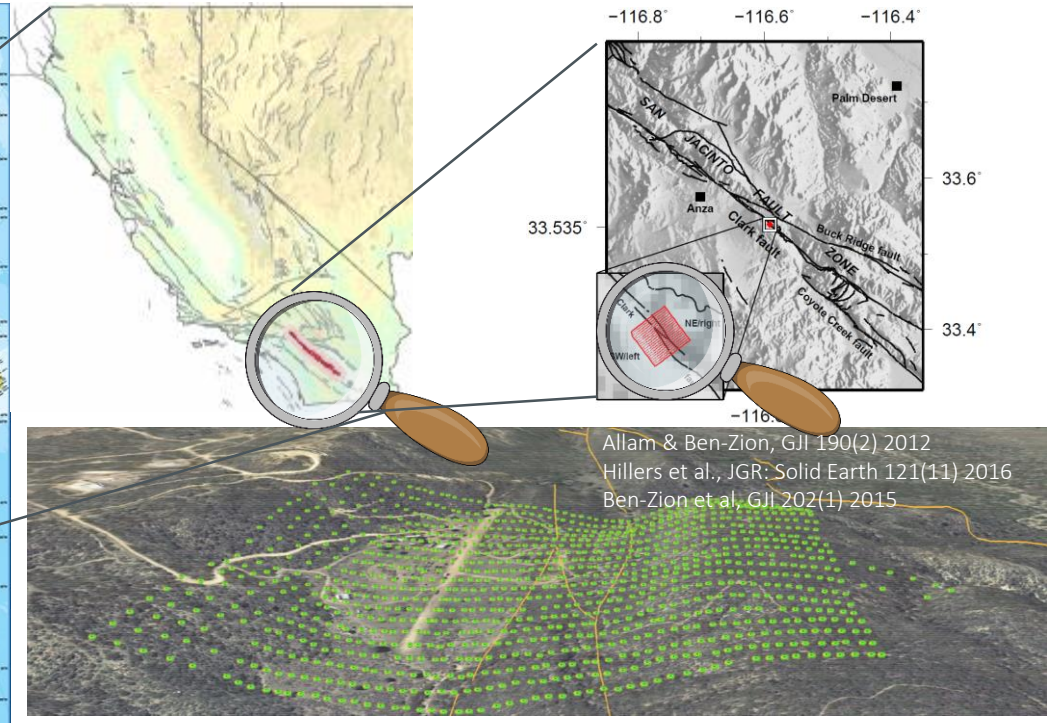

Allam & Ben-Zion, GJI 190(2) 2012
Hillers et al., JGR: Solid Earth 121(11) 2016
Ben-Zion et al, GJI 202(1) 2015

1108-geophones dense array ($\delta_X \approx 10$m, $\delta_Y \approx 30$m) on the San Jacinto Fault, California

$f \sim 10 - 20$ Hz, $\lambda \sim 50 - 200$ m


R. Touma


T. Blondel


A. Derode


M. Campillo

Passive matrix seismic imaging

ocean, wind and human-related noise

raw seismic signal

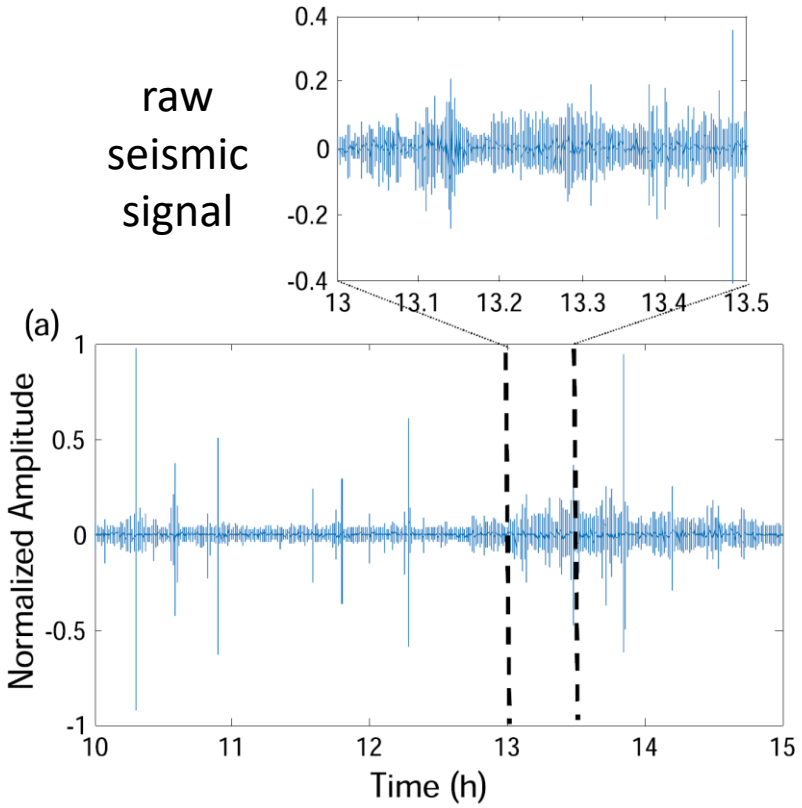

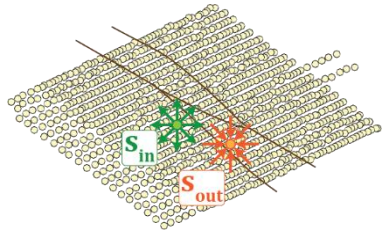

Matrix $\mathbf{R_0}$
in the sensor basis

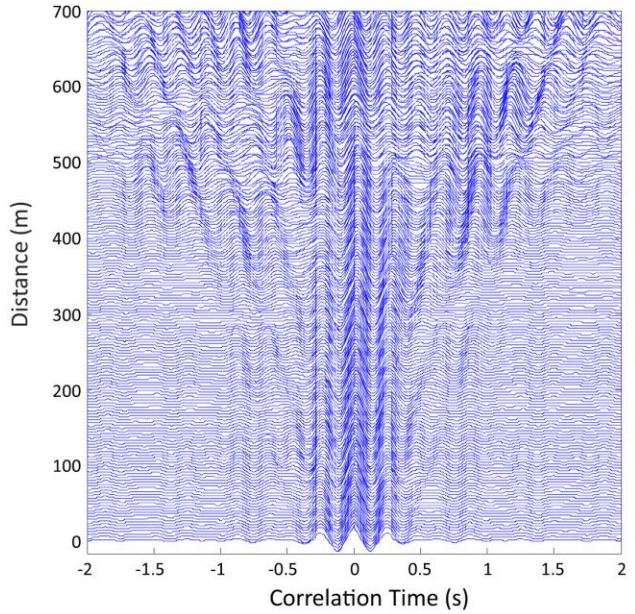

Passive measurement of the reflection matrix $\mathbf{R_0}$ between geophones by cross-correlation of seismic noise

P. Roux et al., Geophys. J. Int., 2016

Broadband focused reflection matrix

Monochromatic focusing

$$\mathbf{R}(z,\omega) = \mathbf{T_0^{\dagger}}(\omega,z)\mathbf{R_0}(\omega)\mathbf{T_0^{*}}(\omega,z)$$

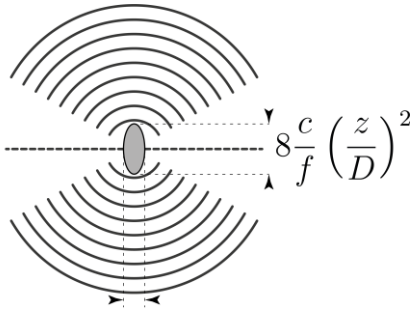

Free-space transmission matrix $\mathbf{T_0}(\omega,z)$

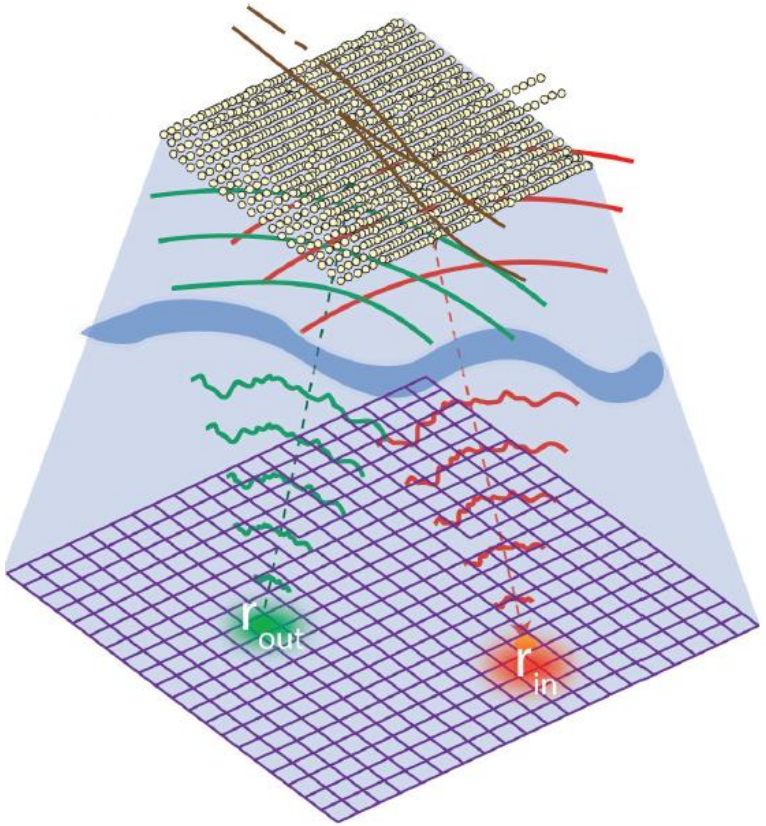

Very rough velocity balground model:
$c_0 = 1500$ m/s

Broadband focused reflection matrix

$$\bar{\mathbf{R}}(z) = \sum_{\omega} \mathbf{R}(z,\omega)$$

Coherent sum over the frequency bandwith
↔
Numerical time gating

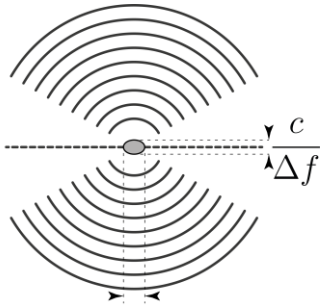

Projection of the reflection matrix in the focused basis
(*redatuming* in seismology)

Berryhill, Geophysics, 1984
Berckhout and Wapenaar, J. Acoust. Soc. Am., 1993

Focused reflection matrix: Local aberration quantification

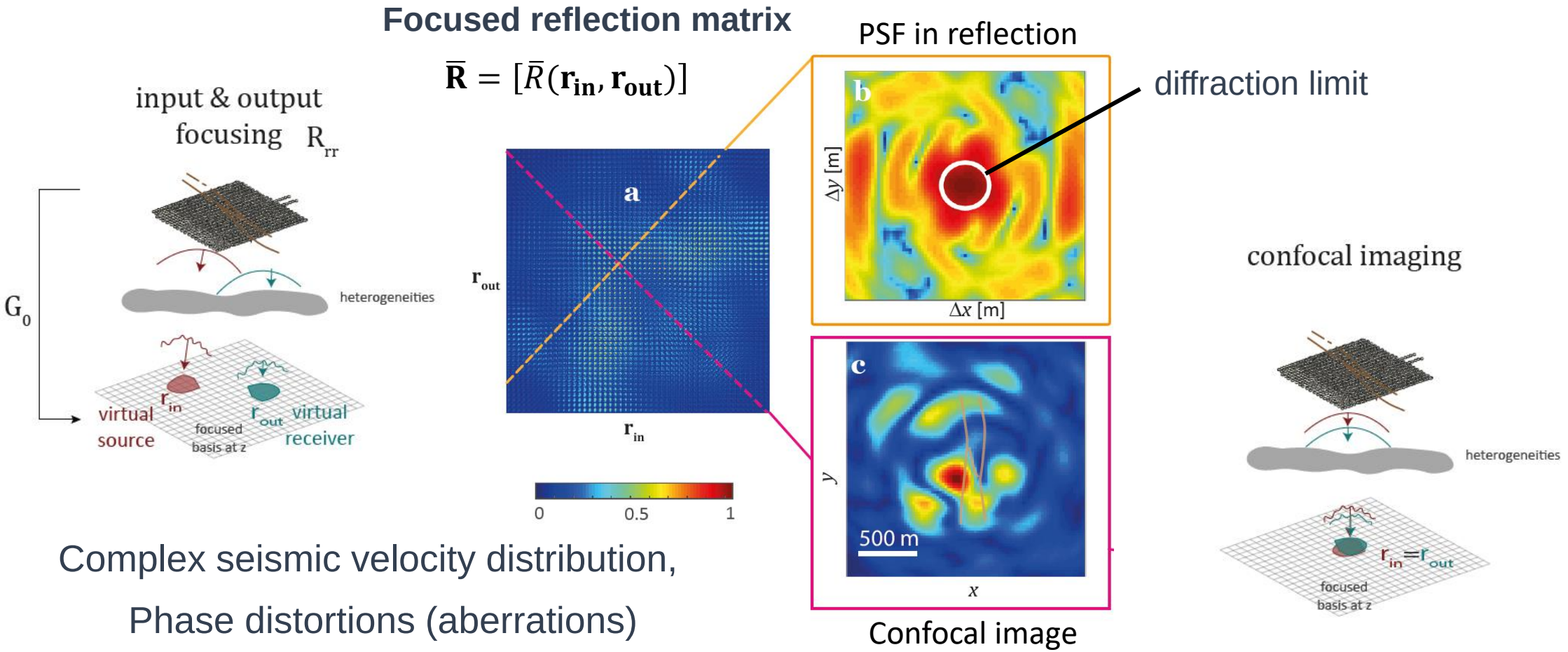

Complex seismic velocity distribution,

Phase distortions (aberrations)

Loss of resolution

The focused reflection matrix enables a local assessment of the aberration level

Touma *et al.*, Geophys. J. Int., 2021

Focused reflection matrix: Confocal imaging

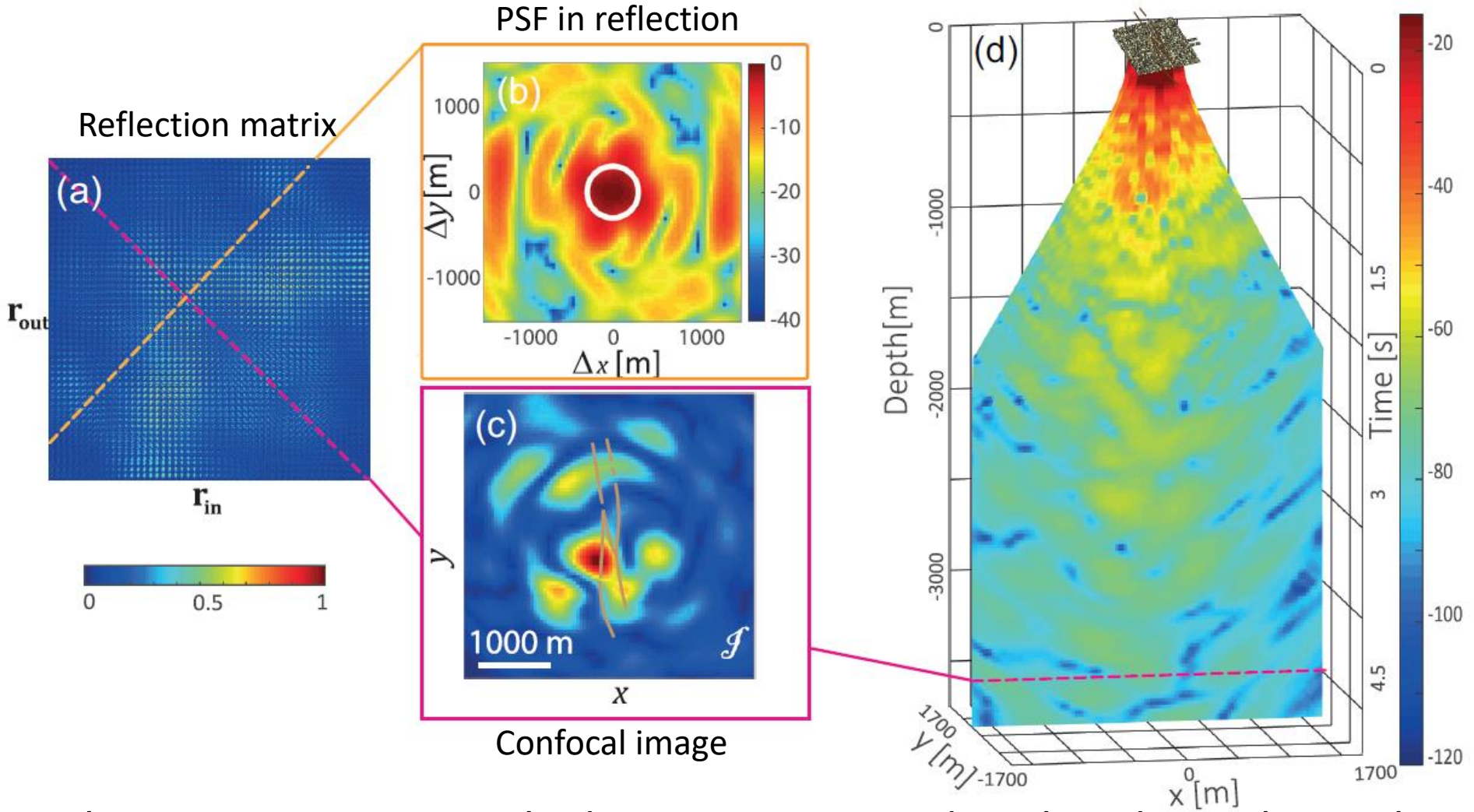

The 2D images are stacked as 3D images and explored as volume slices

However, the confocal 3D image cannot be trusted due to the high aberration level

Touma *et al.*, Geophys. J. Int., 2021

Distortion matrix approach for aberration correction

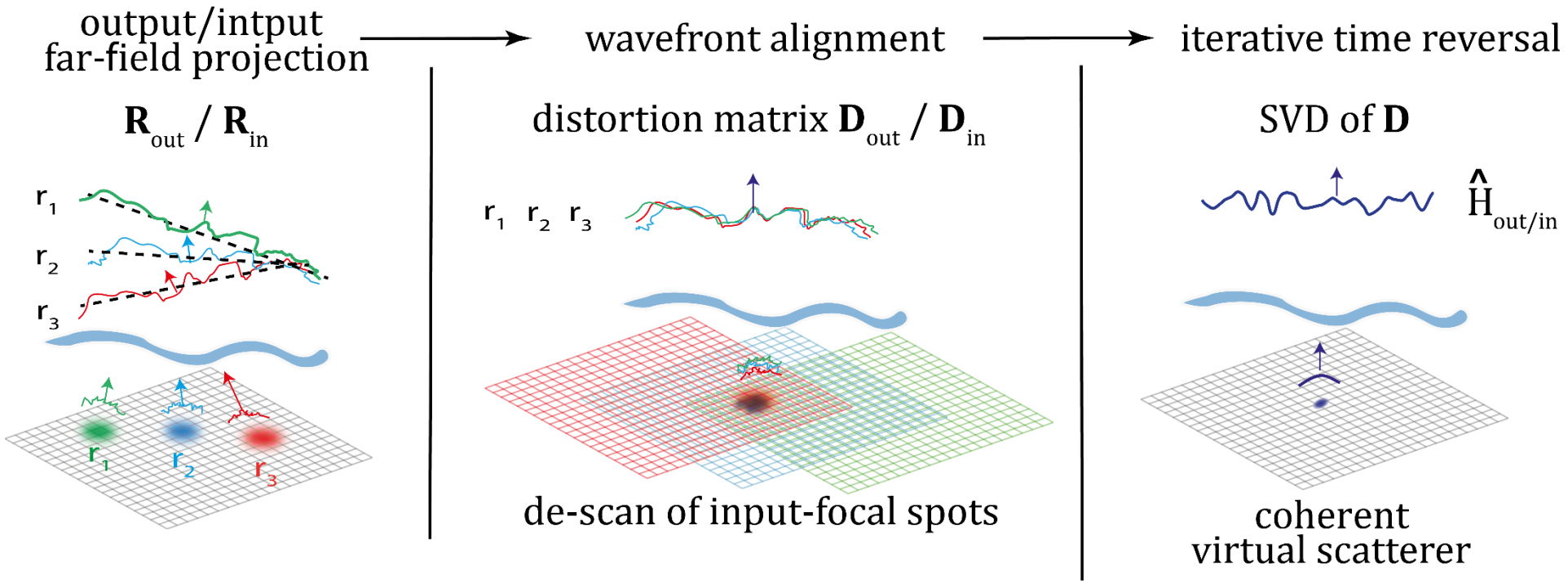

The distortion matrix yields an estimation of the aberration phase transmittance over each isoplanatic patch

Touma *et al.*, Geophys. J. Int., 2021

Distortion matrix approach of seismic imaging

SVD of **D**:
One-to-one association between isoplanatic patches and aberration phase laws

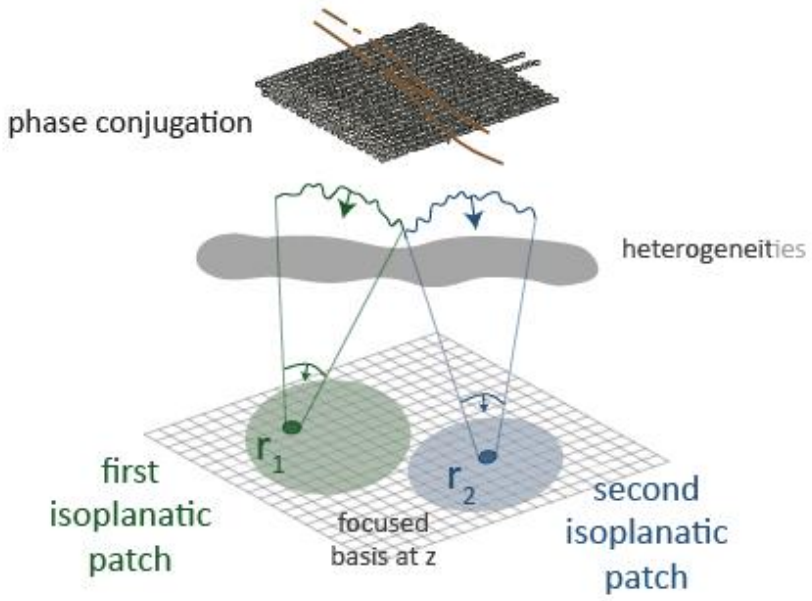

Phase conjugate of the aberration phase law

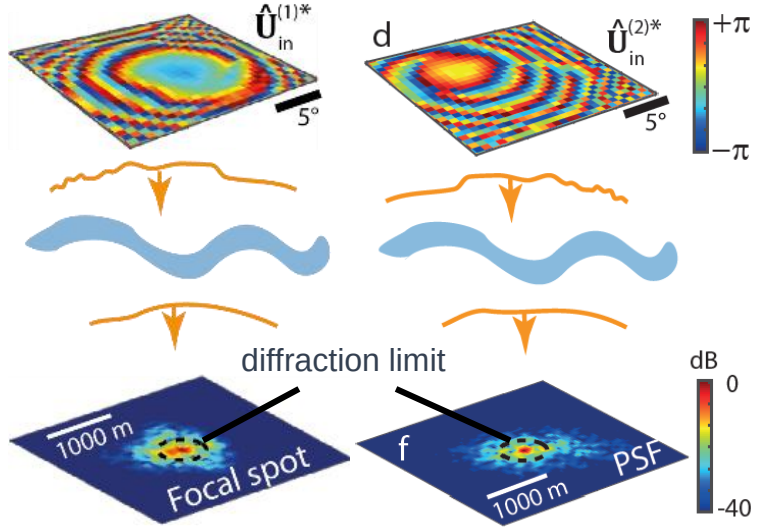

Before correction

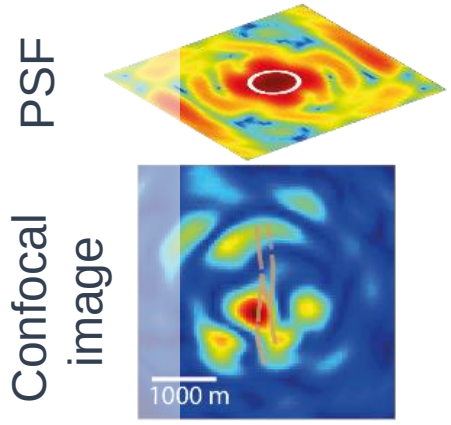

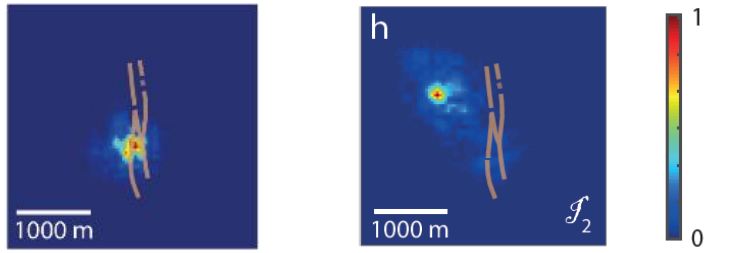

The aberration correction steers the focused energy back to the diagonal

Resolution almost 8× better than the diffraction limit in depth (free space)

Touma *et al.*, Geophys. J. Int., 2021

Input aberration correction

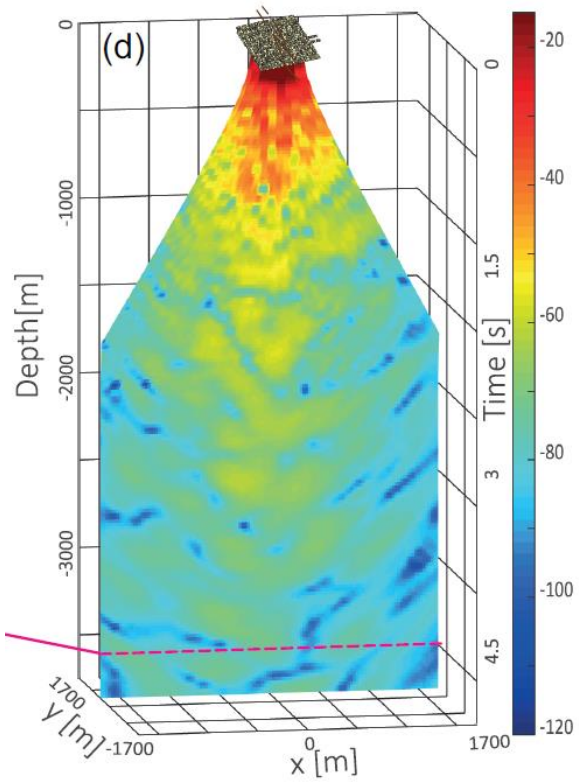

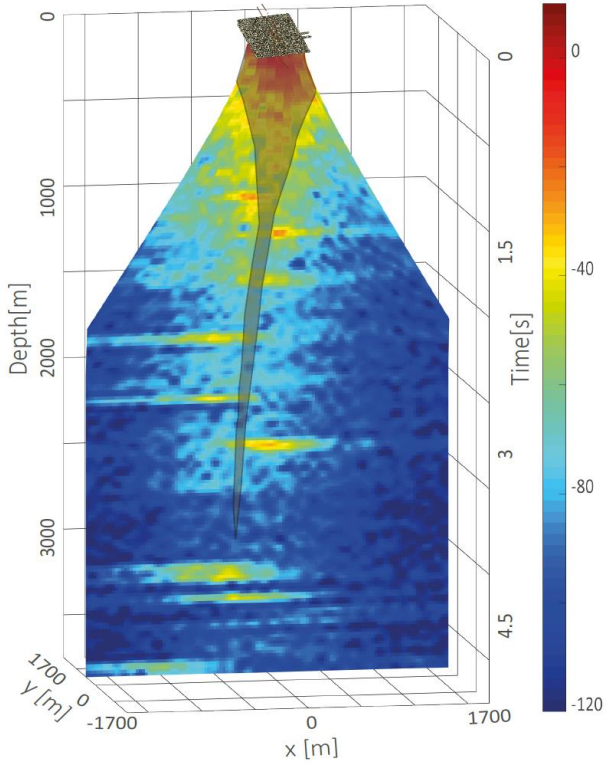

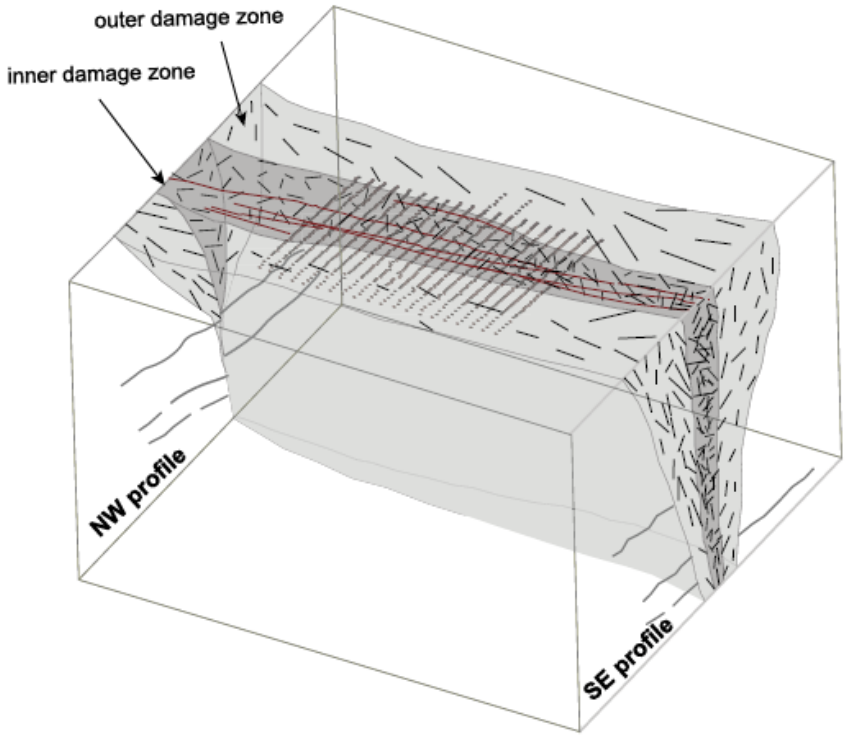

The matrix approach reveals the in-depth structure of the fault (shaded area):

-> Strongly heterogeneous damage area (z<1500 m)

-> Offset between geological units at the fault location

For a more detailed analysis of matrix images, see Touma *et al.*, EPSL, 2022

Passive matrix imaging of La Souffrière volcano

Context

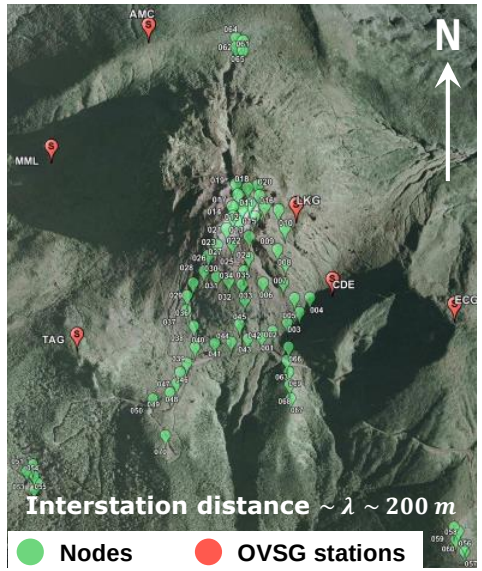

Network of 65 geophones

Seismic noise correlation
(2 months, 10–20 Hz)

Results

Reflectivity images

Homogeneous model
c = 2000 m/s

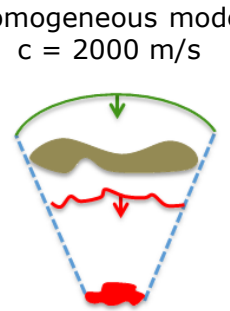

Aberrated focal spot

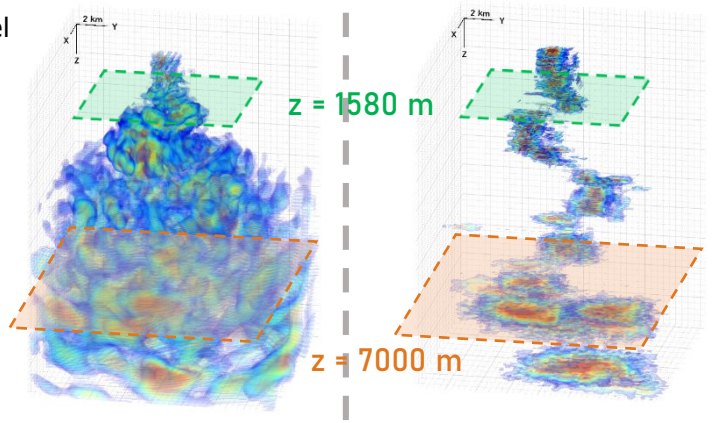

1km
2km

Uncorrected

Corrected

Matrix imaging (1,2)
Adaptive focusing

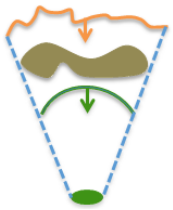

Super-resolution ~ λ

Blondel *et al.*, JGR 2018 (1); Touma *et al.*, GJI 2020 (2); Moretti *et al.*, JVGR 2020 (3)

Problematic

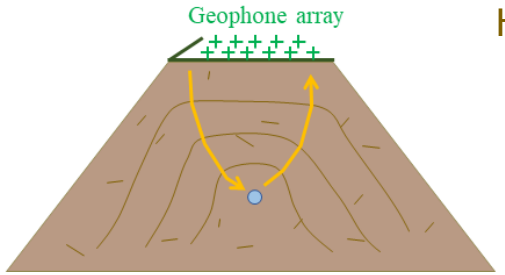

Aberrations
(long-scale variations)

Heterogeneous wave
velocity distribution

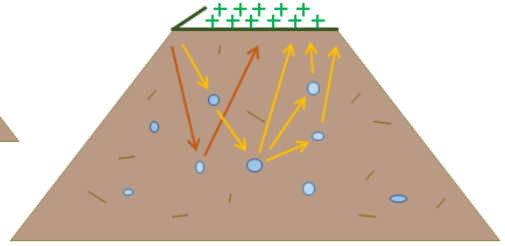

Multiple scattering
(short-scale fluctuations)

E. Giraudat, PhD thesis

Discussion

High resolution 3D image

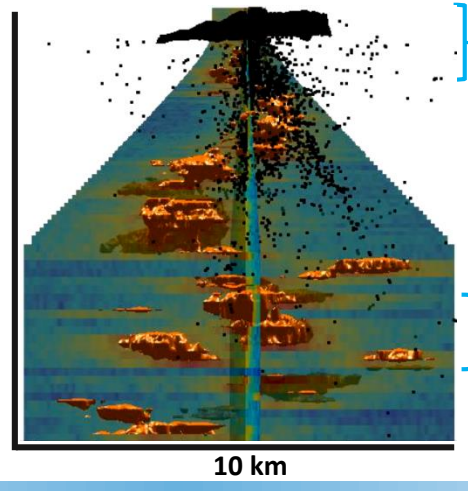

Deep lens
structures (3)

Superficial lateral conduit

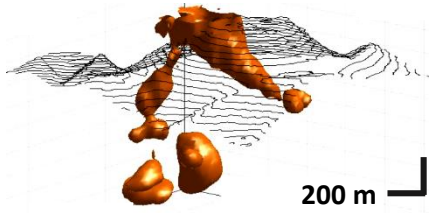

Location of [3-5 Hz]seismic noise

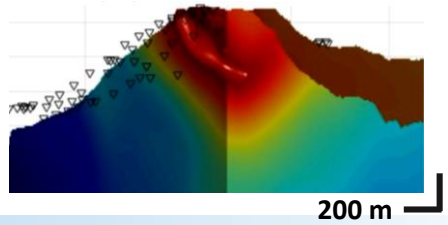

High resolution image of the volcano's internal structure by passive matrix imaging

One open question: Physical origin for super-resolution ?

Diffraction-limited resolution

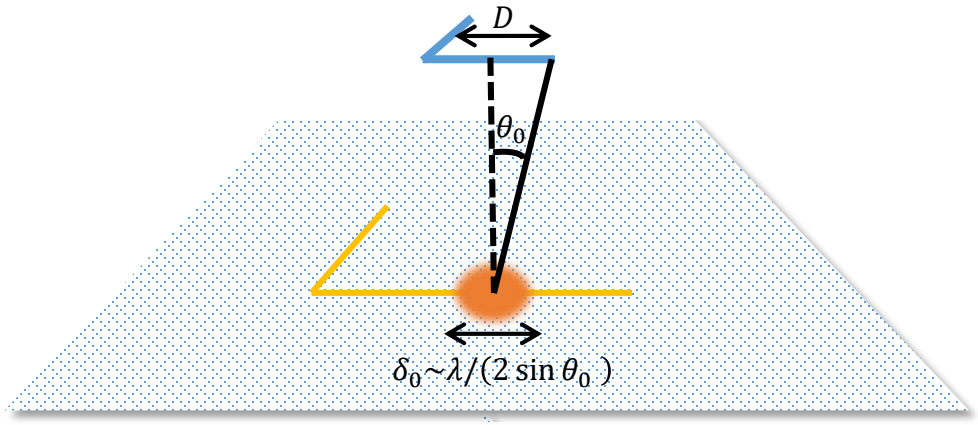

Conversion Rayleigh ↔ Bulk waves

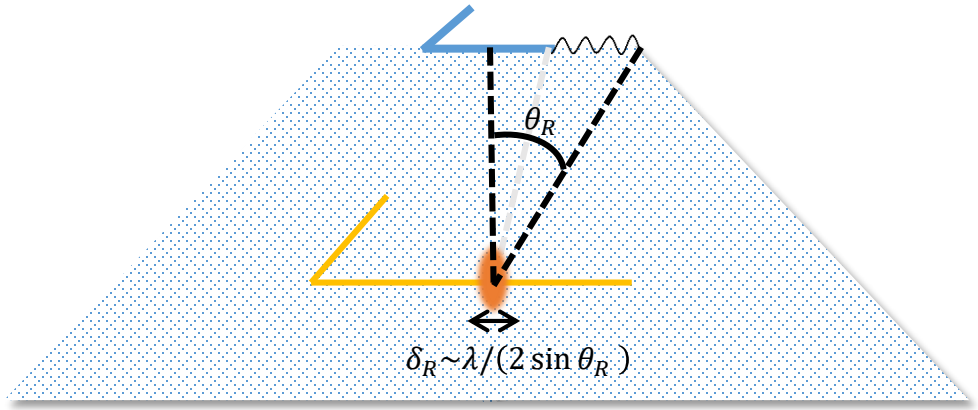

Scattering Lens

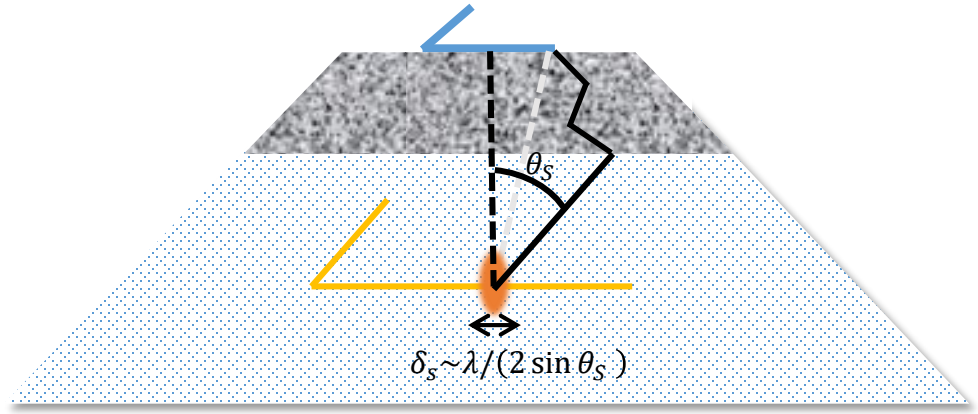

A. Derode and M. Fink, PRL, 1995

Kaleidoscopic Lens

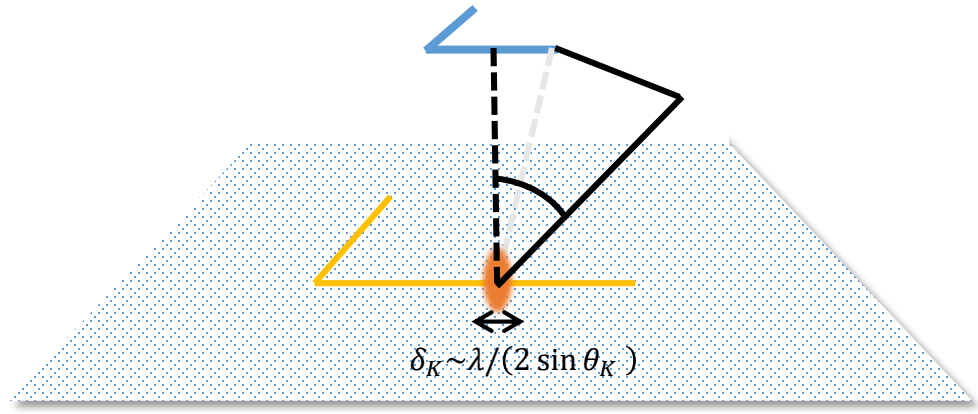

P. Roux and M. Fink, J. Acoust. Soc. Am., 2001

Rayleigh waves, scattering and waveguiding are good candidates to account for super-resolution

Conclusion and perspectives

Institut Langevin
ONDES ET IMAGES

Passive matrix imaging:

Seismic noise, bulk waves
Fault zones, volcanoes
Dense network of geophones (Nyquist criterion)
Specular reflectors / Diffuse scattering
Penetration depth :
From 10 km (10-20 Hz) to 100 km (0.1-0.5 Hz)
Super-resolution ($\sim \lambda$)

Limits:

No correction of axial/dispersive aberrations
Conversion between P- and S-waves

Perspectives:

Bulk wave velocity tomography
Exploit temporal degrees of freedom
(inspired by ultrasound)

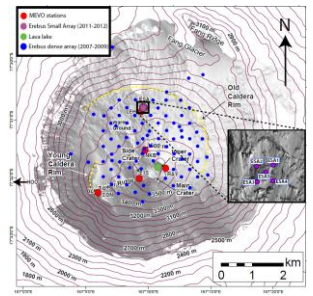

North Anatolian fault (Turkey)

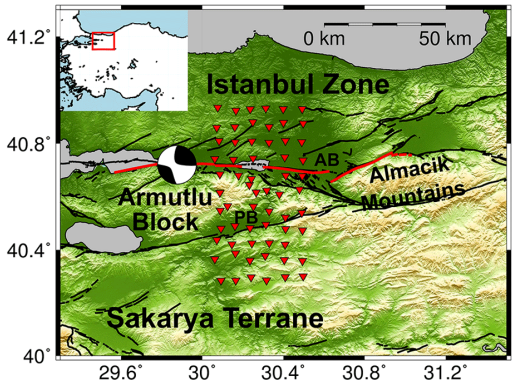

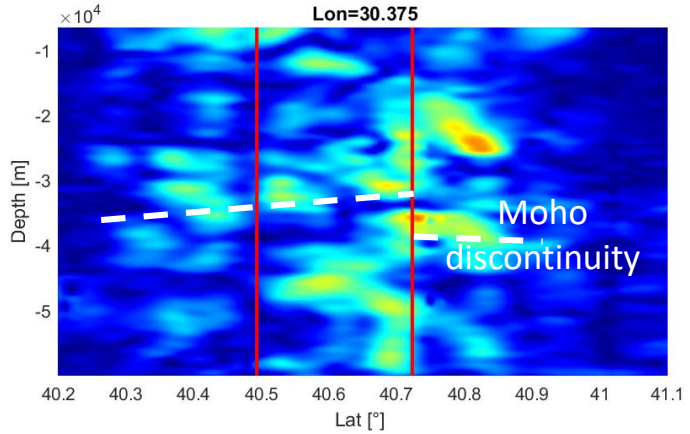

R. Touma et al., *in prep.* 2021

Erebus volcano (Antarctica)

Multiple scattering filter

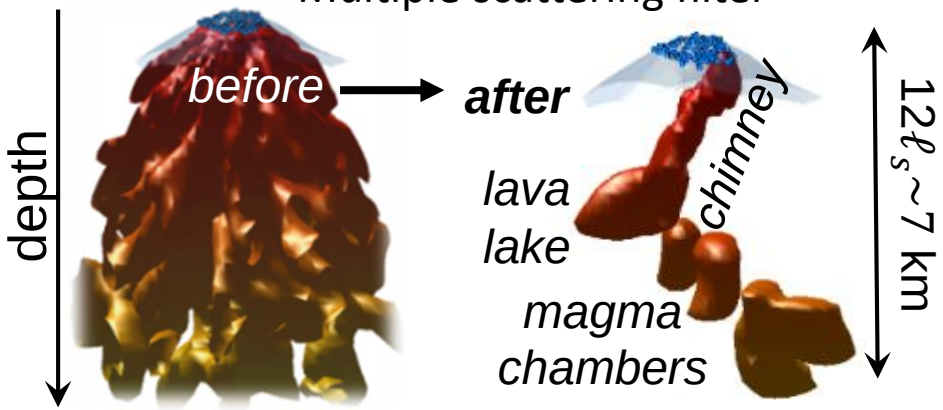

T. Blondel et al., J. Geophys. Res. 2018

Towards Quantitative Matrix Imaging

An ultrasound proof-of-concept

Matrix approach of ultrasound imaging

Institut Langevin
ONDES ET IMAGES

Ultrasound image (liver)

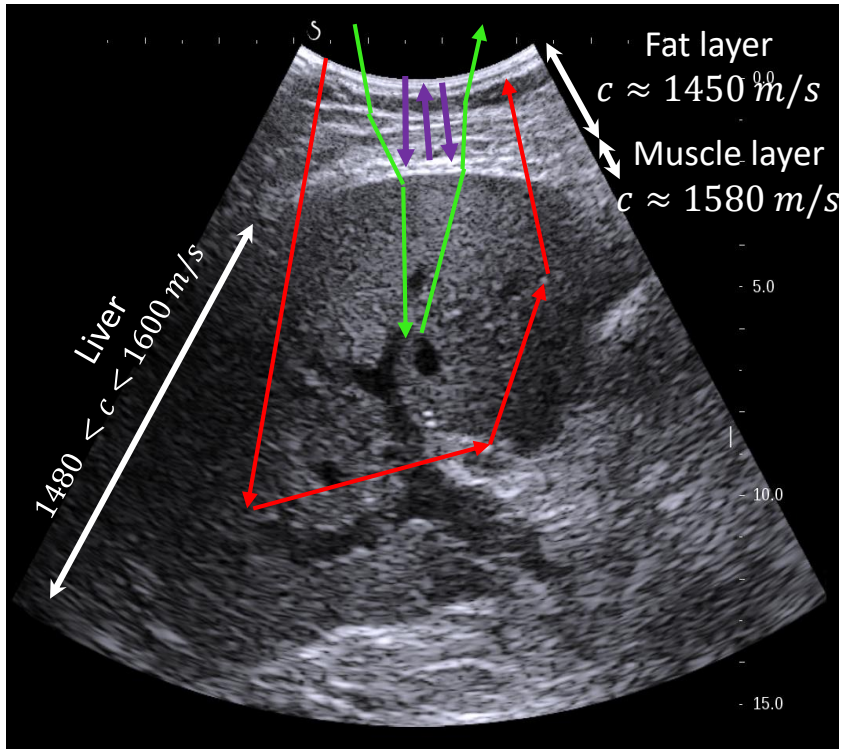

Conventional imaging

Homogeneous speed of sound « c »
Single scattering process
Scatterer position ⇔ echo time of flight
Confocal imaging

Aberration

Resolution and contrast

Multiple reflection

Reverberation artefacts

Multiple scattering

Incoherent background

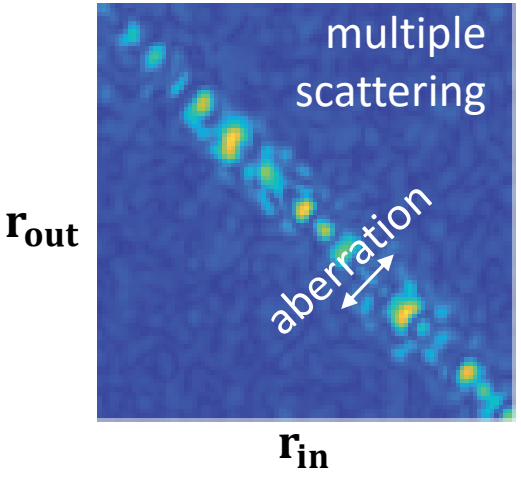

B-mode

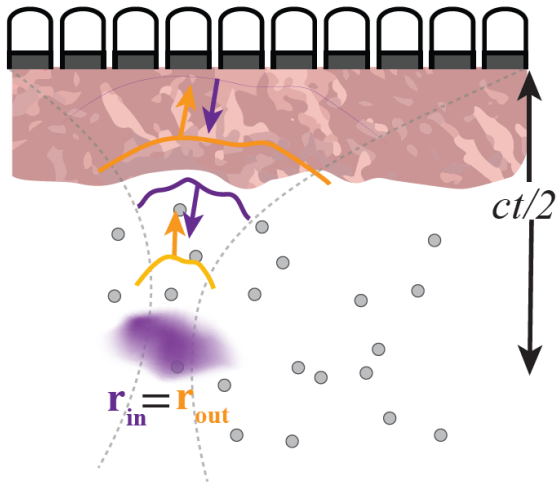

Matrix imaging

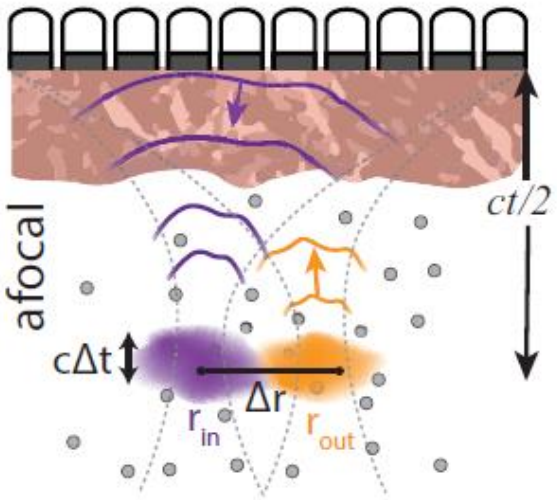

W. Lambert, L.A. Cobus, M. Fink, A. Aubry, PNAS (2020)

Ultrasound Matrix Imaging

Institut Langevin
ONDES ET IMAGES

Imaging deeper and sharper

(*e.g* breast micro-calcifications)

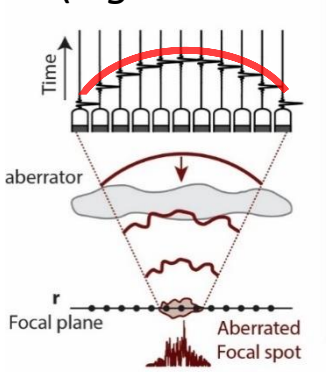

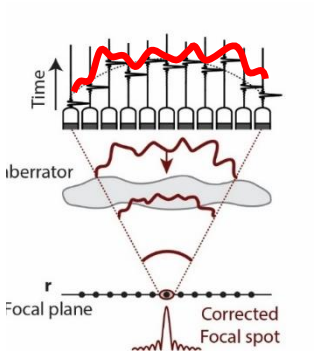

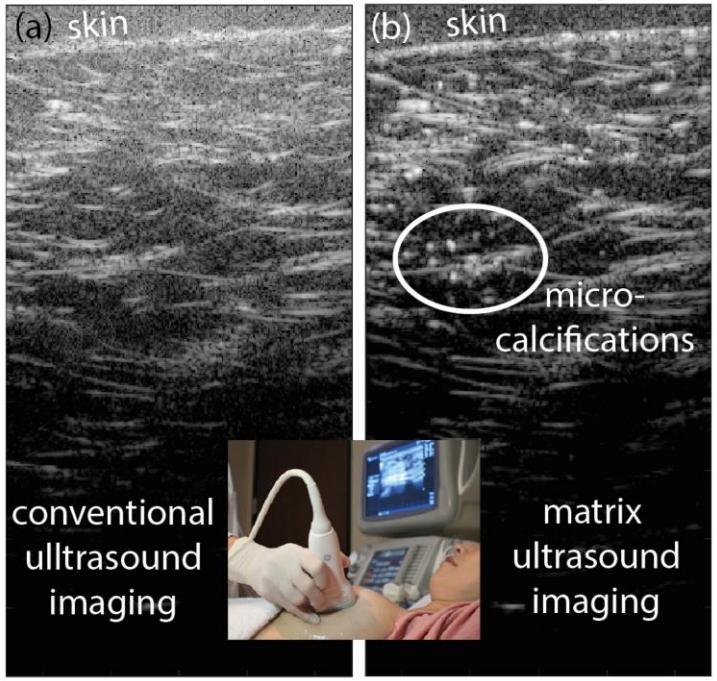

W. Lambert, PNAS, 2020

Remove/Compensate for Reverberations

(*e.g* abdominal wall, skull *etc.*)

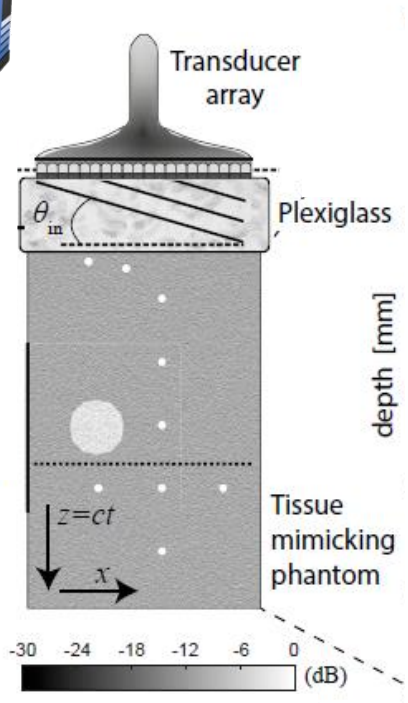

Academic proof-of-concept

(*e.g* tissue mimicking phantom)

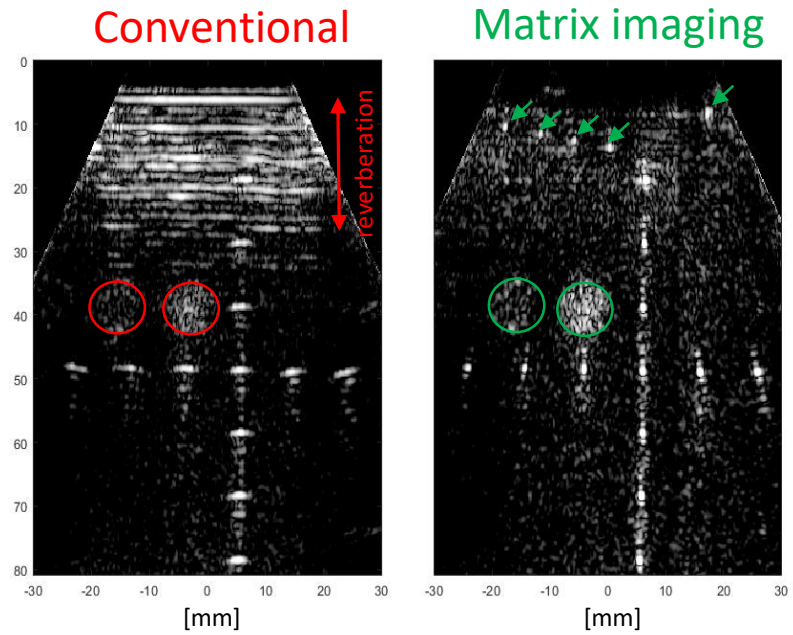

Contrast, transverse and axial resolution drastically improved by matrix imaging

E. Giraudat, PhD thesis

Institut Langevin
ONDES ET IMAGES

Self-portrait of an ultrasonic wave by exploiting scattering in tissues

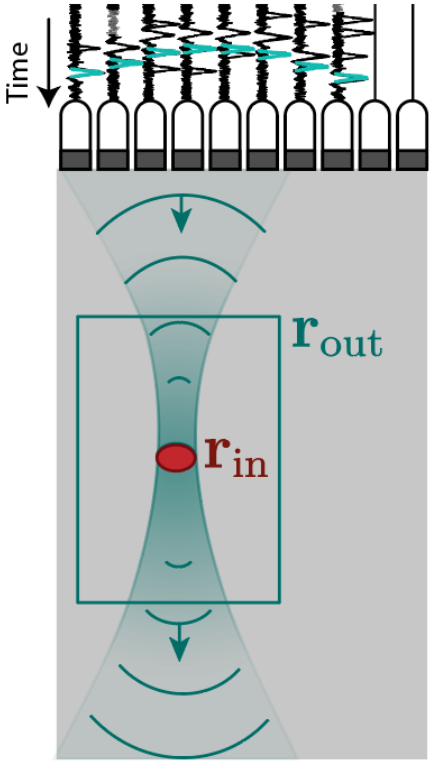

$$\overline{\mathbf{R}}(z) = \sum_{\omega} \mathbf{R}(z,\omega)\, e^{j\omega\Delta t}$$

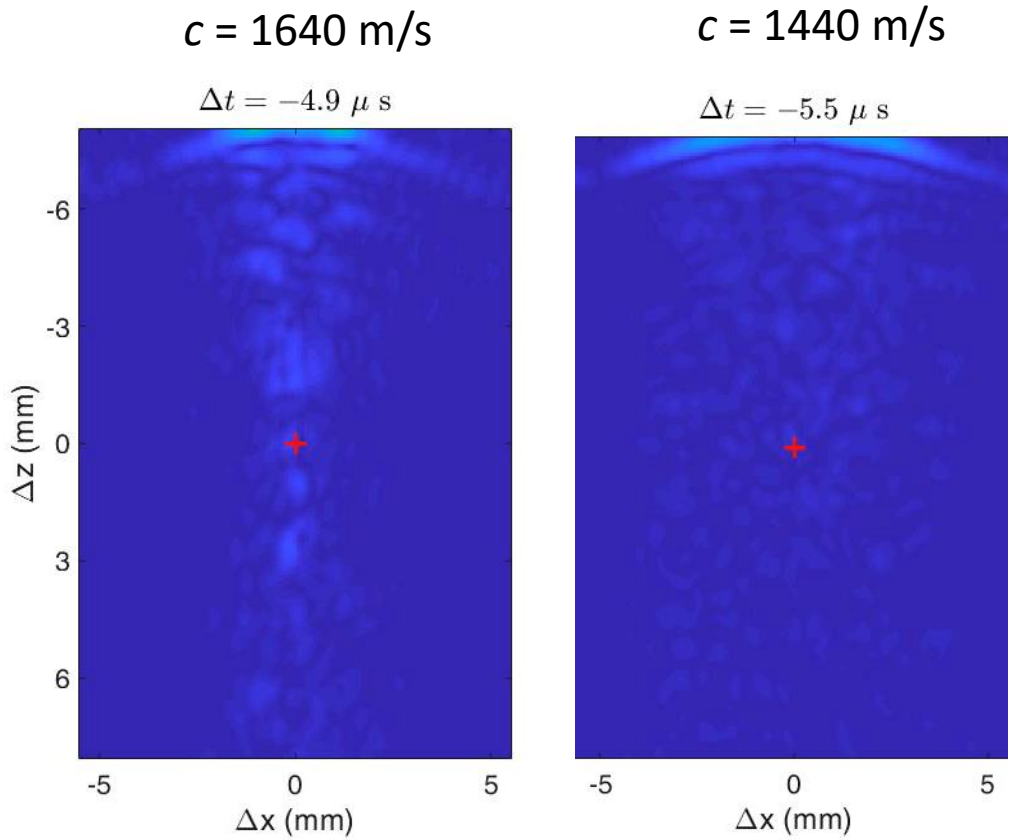

Measure the integrated speed-of-sound at a given pixel by tuning the axial position of the focusing point

William Lambert, PhD thesis

Quantitative Matrix Imaging

Institut Langevin
ONDES ET IMAGES

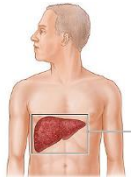

Ultrasound B-mode
(*difficult-to-image* patient)

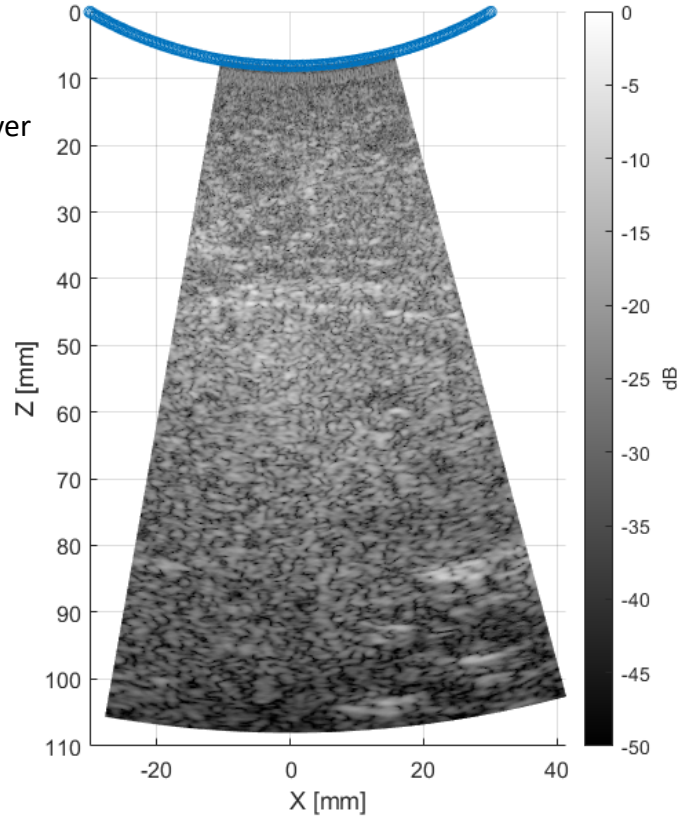

Integrated speed-of-sound
[m/s]

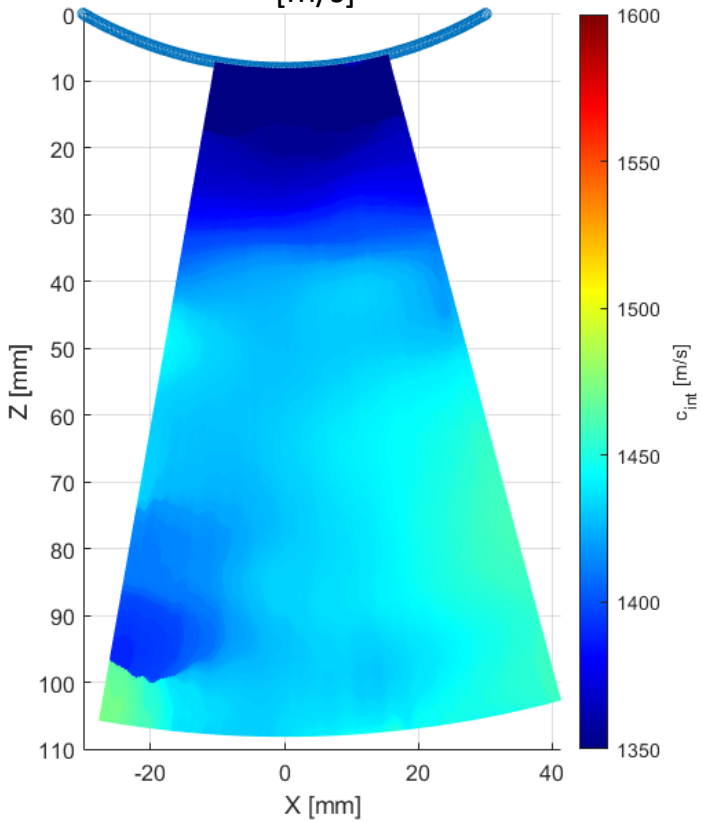

Local speed-of-sound
[m/s]

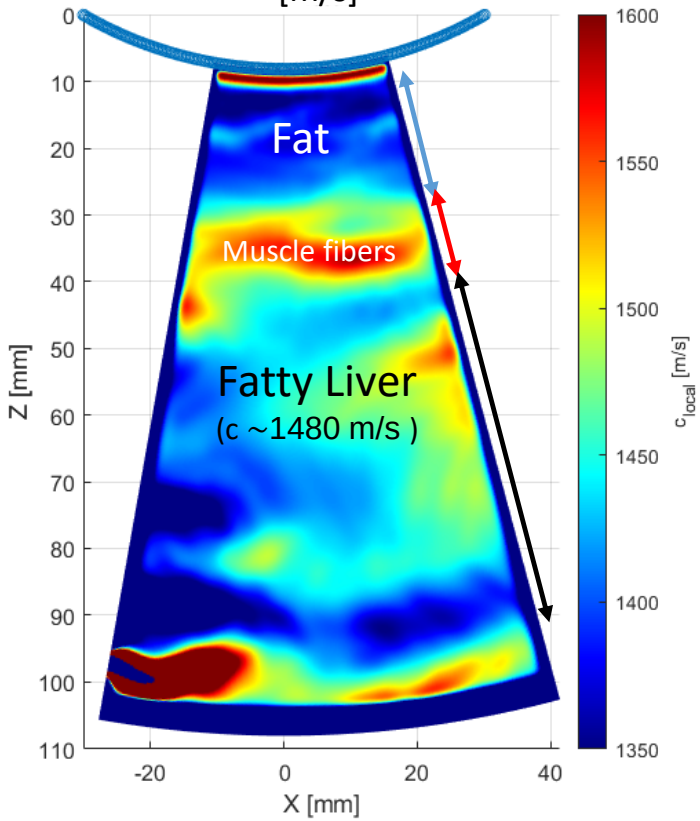

Steatosis diagnosis:
Accumulation of fat droplets
within the liver cells
c_{fat}~1480 m/s vs c_{liver} ~1600 m/s

$$\frac{1}{\hat{c}(\mathbf{r})} = \int_0^z \frac{1}{c(\mathbf{r})} \frac{dz}{z}$$

Tomography of the speed-of-sound,
an important parameter bio-marker for steatosis diagnosis

Flavien Bureau, PhD thesis

Exact repositioning in depth of the ultrasound image

Institut **Langevin**
ONDES ET IMAGES

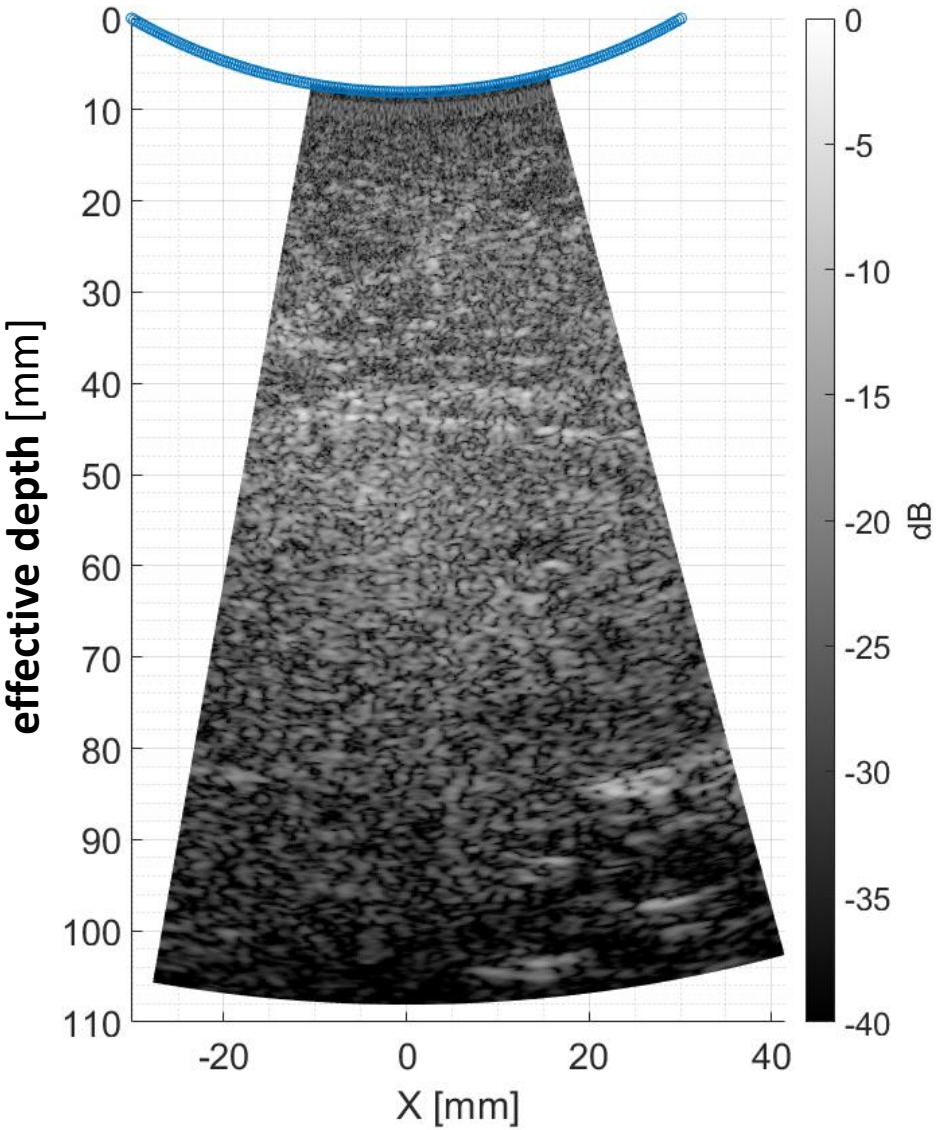

Flavien Bureau, PhD thesis

Exact repositioning in depth of the ultrasound image

Institut **Langevin**
ONDES ET IMAGES

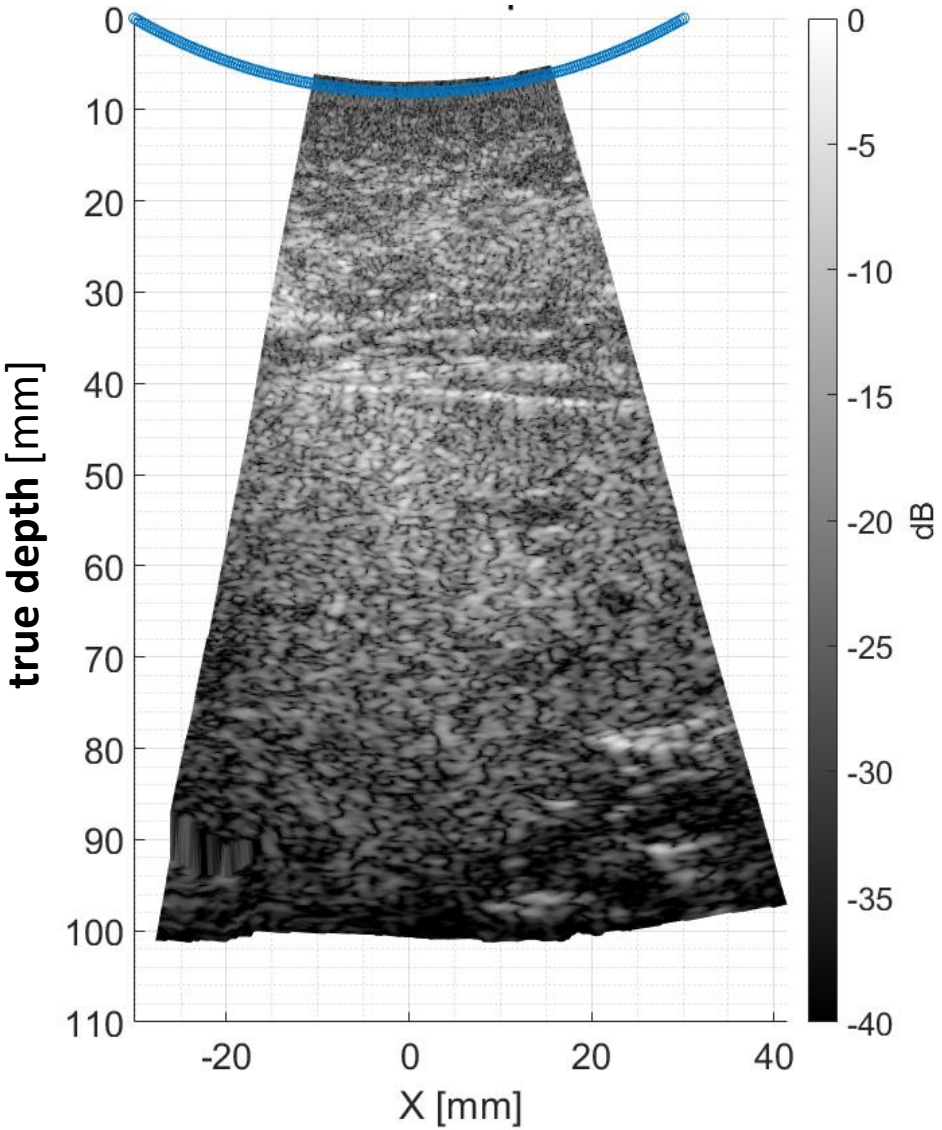

Flavien Bureau, PhD thesis

Quantitative Matrix Imaging

Institut Langevin
ONDES ET IMAGES

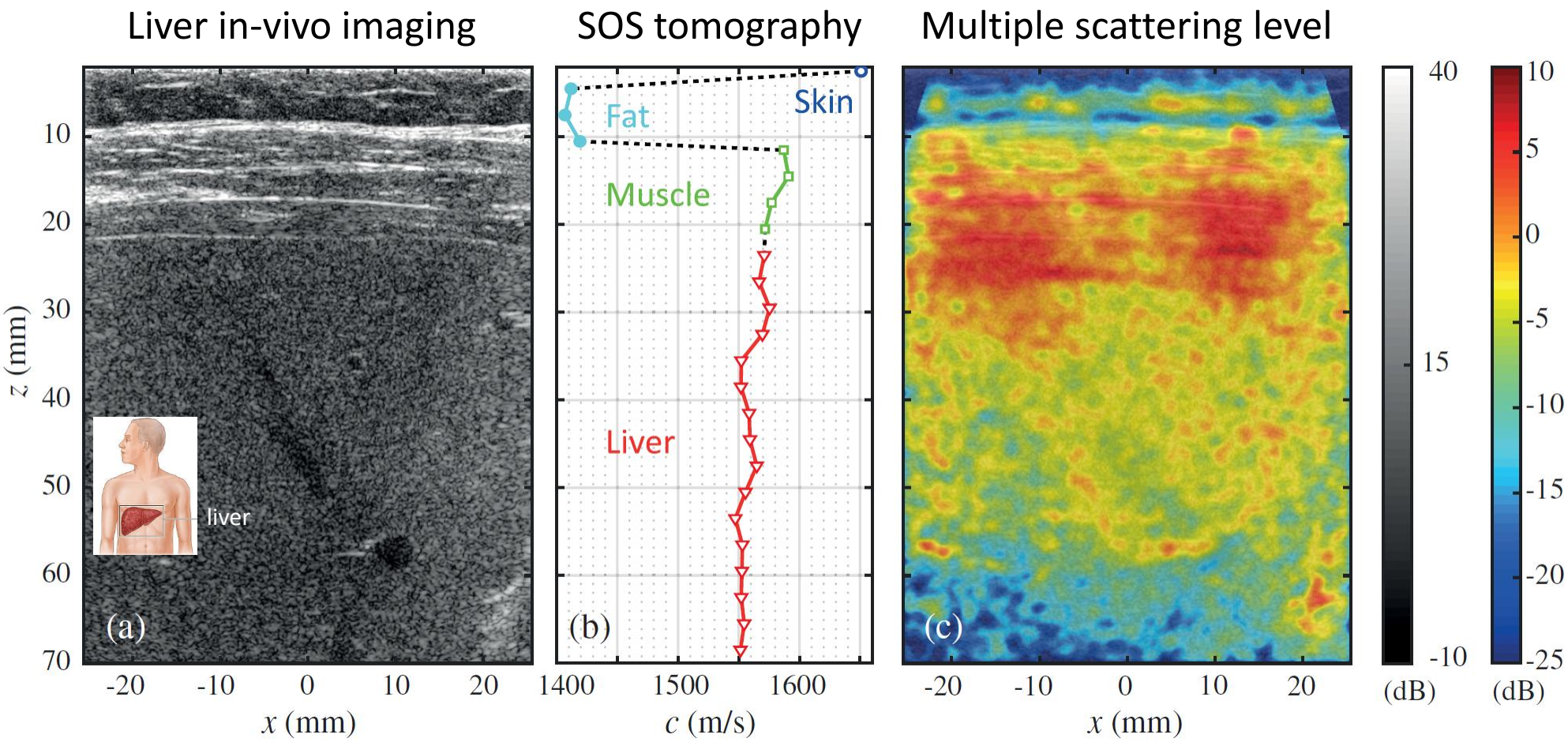

Tomography of multiple scattering,
a new bio-marker for tumor detection?

W. Lambert *et al.*, Phys. Rev. X, 2020

Quantitative Matrix Imaging

Institut **Langevin**
ONDES ET IMAGES

Calf Ultrasound Image

Map of fibers orientation

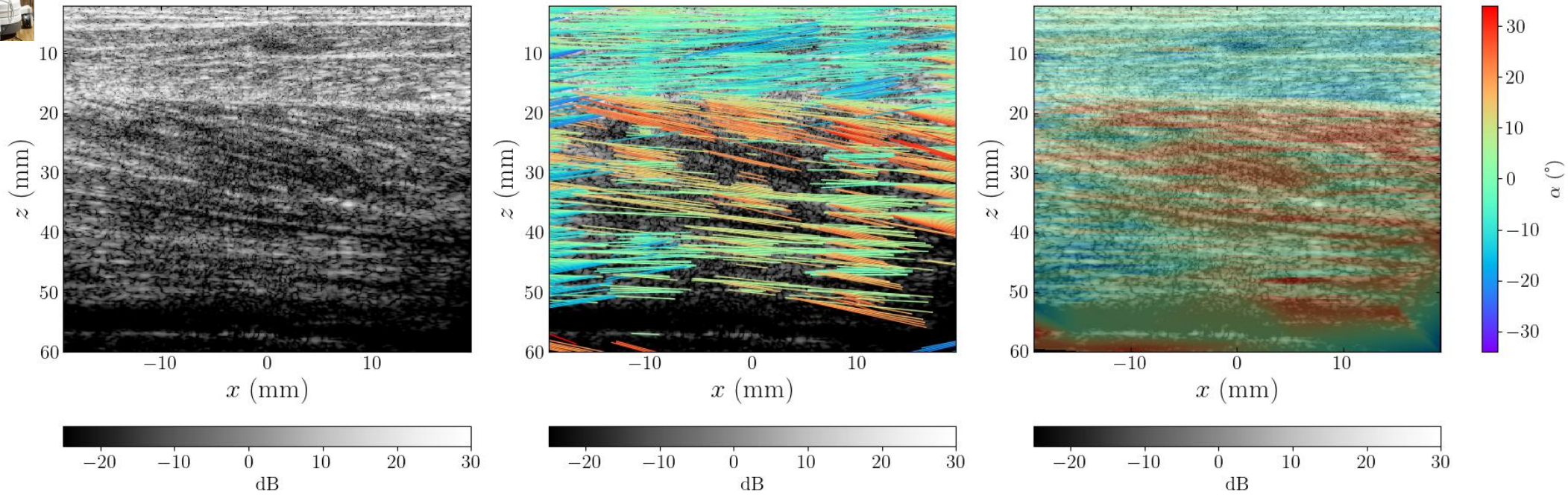

Tomography of scattering anisotropy in fibrous tissues,
an important bio-marker for muscular distrophy, myocardial disease *etc.*

Antton Goicoechea's post-doc

Conclusion & Perspectives

Conclusion and perspectives

Universal matrix approach of imaging in wave physics

Reflection, Non invasive, Label free, Post-processing

Active/Passive measurements
Large dimension sensor networks
High number of spatial degrees of freedom

3D optical imaging of an edematous primate cornea

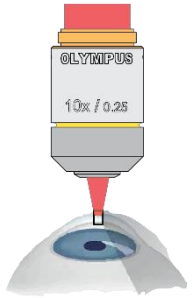

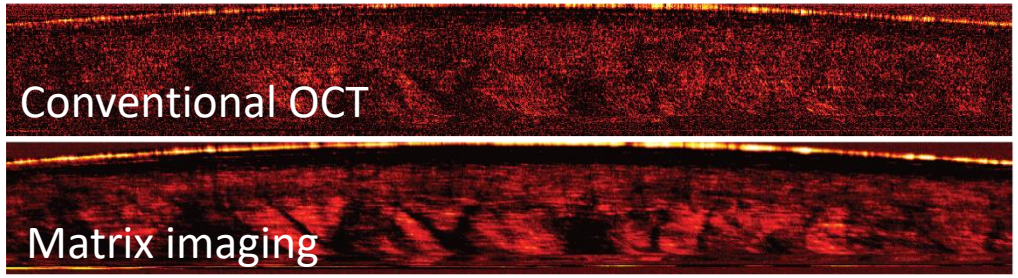

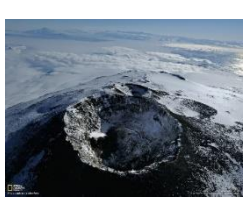

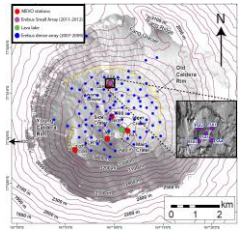

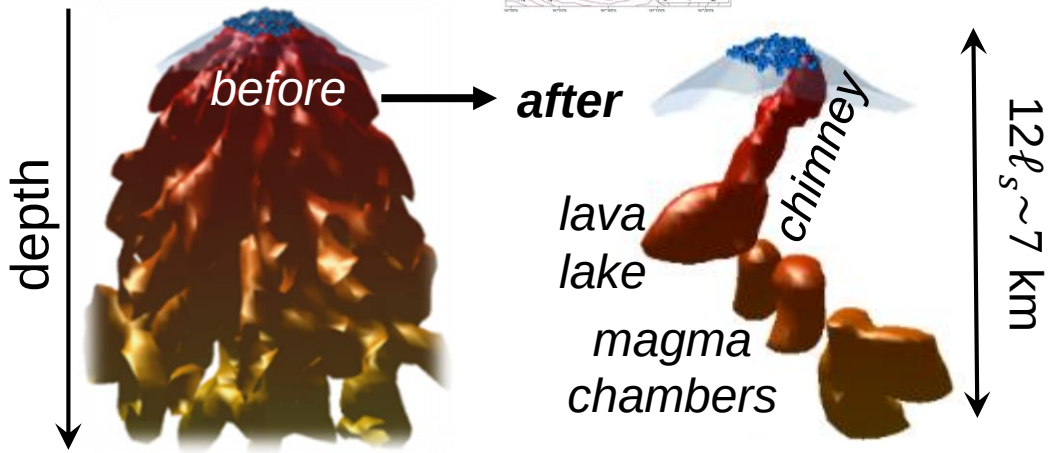

Applications to any research field:
- **Optical microscopy**
- **Ultrasound imaging**
- **Seismology**
- **Radar technology**
- **etc.**

But limited, so far, to
- **single scattering**
- **forward multiple scattering…**

Extend the matrix approach to the time/frequency domain

Go beyond the ballistic time

Control all the spatio-temporal degrees of freedom provided by the scattering medium

Self-portrait of the wave inside the scattering medium

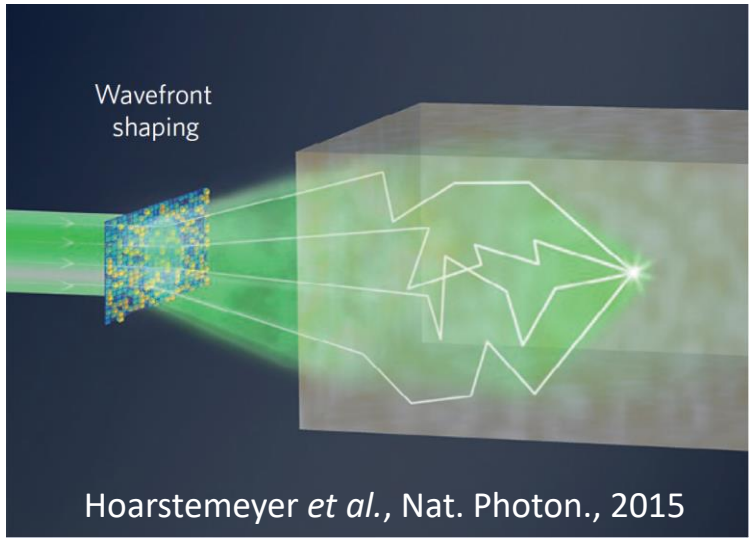

Hoarstemeyer *et al.*, Nat. Photon., 2015

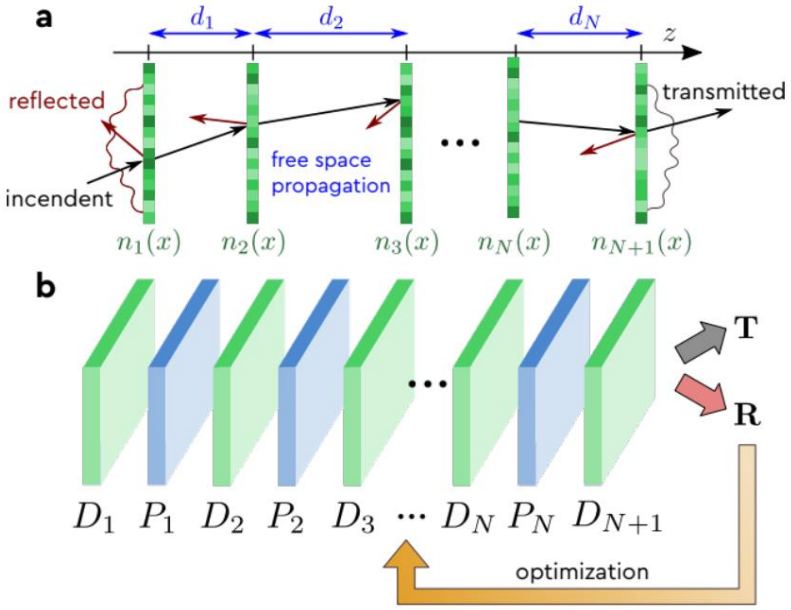

Courtesy of Sebastien Popoff

Depth-by-depth iterative procedure

Deterministic and learning-based approaches for the retrieval of the T-matrix inside the medium

Collaborators

Institut Langevin
ONDES ET IMAGES

OPTICS


Amaury Badon


Victor Barolle


Paul Balondrade


Ulysse Najar

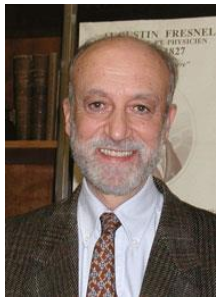
Claude Boccara


Mathias Fink

ULTRASOUND


William Lambert


Laura Cobus

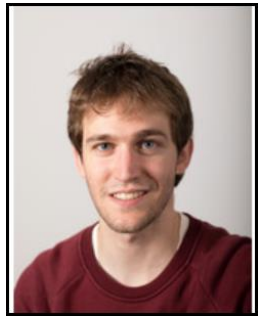
Flavien Bureau


Elsa Giraudat


Arthur Le Ber


Antton Goicoechea

SEISMOLOGY


Rita Touma


Thibaud Blondel


Arnaud Derode


Arnaud Burtin


Michel Campillo

Thanks for your attention!

Institut Langevin, ESPCI Paris, CNRS, PSL University, Paris, France

IDEFIX Seminar – INRIA, Institut Polytechnique de Paris, EDF R&D – March 22nd, 2022